Oil-spill monitoring in Indonesia

Budhi Gunadharma Gautama

IMT Atlantique
Bretagne-Pays de la Loire
École Mines-Télécom

UNIVERSITE BRETAGNE LOIRE

THÈSE / IMT Atlantique

sous le sceau de l'Université Bretagne Loire

pour obtenir le grade de

DOCTEUR D'IMT Atlantique

Spécialité : Signal, Image, Vision

École Doctorale Mathématiques et STIC

Présentée par

Budhi Gunadharma Gautama

Préparée dans le département Signal & communications

Laboratoire Labsticc

Oil-Spill Monitoring in Indonesia

Thèse soutenue le 01 décembre 2017

devant le jury composé de :

René Garello
Professeur (HDR), IMT Atlantique / président

Thomas Corpetti
Directeur de recherche (HDR), LETG-Rennes / rapporteur

Serge Andrefouet
Directeur de recherche (HDR), INDESO Center JI. Baru Perancak / rapporteur

Nicolas Longepe
Chercheur, CLS – Plouzané / examinateur

Emina Mamaca
Chercheur, Ifremer – Plouzané examinatrice

Ronan Fablet
Professeur (HDR), IMT Atlantique / directeur de thèse

N° d'ordre : 2017telb0422

Sous le sceau de l'Université Européenne de Bretagne

IMT Atlantique Bretagne-Pays de la Loire

En accréditation conjointe avec l'**École Doctorale – SICMA**

Thèse de Doctorat

Mention : *STIC – Sciences et Technologies de l'Information et des Communications*

Oil Spill Observation in Indonesia

présentée par

Budhi Gunadharma GAUTAMA

Unité de recherche :	**IMT Atlantique** – Signal et Communication
Laboratoire :	**Lab-STICC**, Pôle CID, Équipe TOMS
Entreprise partenaire :	**CLS FRANCE**
Directeurs de thèse :	**Ronan FABLET**
Encadrant de thèse :	**Grégoire MERCIER et Nicolas LONGÉPÉ**

Soutenue **le 01 Decembre 2017** devant le jury composé de:

M Thomas CORPETTI	Rapporteur
M. Serge ANDRÉFOUËT	Rapporteur
M. René GARELLO - Professeure, IMT Atlantique	Examinateur
Mme. Emina MAMACA	Examinateur

Contents

Acknowledgments xi

Acronyms xiii

Abstract xv

Résumé xvii

Résumé étendu xix

1 Introduction 1

1.1 Context of the thesis . . . 2

1.2 A brief review of INDESO Project . . . 4

1.3 Thesis motivation and outline . . . 6

2 Oil Spill Monitoring in Indonesia 9

2.1 Description of Indonesian waters . . . 10

2.1.1 General aspects of ocean circulation in Indonesia . . . 10

2.1.2 Main issue of Indonesia Marine and Fisheries . . . 11

2.2 Oil spill monitoring as conceived by the INDESO system . . . 18

2.2.1 Operational . . . 18

2.2.2 INDESO sites for the oil spill monitoring . . . 19

2.2.3 System design . . . 21

2.3 Detection of oil spill using EO-based imagery . . . 24

2.3.1 Spaceborne/airborne remote sensing . . . 24

2.3.2 Detection of oil spill based on SAR imagery . . . 27

2.4 Oil spill transport model . . . 31

2.4.1 Introduction . . . 31

2.4.2 Lagrangian 2D Trajectory Model . . . 32
2.4.3 Mobidrift . . . 33
2.4.4 Application of Mobidrift in Indonesia's Oil Spill Trajectory . . . 34
2.5 Conclusion . . . 37

3 Oil spill parameter retrieval 39
3.1 Introduction . . . 40
3.2 Proposed approach . . . 42
3.3 Montara SAR based oil detection . . . 44
3.4 Similarity between SAR oil spill detection and model . . . 47
3.5 Estimation of oil leakage parameters assimilation of SAR images . . . 49
3.6 Application to Montara case study . . . 52
3.7 Conclusion . . . 59

4 Oil spill risk assessment in Indonesian Fisheries Management Area 61
4.1 Introduction . . . 62
4.2 Data and Study area . . . 65
4.2.1 Study Area . . . 65
4.2.2 Data Collection . . . 66
4.2.3 Marine Protected Area Data . . . 71
4.2.4 Marine fisheries data . . . 74
4.2.5 Socio-economic data for fishing activities, tourism services and salt ponds 75
4.3 Proposed methodology . . . 77
4.3.1 Oil spill risk indices . . . 77
4.3.2 Environmental and socio-economical vulnerability indices . . . 80
4.3.3 Global FMA-level risk index . . . 83
4.3.4 MPA-level vulnerability analysis . . . 84
4.4 Results and Discussion . . . 87
4.5 MPA-level risk assessment . . . 89
4.6 Conclusion and Discussion . . . 101

5 Conclusions and Perspectives 105
5.1 Conclusion . . . 106

5.2 Perspectives 108

Bibliography **122**

List of Figures

1.1 Operational Oceanography Schema, Courtesy : INDESO project 4

2.1 Perancak satellite receiving station visibililty circle, Courtesy : INDESO project . 19

2.2 Primary priority (purple) and secondary priority (green) priority areas for oil spill monitoring 20

2.3 Oil Spill monitoring general architecture showing external systems (INDESO Core system with a red star), external interfaces (data providers with a pink star) and applications users (yellow star) 21

2.4 Oil spill observation in INDESO system with SAR detection in North of Java on 25 July 2016 (black box), the wind vector (black arrow), the vessel ID and position showed in triangle with yellow number and the contour of oil spill detected in red 23

2.5 Image AQUA on Montara wellhead location (red dot) on 21 August 2009, no oil slick detected, the purple line is the border of Indonesia territory 25

2.6 Image TERRA on Montara wellhead location on 03 September 2009, oil slick polygon detected in red line, the purple line is the border of Indonesia territory . 25

2.7 Synthetic aperture radar imaging system basic principle 28

2.8 INDESO oil spill report 30

2.9 Bathymetry (meter) of the INDESO configuration. (ETOPOV2g/GEBCO1 + in-house adjustments in straits of major interest) 35

2.10 Sea surface current velocity (m/s) on 01 January 2015 data from the INDESO system 35

2.11 Wind velocity data (m/s) and its direction (black arrow) on 01 January 2015 data from the INDESO system 36

3.1 Position of the Montara oil platform on the map of bathymetry, the red sign is Montara wellhead position and the black box is our boundary box for oil trajectory simulation. 41

3.2 Flowchart of the proposed approach for the assimilation of oil leakage parameters from satellite-based SAR observations 43

3.3 SAR Observation on September 02, 2009 by ENVISAT, red contour outlines the main patches of weathered oil on the sea surface, the red dot is Montara wellhead position and the purple outlines the border of Indonesia (above the line) and Australia water territory (below the line). 48

3.4 Level-set [1] representation of closed contours in a two-dimensional plane : when the contours t=0 (yellow,-) with the value $\phi < 0$ moving forward on t=1 (blue,-) with the value $\phi > 0$ 50

3.5 Spatial density of a set of particles simulated from Lagrangian transport model (3.2). The simulated particle set is depicted as a set of blue dots. We also display the contour of the kernel-based estimate of the spatial density of the simulated particle set. 51

3.6 Minimum RMSE of level set value of images SAR on September 02, 2009 with simulations of one-day oil leakage from August 21, 2009 to August 02, 2009 (a) and oil leakage started on 21 August,2009 with different duration (b) from Montara wellhead platform. 53

3.7 Optimum value of wind drift factor C_w from simulations of one-day oil leakage from Montara wellhead platform from August 21, 2009 to September 02, 2009. . 54

3.8 Optimum value of current drift factor C_c from simulations of one-day oil leakage from Montara wellhead platform from August 21, 2009 to September 02, 2009 . . 54

3.9 Level-set-based distances between the SAR observation of the oil spill on September, 02 2009, and Lagrangian-based drift simulations of twelve-day oil leakage, started on August 21, 2009, within Powell's optimization scheme for wind and current drift coefficients. Red dot show the minimum RMSE value founded (3.513) with the value of $C_C = 1.285$ and $C_w = 0.0493$. 55

3.10 Level-set-based representation of the SAR-derived detection of the oil spill on September 02, 2009, and Lagrangian-based drift simulations for a one-day oil leakage on August 21, 2009, with optimal wind and current drift coefficients, $C_w = 49.3\%$ and $C_C = 122.1\%$ (a) and Lagrangian-based drift simulations for a twelve-days oil leakage started on August 21, 2009 with optimal wind and current drift coefficients, $C_w = 49.3\%$ and $C_C = 128.5\%$ (b). The SAR detection and simulation contours are shows in blue and red line respectively and red dot is the position of Montara oil platform 56

3.11 Optimal level-set-based distances between the SAR observation of the oil spill on September 02, 2009, and Lagrangian-based drift simulations of oil leakage with respect to leakage starting date (x-axis) and duration (y-xis). The optimal level-set-based distances are issued from Powell's optimization of wind and current drift coefficients. 57

4.1 Map of the study area with Indonesian Fisheries Management areas in blue, Indonesian land territory (in white) and its neighboring country (in brown), Marine Protected Area (in red) and ship density map estimated from AIS data to be used as potential source of unintentional and intentional oil spills (in green triangle) . 65

4.2 Ship density on Indonesia marine waters based on the AIS data 69

4.3 SAR-based Detection of oil spills in the framework of INDESO system in Indonesia sea water territory (FMA are depicted in green) from 27 July 2014 until 16 January 2017), the boxes refer to the scene of the SAR images (271 scenes). We report the contours of oil spill detections in black. 70

4.4 Detection of oil spill on the Java Sea using SAR observation (using RADARSAT2 on INDESO system on 25 July 2016 11 :07 :27 (UTC), there are 14 detected oil spill contours (in red) and 40 neighboring ships (in blue) with their ID reference number (in yellow) 71

4.5 Mapping of 7 zones of MPA in FMA 712 (red) along with potential oil spill sources (green triangles) associated with high-traffic points in the area determined from AIS-derived traffic density maps. 85

4.6 Mapping of 14 zones of MPA in FMA 711 (red) along with potential oil spill sources (green triangles) associated with high-traffic points in the area determined from AIS-derived traffic density maps. 86
4.7 Oil spill drift simulations from one source point located at 0° 36' 0" S and 107° 5' 60" E (green triangle) in FMA 711 with 3-day and 6-day durations (resp. black and gray dots) for metocean conditions in the Northwest monsoon from December to February. 90
4.8 Oil spill drift simulations from one source point located at 0° 36' 0" S and 107° 5' 60" E (green triangle) in FMA 711 with 3-day and 6-day durations (resp. black and gray dots) for metocean conditions in the Transition 1 monsoon from March to May. 91
4.9 Oil spill drift simulations from one source point located at 0° 36' 0" S and 107° 5' 60" E (green triangle) in FMA 711 with 3-day and 6-day durations (resp. black and gray dots) for metocean conditions in the SouthEast monsoon from June to August. 92
4.10 Oil spill drift simulations from one source point located at 0° 36' 0" S and 107° 5' 60" E (green triangle) in FMA 711 with 3-day and 6-day durations (resp. black and gray dots) for metocean conditions in the Transition 2 monsoon from September to November. 93
4.11 Oil spill drift simulations from one source point located at 5° 30' 0" S and 106° 54' 0" E (green triangle) in FMA 712 with 3-day and 6-day durations (resp. black and gray dots) for metocean conditions from January to December. 94

List of Tables

2.1 Targeted areas for oil spill monitoring 20

2.2 List of satellite-borne SAR sensors 27

4.1 Oil spills caused by ships in Indonesia FMA between 1975 and 2010 67

4.2 Number of potential oil spill source considered in each FMA 68

4.3 Coverage area of SAR images within each FMA and associated percentage with respect to the total surface area of each FMA 70

4.4 Considered MPA-based ecological data for each FMA : number of species for coral reef fish, sea turtles, mangrove and seabirds, total seagrass area, number of dugong populations, total MPA area. 72

4.5 Fish production and associated economic value in each FMA 75

4.6 Considered socio-economic characteristics of fisheries activities, maritime tourism activities and traditional salt ponds in each FMA. 76

4.7 Oil spill risk indices derived from different data sources for the 11 FMA. We let the reader refer to the main text for the definition of the different indices PR_s k 80

4.8 Vulnerability indices computed for each FMA from MPA-level ecological features. We let the reader refer to the main text for the definition of the different indices PR_end k. 81

4.9 Categorization of the Global Risk Index (GRI) (Eq.4.6). 84

4.10 Synthesis of FMA-level risk and vulnerability indices 87

4.11 Global Risk Index (GRI) for each FMA 88

4.12 Number of particles entering each MPA in FMA 711 and 712 for oil spill drift simulations with January-to-December metocean conditions. AIS-derived Vessel density maps were used to generate oil spill source points. 95

4.13 MPA-level vulnerability indices in FMA 711 issued from oil spill drift simulations for a 3-day drift duration and January-to-December metocean conditions. 96

4.14 MPA-level vulnerability indices in FMA 711 issued from oil spill drift simulations for a 6-day drift duration and January-to-December metocean conditions. 97
4.15 MPA-level vulnerability indices in FMA 712 issued from oil spill drift simulations for a 3-day drift duration and January-to-December metocean conditions. 98
4.16 MPA-level vulnerability indices in FMA 712 issued from oil spill drift simulations for a 6-day drift duration and January-to-December metocean conditions. 99
4.17 Mean MPA-level vulnerability indices in FMA 711 for January-to-December metocean conditions 100
4.18 MPA-level vulnerability indices in FMA 712 under different monsoon conditions. 100

Acknowledgements

During more than three years of my stay in France to study in Telecom Bretagne/IMT Atlantique for my PhD study, I have had the opportunity to learn a great amount of knowledge and gain meaningful and valuable work and life experience. For me this experience would be the best chapter in my life. All of these would not have been possible without the contribution of several persons with whom I have interacted during this period.

In this opportunity I would like to express my grateful to:

- Foremost, I would like to express my sincere gratitude to my advisor Prof. Ronan Fablet, Nicolas Longépé and Prof. Gregoire Mercier for the continuous support of my Ph.D study and research, for his patience, motivation, enthusiasm, and immense knowledge. His guidance helped me in all the time of research and writing of this thesis. I could not have imagined having a better advisor and mentor for my Ph.D study.
- Besides my advisor, I would like to thank INDESO National Capacity Building Committee: Pak Aryo, Pak Berny, Bu Yenung, Pak Aulia, Pak Widodo, Pak Vincent from IPB, Ibu Ita from UNDIP for their encouragement, insightful comments, and motivation.
- INDESO CLS team in Brest and Toulouse: especially Florence, Beatrice and Philippe.
- KKP team: Head of Marine Research Center and Head of Agency for Marine & Fisheries Research & Human Resources with all the staffs in Jakarta and Perancak.
- Government of French and Campus France for the best security social system.
- I thank my fellow labmates in Signal et Communication Departement Telecom Bretagne.
- My family that supporting me, especially my wife for giving two beautiful babies to me at the first place and my mother for supporting me spiritually throughout my life.
- Last but not least to all Indonesian student and my friend in Brest, for all the fun we have had in the last three years.

Acronyms

AIS	Automatic Identification System
ASEAN	Association of Southeast Asian Nations
CIS	Central Information System
CLS	Collecte Localisation Satellites
INDESO	Infrastructure Development of Space Oceanography
ECMWF	European Centre for Medium Range Weather Forecasting
EM	Electromagnetic
EO	Earth Observation
FMA	Fishing Management Area
GRI	Global Risk Index
GUI	Graphical User Interface
IUU	Illegal, Unreported and Unregulated
IR	Infra Red
ITF	Indonesia Through Flow
ITOPF	International Tanker Owners Pollution Federation
JICA	Japan International Cooperation Agency
MPA	Marine Protected Area
MMAF	Ministry of Marine and Fisheries
NCEP	National Center for Environmental Prediction

NRT Near Real Time

OG Oil and Gas

pH potential of Hydrogen

SAR Synthetic Aperture Radar

SLA Sea Level Anomaly

SRS Satellite Receiving Station

SSH Sea Surface Height

SST Sea Surface Temperature

TIR Thermal Infra Red

UV Ultra Violet

ZEE Zone Economic Exclusive

Abstract

Indonesia as the biggest archipelago has a major threat coming from oil spill. Due to the increasing concerns of environment protection for sustainable development, the government of Indonesia in cooperation with government of France developed an ocean observation system with one of its pilot applications is oil spills monitoring. This system is integrated in the operational oceanography systems within the project of Infrastructure Development of Space Oceanography (INDESO). The context of this thesis is in the frame of INDESO project particularly in the monitoring of oil spill in the Indonesian seas. Within the context above, this thesis propose new methodologies and analyses. This thesis involved two main contributions. The first contribution addressed the retrieval of oil spill drift parameters from a joint analysis of SAR observations of an oil spill and of outputs of a Lagrangian oil spill transport model. The proposed framework exploited a Lagrangian oil spill transport model such that the simulated oil spill drift could match a SAR-based observation of an oil spill. To confirm the origin of the oil spill detected on a given date through a SAR observation, we performed simulations with various leakage starting dates, leakage durations, and different values of wind and current weighing coefficients. We applied the proposed methodology on the most famous oil spill accident in Indonesia, the Montara case. The second contribution was the global assessment of oil spill risk in Indonesia. We focused on the 11 Indonesia Fisheries Management Area to support the sustainability development of marine and fisheries. The focus was given to Fisheries Management Areas as a means to provide synoptic analysis over the entire Indonesian maritime territory. In this analysis we proposed methodology that considered the oil spill from different source and their impacts not only to the environment, but also from social and economic perspectives. For the assessment of vulnerability of Marine Protected Areas to oil spill pollution, we also exploited the oil spill trajectory model. The result of this study can be used in the mitigation planning to reduce the negative impacts of oil spill.

Keywords: *oil spill, Indonesia, Synthetic Aperture Radar, trajectory model, oceanography operational.*

Résumé

L'Indonésie, l'une de plus grands archipels, a été menacé avec la pollution provenant de la marée noire. Le gouvernement d'Indonésie en coopération avec le gouvernement Français a développé un système d'observation de l'océan par satellite afin de supporter de développement durable. Ce système est intégré dans les systèmes d'océanographie opérationnelle dans le cadre du projet de développement des infrastructures de l'océanographie spatiale (INDESO). Le contexte de cette thèse est dans le cadre du projet INDESO notamment dans applications d'INDESO pour suivre des déversements de pétrole dans les mers d'Indonésie. Dans ce contexte, cette thèse propose de nouvelles méthodologies et analyses. Cette thèse comportait deux contributions principales. La première contribution est sur la récupération des paramètres de dérive des déversements d'hydrocarbures à partir d'une analyse conjointe des observations SAR (Synthetic Aperture Radar) et des résultats d'un modèle de transport de déversement de pétrole. Pour confirmer l'origine du déversement de pétrole détecté à une date donnée par une observation de SAR, nous avons effectuaient des simulations avec différentes dates de début de fuite, duré de fuite et différentes valeurs de pondération deux facteurs dominants i.e. vent et courant. Nous avons appliqué la méthodologie proposée sur le plus grand accident en Indonésie, l'accident de Montara. La deuxième contribution est l'évaluation globale du risque de déversement d'hydrocarbures en Indonésie. Nous sommes concentrés sur la zone de gestion des pêches de l'Indonésie. Dans cette analyse, nous avons proposé une méthodologie qui considère le déversement de pétrole, qui a des sources différentes et leurs impacts à l'environnement, mais aussi sur les perspectives sociales et économiques. Pour l'évaluation de la vulnérabilité des zones marines protégées, nous avons également exploité le modèle de 2D lagrangien. Le résultat de cette étude peut être utilisé dans la planification d'une action pour réduire les impacts négatifs du déversement d'hydrocarbures.

Mots clés: déversement d'hydrocarbures, Indonésie, Synthétique Aperture Radar, modèle de trajectoire, océanographie opérationnelle.

Résumé étendu

Note : Les thèses accomplies dans un établissement français mais écrits dans une autre langue doivent fournir un résumé français.

Introduction

L'Indonésie est un pays maritime avec plus que 17000 îles. Marine et la pêche sont la principal collaborateur à la croissance d'économique. D'autre part, l'Indonésie a une menace majeure venant de la fuite de pétrole. Dans les eaux océaniques et côtières, il y a deux sources de fuite de pétrole, sorties intentionnelles et involontaires. L'exemple de sorties intentionnelles est la fuite de pétrole venant de décharges opérationnelles en expédiant. Il y a quelques possibilités que la décharge est légale mais dans la plupart des cas ils sont illégaux. Le risque est plus grand depuis il y a trois voies de navigation maritime majeures en Indonésie qui connectent l'océan Indien, l'Océan Pacifique et le Sud-est la Mer de la Chine. Cette trois voies ont la haute densité de trafic. Le trafic maritime dense est devient potentiellement la source de fuite de pétrole intentionnelle. Sur côté non intentionnel, l'accident de déversement d'hydrocarbures survenu à la plate-forme de Montara est l'un des exemples les plus graves de déversement involontaire.

En raison des croissantes de préoccupations de la protection de l'environnement pour le développement durable, le gouvernement indonésien a développé un système d'observation océanique avec sept applications pilotes : lutte contre la pêche illégale, surveillance des stocks de poissons, surveillance des récifs coralliens, surveillance des déversements d'hydrocarbures, l'aquaculture de crevettes et d'algues, gestion intégrée des zones côtières et monitorage de mangrove. Ce système est intégré dans les systèmes d'océanographie opérationnelle dans le cadre du projet de développement des infrastructures de l'océanographie spatiale (INDESO). Le contexte de cette thèse est dans le cadre du projet INDESO notamment dans l'application de suivi des déversements de pétrole dans les mers Indonésiennes.

Le système d'Indeso devrait aider le gouvernement indonésien à réduire et à préparer la planification de l'atténuation de l'impact des déversements de pétrole. Malgré le système de détection SAR que mis en place dans le système INDESO, il y a un besoin d'informations complémentaires sur la planification de l'atténuation. Pour prévenir l'impact des déversements de pétrole dans l'environnement, il est essentiel de surveiller l'océan continuellement et d'utiliser des systèmes de prévision pour prévoir sa dérive. L'information ordinaire basée sur l'océanographie opérationnelle à partir des observations et des modèles doit être combinée avec le modèle de trajectoire du déversement d'hydrocarbures afin d'obtenir la position d'évolution du déversement d'hydrocarbures. Dans ce travail, le transport pétrolier à la surface de la mer est modélisé par un modèle 2D lagrangien nommé Mobidrift. Dans ce contexte, nous avons utilisé le cas de Montara comme cas d'étude pour implémenter un schéma d'assimilation de la détection basée sur SAR dans le modèle de dérive. Pour assimiler l'image SAR, nous proposons une méthodologie basée sur une approche Level Set. Nous comparons le contour du déversement d'hydrocarbures de la détection SAR avec le contour des particules simulées par le modèle de trajectoire. Avec cette comparaison, l'objectif est de déterminer ou de confirmer la source des pollutions. L'objectif est également de mieux comprendre les phénomènes de dérive, et au moins de régler certains facteurs tels que la pondération du vent et des effets du courant dans l'advection totale, le temps et la durée de la fuite.

En outre, pour soutenir le développement durable de la marine et de la pêche, nous devons évaluer le risque lié au déversement d'hydrocarbures. L'Indonésie a un territoire de l'eau unique puisque c'est un grand archipel pays. Le gouvernement de l'Indonésie a divisé ses zones économiques exclusives (ZEE) en 11 zones de gestion des pêches (FMA/Fishing Management Area). Chaque FMA a des caractéristiques différentes. Nous analysons le risque de déversement d'hydrocarbures dans 11 FMA en Indonésie à partir de différentes sources potentielles de pollution. Dans ce travail, nous synthétisons tous les rapports de différentes institutions liés pour trouver les données caractérisées de facteurs importants avec ses variables qui déterminent les amplitudes de risque. Cinq variables sont sélectionnées pour la probabilité d'occurrence de déversements de pétrole, tels que le nombre d'accidents de navires, de plates-formes pétrolières offshore et de raffineries de pétrole, la densité du trafic maritime, les ports transportant du pétrole et les polygones de pétrole détectés par SAR dans les systèmes d'INDESO. En facteur écologique, nous choisissons deux variables liées qui sont le nombre d'espèces importantes et la

superficie de Marine Protegée Région(Marine Protected Area/MPA). Cinq variables liées à l'impact des marées noires sur le facteur socioéconomique sont retenues (nombre de production de capture marines et leur valeur économique, nombre de centres de production de sel, nombre de bateaux de pêche operationel et nombre de services de tourisme). Nous calculons l'indice général de vulnérabilité à partir de ces trois facteurs. Ensuite, nous classons le risque de déversement d'hydrocarbures dans chaque zone en quatre catégories (minimale, faible, moyenne et élevée). Pour les zones classées à haut risque, nous simulons le déversement de pétrole à partir de différents points sources pour différentes saisons et durées afin d'analyser en détail le risque. Avec cette analyse au moins peut être une contribution sur l'élaboration de la politique nationale sur la planification de l'atténuation des déversements d'hydrocarbures.

Première contribution : Récupération de paramètre de fuite de pétrole

L'accident de déversement de pétrole de Montara en 2009 a souligné les besoins urgents de surveillance opérationnelle des déversements de pétrole dans la mer Indonésiennes. L'exploitant, PTTEP Australasia (Ashmore Cartier) Proprietary Limited (PTTEP AA), a initialement estimé la fuite d'huile à 400 barils (soit environ 64 tonnes) de pétrole brut perdu par jour. La libération incontrôlée a débuté le 21 août 2009 et le pétrole a continué à être libéré jusqu'au 3 novembre 2009, date à laquelle le puits a été maîtrisé. La plate-forme de tête de puits de Montara est située dans les territoires australiennes à la latitude $12°40'20.5''$N and longitude $124°32'22.2''$E. Suite à l'accident de Montara, le Ministère des Affaires Maritimes et de la Pêche d'Indonésie a initié le développement de systèmes de surveillance des océans, en combinaison avec l'océanographie opérationnelle, notamment dans le cadre du projet INDESO. Dans ce contexte, la présente étude porte sur l'assimilation des observations déversements d'hydrocarbures par SAR (Synthetic Aperture Radar) satellite dans un modèle de trajectoire pétrolière. Il repose sur des simulations lagrangiennes du transport de particules à la surface de la mer. La comparaison à base de Level Set méthode. En utilisant le déversement d'hydrocarbures de Montara, nous démontrons la pertinence du modèle proposé et du schéma numérique associé pour l'optimisation des paramètres de fuite de pétrol. Les paramètres sont la date de début de la fuite, sa durée et ses coefficients de dérives du courant et vents.

Notre approche implique trois composants principaux :

- Un modèle Lagrangien de transport 2D

  Modèle simule l'advection de particules à la surface de la mer dans des conditions de vent et de courant données. Le modèle de transport considéré, à savoir le modèle Mobidrift développé par Collecte Localisation Satellite (CLS). Dans le modèle de Mobidrift, les fluides sont modélisés par un ensemble de particules déterministes. Pour une source définie par une plate-forme pétrolière fixe, nous fournissons au modèle Mobidrift l'emplacement de la source, l'heure de début de la libération des particules et la durée de la fuite. Pour chaque particule libérée de la position initiale, nous appliquons le modèle de transport 2D considéré pour dériver sa trajectoire jusqu'à la date finale de la simulation. Dans nos simulations, nous considérons généralement environ 500 particules libérées sur une base quotidienne. Formellement, le modèle de Mobidrift repose sur l'advection bidimensionnelle des particules par un déplacement de surface donné par une somme pondérée du courant de marée et des vitesses du courant induites par le vent.

- La détection des déversements d'hydrocarbures à partir d'observations SAR par satellite

  Dans cette étude, la première image SAR couvrant l'événement Montara est utilisée. Il a été observé le 02 septembre 2009 à 10h 07 UTC par la mission européenne ENVISAT. La résolution spatiale est de 75×75 mètres avec une largeur d'andain de 400 km. Depuis l'éruption de la plate-forme de Montara au 21 août 2009, cette image a été prise 12 jours après l'accident. Comme l'a observé le capteur SAR, la nappe de pétrole est toujours connectée à la plate-forme de la tête de puits, avec une longueur estimée à 160 km.

- La définition d'une mesure de similarité entre les ensembles de particules simulés et la détection de déversements d'hydrocarbures à partir d'observations SAR par satellite.

  Un élément clé de notre approche est la définition d'une mesure de la qualité de l'adéquation entre le déversement de pétrole détecté et la simulation des trajectoires des modèles de transport. Cela revient à définir une mesure de similarité entre un ensemble de particules et un contour dans un plan bidimensionnel. Nous exploitons les représentations implicites de niveaux définis par Osher et Sethian.

Application au cas de Montara

Pour étudier la sensibilité des simulations du modèle de transport en fonction des paramètres de fuite de pétrol, nous effectuons d'abord une assimilation avec une fuite tous les jours allant du 21 août au 02 septembre. Cette première simulation utilise différentes dates de fuite avec une durée d'un jour. Le résultat montre que les cinq premiers jours de fuite donnent la valeur minimale de RMSE. Pour chaque date, nous résolvons la minimisation de la valeur du level-set pour estimer les facteurs de dérive du vent et du courant (Cw et Cc). Nous rapportons dans la série des paramètres optimaux Cw et Cc liés aux simulations. Pour la source de fuite le 21 août 2009 avec une durée d'une journée, le RMSE minimum a été atteint pour les facteurs de dérive optimaux Cw = 0,0493 et Cc = 1,221 Les valeurs du facteur de dérive du courant optimal vont de 1,2 à 1,3. Les facteurs de dérive du vent optimaux récupérés vont d'environ 0,037 à 0,049. Dans l'ensemble, ces expériences initiales soulignent la plus grande contribution des fuites de pétrol, qui sont survenues depuis les cinq premiers jours, au déversement d'hydrocarbures détecté lors de l'observation SAR le 2 septembre 2009.

Ensuite, nous essayons de simuler la fuite avec une durée différente. Cette simulation montre que le RMSE diminue à mesure que la durée augmente. Le RMSE minimum a été atteint pour la source de fuite le 21 août 2009 avec une durée de 12 jours. La majeure partie de la surface du déversement de pétrole détecté est en fait expliquée par les fuites survenues sur les 5 premiers jours pour sa durée maximale (12 jours pour la source de fuite 21 août 2009, 11 jours pour la source de fuite 22 août 2009, 10 jours pour le 23 août 2009, etc.)

Les séries de distances basées sur les level sets montrent une nette tendance à la hausse, qui souligne l'impact des premières fuites d'huile le 21 août. Ces résultats confortent clairement l'existence d'une fuite continue d'huile pendant au moins 5 jours à partir du 21 août. 2009 avec le minimum RMSE atteint pour fuite de pétrol le 21 août 2009 avec une durée de 12 jours. Les facteurs de dérive optimaux estimés, respectivement Cw = 0,0493 et Cc = 1,285, sont réalistes et en accord avec les expériences rapportées ci-dessus et les travaux antérieurs.

La comparaison entre les simulations de modèles de transport et la détection de déversements d'hydrocarbures dérivés de SAR le 2 septembre 2009 met en évidence l'amélioration de l'appariement associé aux cinq premiers jours avec une durée allant jusqu'à l'hypothèse de fuite du 02 septembre par rapport à l'hypothèse de fuite journalière avec les nominale facteurs de dérive du vent et du courant optimisés.

Deuxième Contribution : Évaluation du risque de déversement d'hydrocarbures en Indonésie FMA

Les ressources marines et côtières sont d'une importance ressources pour l'Indonésie. La pêche de capture est l'une des ressources alimentaires les plus importantes. La production de 2005 à 2014 a augmenté en moyenne de 3,58% par an. De 4 408 499 tonnes en 2005, la production de poisson a atteint 6 037 654 tonnes, avec une valeur commerciale de plus de 7,5 milliards de dollars en 2014. La production de poissons comprend des espèces pélagiques grandes et petites et des stocks démersaux ainsi que des crustacés, des mollusques et les algues. Pour améliorer la gestion des ressources marines et halieutiques, le Ministère de la marine et de la pêche de l'Indonésie a divisé les territoire marines en 11 zones de gestion des pêches. L'Indonésie implique également une très grande biodiversité d'espèces avec une variété d'espèces importantes telles que les poissons de récifs coralliens, les cétacés, les tortues de mer, les mangroves, les algues, les dugongs et les oiseaux de mer. Dans certaines régions spécifiques, le gouvernement de l'Indonésie a créé en 2013 des aires marines protégées pour une superficie totale de 17 144 702 ha. Plusieurs études ont analysé les pollutions par déversement d'hydrocarbures en termes de dommages écologiques et de vulnérabilité pour la gestion des zones côtières et des zones côtières. Quelques études ont ciblé à la fois la vulnérabilité environnementale et socio-économique à la pollution par les hydrocarbures. On peut citer la combinaison de facteurs environnementaux et socioéconomiques dans l'île de Noirmoutier (France), la détermination des niveaux de risque de déversement dans les côtières de la Thaïlande ou l'évaluation des niveaux de risque de déversement dans la mer de Bohai (Chine). Cette dernière analyse différentes sources de déversement d'hydrocarbures, à savoir les pollutions de navires et de plateformes de pétrol.

Dans ce contexte, l'objectif de cette étude est de fournir des informations pratiques pour améliorer les politiques de prévention et de gestion des déversements d'hydrocarbures pour le gouvernement Indonésien, en mettant l'accent sur les zones de gestion des pêches. La méthodologie proposée comporte deux étapes principales :

- l'évaluation des niveaux global de risque de déversement d'hydrocarbures à l'échelle des zones de gestion des pêches,

- pour les zones de haut risque, une analyse plus poussée à des échelles spatiales plus fines à l'aide de simulations de dérive d'hydrocarbures.

Pour ces deux niveaux, la vulnérabilité d'une zone est évaluée à la fois en termes d'impacts écologiques et économiques. L'impact écologique est évalué par rapport à un indice de biodiversité et à la surface des MPA, tandis que les impacts économiques prennent en compte la valeur économique des ressources exploitées ainsi que le niveau d'emploi direct et indirect des activités de pêche et des services maritimes . Notre étude met clairement en évidence de fortes divergences dans la vulnérabilité aux déversements d'hydrocarbures dans les zones de gestion des pêches considérées. Ces connaissances sont d'un intérêt majeur pour mettre en œuvre des plans de surveillance et de prévention spatialisés appropriés. Notre zone d'étude comprend les eaux marines Indonésiennes. Décret Ministériel numéro 18 de 2014, ils étaient divisés en 11 Zones de Gestion des Fisheiries, à savoir : (1) FMA 571 pour le détroit de Malacca et la mer d'Andaman, (2) FMA 572 pour l'Océan Indien de Sumatera Ouest et de 3) FMA 573 pour l'océan Indien du sud de Java, sud de Nusa Tenggara, mer de Savu et mer de Timor Est, (4) FMA 711 pour le détroit de Karimata, la mer de Natuna et la mer de Chine Sud (5) FMA 713 pour le détroit de Makassar, Bone Bay, la mer de Flores et la mer de Bali, 7 FMA 714 pour la baie de Tolo et la mer de Banda, 8 FMA 715 pour la baie Tomini, la mer de Maluku, la mer de Seram et la baie Berau. 9) FMA 716 pour la mer de Sulawesi et au nord de l'île Halmahera, (10) FMA 717 pour la baie de Cendrawasih et l'océan Pacifique et (11) FMA 718 pour la baie d'Aru, la mer Arafuru et la mer de Timor Est. Chaque FMA comprend des zones marines protégées.

Les facteurs suivants considérés comme des possibles proxy pour les occurrences de déversement d'hydrocarbures :

- le nombre d'accidents de navires ;
- le nombre de navires ;
- l'emplacement de toutes les plateformes pétrolières dans la mer d'Indonésie ;
- l'emplacement des raffineries de pétrole en Indonésie ;
- la liste des ports ayant des activités de distribution de pétrole ;
- la zone totale de détection des déversements d'hydrocarbures dérivés des SAR.

Dans le but d'évaluer l'impact des pollutions par déversement de pétrole en termes d'impact environnemental, social et économique, nous avons collecté les informations suivantes pour chaque FMA et MPA :

- le nombre d'espèces pour les groupes d'espèces importants (c'est-à-dire les poissons des récifs coralliens, les cétacés, les tortues de mer, les mangroves, les algues, les dugongs et les oiseaux marins) ;
- le nombre d'MPA et la zone associée ;
- les productions totales de poisson et les valeurs économiques associées ;
- le nombre de services de tourisme ;
- le nombre de centres d'étangs de sel ;
- le nombre de navires de pêche en operationel ;

Nous calculons d'abord les indices de risque de déversement d'hydrocarbures pour différentes sources de déversement . Nous définissons ensuite les indices de vulnérabilité par rapport à impacts écologiques et socio-économiques. Ces indices sont utilisés pour définir global indices de risque (GRI) au niveau de FMA. Apres, nous explorons une analyse de vulnérabilité à des échelles spatiales plus fines sur l'MPA.

L'identification des indices de risque utilise le pourcentage de risque moyen. Le pourcentage de risque moyen est le pourcentage de risque de la variable critique divisé par le nombre de variables critiques considérées à l'échelle nationale. Dans le calcul du pourcentage de risque de la variable critique, nous avons envisagé d'utiliser le facteur de pondération pour certaines variables. Par exemple, pour calculer le pourcentage de risque lié aux accidents de navires, nous avons utilisé trois facteurs de pondération pour trois classes différentes de ITOPF. Pour certaines autres variables pour lesquelles nous n'avons pas eu suffisamment d'informations détaillées, nous avons considéré ne pas utiliser le facteur de pondération.

En plus de l'analyse d'évaluation des risques au niveau FMA ci-dessus, nous avons effectué une analyse au niveau de l'MPA. Ces échelles spatiales plus fines préconisent également d'envisager des échelles temporelles plus fines, car les conditions météorologiques (métocéaniques) peuvent grandement affecter la dynamique d'un déversement d'hydrocarbures et son impact régional sur l'environnement côtier et extracôtier et les activités humaines associées. Pour les

différentes sources de déversement de pétrole identifiées ci-dessus, nous visons à évaluer leur impact potentiel sur les MPA et comment cet impact peut évoluer en relation avec les variabilités des conditions métocéaniques.

Le schéma proposé a exploité Mobidrift développé par CLS France pour simuler la dérive d'un déversement d'hydrocarbures conditionnellement à des conditions métocéaniques données. Nous avons considéré le paramètre suivant : un facteur de dérive du vent Cw = 0,03, un facteur de dérive du courant de surface de la mer Cc = 1,0 et 500 particules. Nous avons effectué des simulations de dérive pour une durée comprise entre 3 et 6 jours de janvier à décembre avec un pas de temps de 6 heures. En tant que source de déversement de pétrole, nous pourrions considérer les différentes sources. Ici, nous avons utilisé la carte de densité du navire comme source de déversement d'hydrocarbures. Nous avons utilisé les conditions météorologiques pour l'année 2015 comme conditions de référence. Pour une simulation donnée, nous avons évalué le nombre de particules entrant dans une MPA.

Concernant les indices de vulnérabilité liés à l'environnement, notre résultat montre que 4 zones, soit FMA 573, 711, 717 et 718, ont été classées comme zones à haute vulnérabilité. FMA 712, 715 et 716 impliquaient un niveau moyen, FMA 713 et 714 seulement un niveau bas, et FMA 571 et 572 un niveau minimal. D'autre part, concernant impacts socio-économiques, les FMA 711, 712 et 713 (mer de Natuna, mer de Java et détroit de Makassar) représentent un niveau de risque élevé. La FMA 717 représentait un niveau de risque minimal et les 7 FMA restantes un niveau à faible risque.

Les valeurs GRI pour toutes les FMA indiquent clairement les zones FMA 711 et 712 en tant que zones à haut risque. L'FMA 711 est la plus vulnérable car elle présente un risque élevé pour les différentes sources de déversement d'hydrocarbures et présente également une grande vulnérabilité en termes d'impacts environnementaux et socio-économiques. En revanche, la FMA 712 décrit un niveau de vulnérabilité élevé en termes de facteurs socio-économiques mais seulement un niveau de vulnérabilité moyen en termes d'impact environnemental. Deux zones, FMA 573 et 713, sont classées comme zones à risque moyen. FMA 573 implique un impact à haut risque en ce qui concerne les facteurs environnementaux mais un niveau à faible risque en termes d'exposition aux déversements d'hydrocarbures et d'impacts socio-économiques. La FMA 713 décrit un niveau de risque / vulnérabilité élevé en termes d'impacts socio-économiques et d'exposition aux déversements d'hydrocarbures, mais un niveau de risque moyen concernant

les facteurs environnementaux. Dans l'ensemble, les autres FMA semblent relativement sûres en ce qui concerne la pollution par les hydrocarbures, avec un niveau de risque faible pour les FMA 571 et 715 et un niveau de risque minimal pour les FMA 572, 714, 716, 717 et 718.

A la base de l'analyse FMA ci-dessus, nous avons effectué une analyse de vulnérabilité à des échelles spatiales et temporelles plus fines dans les deux FMA à haut risque, à savoir FMA 711 et 712. Pour FMA 711, nous avons effectué des simulations Mobidrift avec 107 points de source que nous avons obtenus à partir de la carte de densité. Nous présentons des simulations avec deux durées (3 et 6 jours) pour différentes conditions métocéaniques de janvier à décembre. La variabilité saisonnière de ces conditions metocéan affecte clairement la dérive du déversement de pétrole et ses impacts sur les MPA proches. Nous présentons également des exemples de simulation pour FMA 712, qui impliquent 357 points source de déversement d'hydrocarbures. Nous avons exécuté la simulation avec des durées de 3 jours et de 6 jours pour les conditions météorologiques de janvier à décembre.

La simulation montre que MPA 711.7 est la plus vulnérable tout au long de l'année. Cette AMP est plus vulnérable lors de la mousson NordOuest et Transition 2. Par conséquent, la surveillance devrait être renforcée dans cette région pendant cette période. MPA 711.6 et MPA 711.9 sont d'autres MPA vulnérables dans la zone FMA 711. Le MPA 711.6 a été menacé sur la mousson du NordOuest et le MPA 711.9 sur la mousson du SudEst. Dans un zone de l'FMA 712, l'MPA 712.1 était l'MPA la plus menacée par le déversement d'hydrocarbures. Cette MPA est plus vulnérable sur la mousson de SouthEast, Transation 1 et Transation 2. MPA 712.1 a besoin de plus de surveillance sur la mousson de la Transation 2 car à cette période les deux déversements de pétrole provenant de la simulation de 3 et 6 jours ont été menacés dans cette zone. Les autres MPA qui ont besoin d'attention sont MPA 712.3 et 712.6. Le MPA 712.3 a été menacé sur la mousson NordOuest et le MPA 712.6 sur la mousson Transition 2 et SouthEast.

Dans FMA 712, le niveau de risque est le plus élevé. La mer de Java joue un rôle important en termes d'activités maritimes et de production halieutique, tandis que le trafic maritime est dense et que de nombreuses activités qui sont liées à la production et à la distribution de pétrole et de gaz. Les îles Seribu (MPA 712.1) au nord de Jakarta sont les MPA les plus menacées. Cette MPA est menacée presque toute l'année de janvier à décembre avec le niveau de risque le plus élevé pendant la mousson du SudEst de juin à août. Située au nord de Semarang (capitale

de la province centrale de Java) avec un trafic maritime dense, Karimunjawa (MPA 712.6) est la deuxième MPA la plus menacée de la FMA 712 mais avec un niveau de risque faible.

Dans l'FMA 711, l'MPA les plus vulnérables sont les îles Batam (MPA 711.7 et 711.6) et Îles Tambelan et Karimata (MPA 711.9 et 711.11). Les îles Batam sont vulnérables en raison de leur emplacement près des ports de Singapour qui ont une densité de trafic maritime très élevée. L'amélioration de la surveillance devrait être effectuée sur ces îles. La surveillance et l'atténuation devraient être axées sur la période de mousson du NordOuest de décembre à février et sur la période de transition de mars à mai. Les autres MPA de la FMA 711 qui requièrent une attention particulière sont les MPA des îles Tambelan et Karimata situées dans le détroit de Karimata. Les îles Tambelan et Karimata sont proches des grandes voies maritimes. Pour cette MPA, l'accent devrait être mis sur la période de juin-août (mousson SudEst), avec une menace principale liée à des dérives relativement plus longues (durée de 6 jours).

Conclusion and Discussion

La surveillance des déversements d'hydrocarbures dans les mers indonésiennes est l'un des principaux objectifs du projet INDESO. Dans ce cadre, cette thèse visait à proposer de nouvelles méthodologies et analyses. Cette thèse comportait deux contributions principales. La première contribution portait sur la récupération des paramètres de dérive des déversements d'hydrocarbures à partir d'une analyse conjointe des observations SAR d'un déversement d'hydrocarbures et des résultats d'un modèle de transport de déversement de pétrole lagrangien. Nous avons appliqué la méthodologie proposée sur le plus grand accident de déversement d'hydrocarbures en Indonésie, à savoir Montara. La deuxième contribution a été l'évaluation globale du risque de déversement d'hydrocarbures en Indonésie. Nous nous sommes concentrés sur la zone de gestion des pêches de l'Indonésie pour soutenir le développement durable de la marine et des pêches. Dans cette analyse, nous avons proposé une méthodologie qui a pris en compte le déversement de pétrole provenant de différentes sources et leurs impacts non seulement sur l'environnement, mais aussi sur les perspectives sociales et économiques. Pour l'évaluation de la vulnérabilité des zones marines protégées à la pollution par les hydrocarbures, nous avons également exploité le modèle de la trajectoire des déversements d'hydrocarbures.

L'étude sur l'assimilation des images SAR dans les modèles de trajectoires de déversements d'hydrocarbures ouvre de nouvelles voies de recherche pour la surveillance opérationnelle des

déversements d'hydrocarbures par satellite. Les travaux futurs étudieront plus avant l'assimilation des paramètres de fuite d'huile à partir d'observations multi-date ainsi que d'autres configurations de fuites d'huile, telles que les rejets illégaux d'huile provenant des navires et des suintements d'huile naturelle. Les deux nouvelles applications seraient d'un intérêt majeur dans le cadre du projet INDESO. L'analyse du risque de déversement d'hydrocarbures a montré que plusieurs zones sont classées comme zones hautement vulnérables. Dans ces zones à haut risque, les données océanographiques telles que la bathymétrie et les informations sur les courants, les vents et les marées devraient être mieux préparées et préparées à l'avance en vue d'être pleinement opérationnelles en cas de désastres pétroliers le plus souvent inattendus. On peut envisager de développer et de paramétrer des modèles de dérive des déversements d'hydrocarbures spécifiques aux zones pour les zones à haut risque. En ce qui concerne la mise en œuvre des outils de surveillance des déversements d'hydrocarbures proposés, une question critique si la disponibilité des données à l'appui. Dans notre étude, nous avons calculé les indices de risque de déversement d'hydrocarbures à partir de simulations de dérive de pétrole en utilisant uniquement les positions des navires comme sources. Les informations sur les positions des plates-formes pétrolières amélioreraient encore l'analyse du risque de déversement d'hydrocarbures et la cartographie de ce risque à l'échelle nationale et régionale. La simulation de déversement d'hydrocarbures sera meilleure compte tenu du processus d'évaporation et d'émulsification. Dans le futur, la simulation utilisant le réglage 3D permettra d'identifier plus clairement l'impact du déversement d'hydrocarbures sur l'environnement marin. L'expertise en modélisation des trajectoires d'objets et en analyse d'images satellitaires pour les applications marines reste assez limitée en Indonésie. Cette thèse peut être utilisée pour soutenir le fonctionnement d'Indeso en particulier pour la surveillance des déversements d'hydrocarbures en territoire maritime indonésien. Notre travail peut être utilisé dans l'application de la loi, la réponse et la planification de l'atténuation. À l'avenir, on peut s'attendre à ce que la pollution marine attire de plus en plus l'attention des parties prenantes, car les activités maritimes et de pêche ont tendance à être les plus importantes sources de croissance d'économie. La pollution marine ne se limite pas à la pollution par les hydrocarbures. Les océans du monde font maintenant face à des montagnes de débris. Le territoire maritime de l'Indonésie est l'un des plus touchés. L'Indonésie est également soupçonnée d'être l'un des plus grands pollueurs marins du monde. À cet égard, INDESO est un outil essentiel pour soutenir le gouvernement de l'Indonésie dans la lutte contre ce problème. Avec les

données d'observation complètes acquises au sein d'INDESO ainsi que les outils de modélisation et d'analyse mis en œuvre sont manifestement d'un grand intérêt pour résoudre ce problème. Par exemple, on pourrait combiner la détection aux débris marins aux modèles de trajectoires de dérive pour prévoir impact de la pollution par les débris marins sur le écosystèmes côtiers indonésiens. La détection des débris marins est un véritable défi car les débris sont relativement petits et se retrouvent principalement dans le sous-sol. De nouvelles solutions et un plan opérationnel doivent ensuite être développés en réponse aux besoins opérationnels.

Chapitre 1

Introduction

1.1 Context of the thesis 2

1.2 A brief review of INDESO Project 4

1.3 Thesis motivation and outline 6

1.1 Context of the thesis

Indonesia is one of the biggest archipelago country with more than 17000 islands. It is more than 4 000 km wide from West to East with various resources from its ocean. This marine ecosystem has a major threat coming from oil spill. In the ocean and coastal waters, there are two sources of oil spill, it may result from intentional or unintentional releases. The example of intentional releases is oil spill coming from operative discharges by shipping. There are some possibilities that the discharge are legal but in most cases they are illegal. Indonesia has three major sea lanes that connect Indian Ocean, Pacific Ocean and South East China Sea with high density of sea traffic. The high sea traffic potentially becomes the source of intentional oil spill.

On the unintentional side, oil spill accident such as the one occurring at the Montara platform is one of the most serious example of unintentional spill. Montara oil leakage was happened on 21 August 2009 for the duration 73 days with estimated 400 barrels of crude oils lost per day. The Montara case became complicate since the location of the oil rig is not in the Indonesian waters so there was a dispute related to the claim whether the oil spill impacted Indonesia water territory. We will further discuss the Montara oil spill in the Chapter 3

Beside oil rig platform accidents, other common pollution incidents occur during terminal operations when oil is being loaded or discharged. Some cases happened in North and South of Java. Due to the increasing concerns of environment protection for sustainable development, the Government of Indonesia in cooperation with Government of France developed an ocean observation system with seven pilot applications, i.e. combating illegal fishing, monitoring fish stock, monitoring coral reef, oil spills monitoring, shrimp and seaweed farming, and integrated coastal zone management and mangrove. This system is integrated in the operational oceanography systems within the project of Infrastructure Development of Space Oceanography (INDESO).

The context of this thesis is in the frame of INDESO project particularly in the monitoring of oil spill in the Indonesian seas. In this thesis, we will first provide a brief overview of INDESO project, including the observation of oil spill using Synthetic Aperture Radar (SAR) images. In operational oceanography system, earth observation satellite data and in situ observation are eventually processed with model in order to get the information needed. In the INDESO oil spill application, space-borne SAR images are used to cover large ocean areas to look for possible oil pollution. Its main advantage compared to space-borne optical sensors is its capability to

monitor the ocean day and night, even in cloudy condition. However, in SAR observation, the wind is essential as it influence sea surface roughness and and may prevent to detect an eventual oil spill.

Apart from the detection and monitoring system, the trajectory drift model is essential in the operational system for oil spill forecast. Wind and surface current data from the operational oceanography system are used as inputs of the model. We assimilate the detection of SAR and the trajectory model using a new proposed methodology. As the test case, we applied this method on the Montara event. We optimized the model using variation of starting date of leakage, duration of leakage and value of coefficient wind and current. The result of assimilation of SAR detection and the trajectory model is important in the preparation and mitigation during oil spill crisis to reduce the oil spill impact to the ecosystem.

Meanwhile, the analysis of oil spill risk by taking into account the environment and socioeconomic factors on the Indonesia's Fisheries Management Areas (FMA) and Marine Protected Areas (MPA) is important as well. The characteristics of the Indonesian archipelago country may render this analysis quite complex.

The main objective, motivation and outline of this thesis are introduced in 1.3.

1.2 A brief review of INDESO Project

The Ministry of Marine and Fisheries (MMAF) in Indonesia is the government organization which is responsible for the management of marine and fisheries resources policies based on the sustainable development as stated in the Law No.32/2014. Indonesia has various natural resources which one of them is fisheries. Fisheries are a key activity in rural areas and can generate local economic growth. Meanwhile, Indonesia is highly vulnerable to human activities processes leading to the degradation of marine ecosystems like voluntary and accidental oil pollutions. The negative extensive impact of oil spill may affect not only the environment but also the human life from social and economic aspects. Oil pollutions easily destroy mangrove ecosystems, coral reef development and fish stock and also threat the society and economy since fisheries contribute extensively to the total of food agriculture.

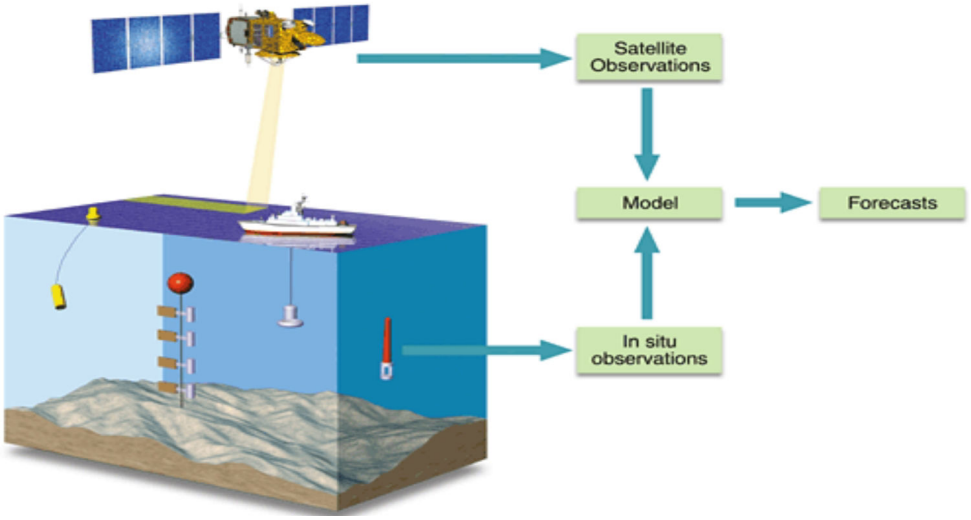

FIGURE 1.1 – Operational Oceanography Schema, Courtesy : INDESO project

The increase of oil spill events makes growing concerns on the protection of marine and fisheries. Some examples of oil spill accidents like the Prestige wreck and Deepwater Horizon at international level and Montara case at national level imposed the need to creating operational monitoring and forecasting center for oil spill. Oil spill monitoring system is one of the application of operational oceanography system that was developed in the INDESO project. Figure 1.1 shows the general system of operational oceanography. In this system, the satellite observation

and the data from *in situ* observation are combined with the model of trajectory of oil spill. The combination of operational oceanography systems and oil-spill models has been demonstrated as a very encouraging measure to minimize oil-spill impacts [2]. Using this combination, comprehensive information can be provided to predict and mitigate the oil spill.

1.3 Thesis motivation and outline

Despite the operational SAR-based detection system set up in INDESO system, there is a need for more supporting information on the mitigation planning. To prevent the impact of oil spills in the environment, there is a crucial need to continuously monitor the ocean and to use forecasting systems to predict its drift. The routinely information based on operational oceanography from observations and models have to be combined with trajectory model of oil spill in order to get the evolution position of oil spill. In this work, the oil transport on the sea surface is modeled by a Lagrangian 2D model named Mobidrift.

In this context, we used the case of Montara as a study case to implement an assimilation scheme of SAR-based detection within the drift model. To assimilate the SAR image, we propose a methodology based on a Level Set approach. We compare the contour of oil spill from the SAR detection with the contour of particles simulated by the trajectory model. With this comparison, the objective is to determine or confirm the source of pollutions. The aim is also to further understand the drift phenomena, and at least tune some factors such as the weighting of wind and current effects within the total advection, the time and duration of leakage.

Furthermore, to support the sustainability development of marine and fisheries we need to assess the risk linked to oil spill. Indonesia has unique water territory since it is an archipelago's country. The Government of Indonesia divided its Economic Exclusive Zones (EEZ) into 11 Fisheries Management Area (FMA). Each FMA has different characteristics. We analyze the risk of oil spill in 11 FMA in Indonesia from different potential sources of pollution. In this work, we synthesize all related reports of different institutions to find the characterized data of important factors with its variables that determine the risk magnitudes. Five variables are selected related to the occurrence probability of oil spills, such as the numbers of ship accidents, oil offshore platform and oil refineries facilities, maritime traffic density, ports with oil transportation activities, and oil spill polygon detected by SAR in INDESO systems. In ecological factor, we choose two variables related (i.e number of important species and area of MPA). Five variables related to impact of oil spills in social economic factor are selected (i.e number of marine capture fisheries production and their economic value, number of salt production center area, number of fishing boat operated and number of water tourism service). We calculate the general vulnerability index from those three factors. Then, we categorize the risk of oil spill on each zone in four

categories (minimal, low, medium, and high). For the zones categorized in high risk, we simulate the oil spill from different source points for different seasons and durations in order to analyze in details the risk. With this analysis at least can be one of contribution on the national policy development on the oil spill mitigation planning.

With respect to the content of our research and for the sake of clarity, this thesis is organized in five chapters : Introduction, Oil Spill Monitoring in Indonesia, Oil Spill Parameter Retrieval, Oil Spill Risk Assessment of Indonesia's Fisheries Management Area and Conclusions/Perspectives.

Out of this first Introduction Chapter, **Chapter 2** provides a brief overview of oil spill monitoring in the Indonesian waters. We will start by a review of the state-of-the-art concerning oil spill observation by satellite remote sensing, with a focus on SAR imagery. The current situation of oil spill observation system in Indonesia will be discussed further including the detail system of INDESO. We will also exposed the review of state-of-the-art of sea surface transport models and the exploration of Lagrangian 2D model that is used in our trajectory model. We will explore the CLS model so called Mobidrift and its application on Indonesian oil spill case.

Chapter 3 will present our first work on the oil spill parameter retrieval. Chapter 3 proposes a method based on Level Set to assimilate the SAR images and the simulation of 2D Lagrangian model. By optimizing the factor of wind and current coefficient, start and duration of leakage, we will attempt to backtrack the SAR-observed oil spill up to its origin.

Chapter 4 is the second contribution from this work. In the Chapter 4, we will expose the risk analysis of oil spill in Indonesia. We will synthesize various reports from different institutions and calculate the risk of oil spill from environmental, social and economic perspectives. Using the oil spill trajectory model, we analyzed the oil spill risk of marine protected area in the most vulnerable fishing management area.

Chapter 5 will conclude this PhD thesis and will provide some perspectives for future work.

Chapitre 2

Oil Spill Monitoring in Indonesia

2.1 Description of Indonesian waters 10
2.1.1 General aspects of ocean circulation in Indonesia 10
2.1.2 Main issue of Indonesia Marine and Fisheries 11
2.2 Oil spill monitoring as conceived by the INDESO system 18
2.2.1 Operational 18
2.2.2 INDESO sites for the oil spill monitoring 19
2.2.3 System design 21
2.3 Detection of oil spill using EO-based imagery 24
2.3.1 Spaceborne/airborne remote sensing 24
2.3.2 Detection of oil spill based on SAR imagery 27
2.4 Oil spill transport model 31
2.4.1 Introduction 31
2.4.2 Lagrangian 2D Trajectory Model 32
2.4.3 Mobidrift 33
2.4.4 Application of Mobidrift in Indonesia's Oil Spill Trajectory 34
2.5 Conclusion 37

2.1 Description of Indonesian waters

Indonesia is located in Southeast Asia between 6 ° N and 11° S in latitude and 95° and 141° in longitude. It is located between two oceans and two continents, Pacific Oceans in the east and Indian Ocean in the West and South, Asia continent in the North and Australia in the South. Indonesia sea territorial is combined between shallow and deep water. The bathymetry of Malaca Strait, Natuna Sea and South China Sea, Java Sea and Kalimantan Strait are not exceed 200 meters. Meanwhile to the East, Irian Jaya/Papua, the Aru islands, the islands group of Nusa Tenggara, Sulawesi, Maluku and Halmahera are surrounded by deep seas. Many places in this area can reach until 5,000 meters depth.

2.1.1 General aspects of ocean circulation in Indonesia

Wind and ocean current are important factors to determine the direction of trajectory particles of oil spill. Ocean current of the Indonesian archipelago is characterized by strong seasonal variations in the upper oceanic circulation. The circulation is influenced by monsoonal winds. Meanwhile in the wind distribution, the variation of seasonal solar heating over the continents of Asia and Australian drives the monsoons. This phenomena changes wind direction twice a year [3]. Indonesia has tropical climate with two typical monsoons i.e southeast monsoon that prevails from June to August and northwest monsoon from December to February with its first transition period from September to November, and second transition from March to May [4]. Southeast monsoons tend to produce upwelling. This upwelling cools the waters and increases the content of Chlorophyl-A, which is nutrients for fishes. The Southern coast of Java is very productive in this season. Meanwhile, the inverse conditions happen during the northwest monsoons.

Besides upwellings that are detected in some areas such as West Sumatra, Makassar Strait, South Java, South Bali, in the Banda and Arafuru Seas, and in the Sunda Strait, there is another important coast and ocean process in the Indonesian waters that influences the fisheries, the so-called Indonesian Through Flow (ITF). Many researches [5], [6], [7], [8] and [9] worked on these upwelling and ITF phenomena. The ITF flows from the Pacific Ocean to the Indian Ocean through Indonesian waters because of the global weather patterns. This phenomenon influences not only the climate system but also marine productivity and pelagic fish migration. Other

phenomenon influencing marine productivity is the Sea Surface Temperature (SST) anomalies due to El Niño [10]. El Niño produces abnormal upwelling developments in some specific areas.

2.1.2 Main issue of Indonesia Marine and Fisheries

Oceans play important role for Indonesia economic development. Indonesia sea water is one of the primary route to connect the world for trade and commerce. It plays important role in social economic development since most of population live in coastal areas. The effects of development such as urbanization, pollution, oil spills, accidents, etc push the negative impacts to the community.

In the marine and fisheries, fluctuations in fish stocks and the preservation of natural habitats and resources are urgent problems. The Illegal Unreported and Unregulated (IUU) fishing is one of most serious problems. Oil pollution is also a serious threat, affecting mangrove ecosystems, coral reef development and even fish stock. The government of Indonesia in particular Ministry of Marine and Fisheries (MMAF) needs to develop efficient policy to tackle these issues affecting both the society and the economy. To manage these problems, ocean forecasting systems and operational services are needed to produce information to monitor, and eventually mitigate them.

Oil spill is one of the main sources of marine pollution in Indonesia. Some regions are very fragile to oil spill, i.e. Malacca Strait and Riau Islands water. For the first area, this is due to its high density of tanker traffic. Local media reported several incidents on the coasts of Batam and Bintan islands. These incidents impacted the local tourism and fisheries. Until now, in Batam and Bintan islands, the causes of several pollution incidents are still unknown. One of the largest accidents in Malacca Strait happened in 1997. A collision between tanker Evoikos and Orapin Global spilled more than 20.000 tonnes of oil to Indonesian and Malaysian waters. Riau Islands water has many activities linked to Oil and Gas (O&G) exploitation and refinery. Besides oil spill, waste from oil refinery, offshore exploration and shipping activities are the other sources of pollution in Indonesia seas. Shipping activities contribute to pollution from its ballast water, domestic waste and oil waste from tank cleaning.

Related to the water pollution, Indonesia has some regulations. Ministry of Environment Decree on No. 51 Year 2004 regulates the marine water quality standard and President Regulation No. 109 Year 2006 is more specified on Oil Spill on Sea National Contingency Plan. On

the Ministry of Environment Decree on No. 51 Year 2004, there are several specified parameters for marine water quality standard. It depends on the type of the uses i.e port, marine tourism, and marine biota. The President Regulation No. 109 Year 2006 states that when oil spill happens in the sea, the owner of the ship/operator and the highest leader in the O&G company oil exploitation have the responsibility to compensate the State for the recovery of oil, conduct the environmental assessment, take care of the community losses and all environmental damages.

Besides the two aforementioned regulations, Indonesia has ratified and adopted some international standards, instruments, conventions and protocols into laws and regulation. Some laws and regulations related to the oil spill are the Presidential Decree No.19/1978 on Ratification of International Convention on the Establishment of an International Fund for Oil Pollution Damage and the Presidential Decree No.46/1986 on Ratification of International Convention for the Prevention of Pollution from Ships.

Beside the preparation of law and regulations, Indonesia has carried out a set of exercises on combating oil spill at sea. These exercises have been mostly conducted with international cooperation. Japan and 5 ASEAN (Association of Southeast Asian Nations) countries (Brunei, Malaysia, Indonesia, Singapore and Philippines) have actively cooperated to enhance the oil spill response and preparedness with Indonesia.

In this thesis, we will focus on the issue of ocean pollution particularly pollution from oil spills. We will analysis the oil spills related to marine and fisheries in the frame of INDESO project systems. Later in the Chapter 3, SAR-detected oil spill will be assimilated with an oil transport model. A new methodology will be proposed and applied on case of the large oil spill accident. Then, in Chapter 4 we will conduct the assessment of oil spill risk in the Indonesia sea water territory related to the marine and fisheries resources.

2.1.2.1 Indonesia as archipelago, marine and fisheries are key activities

MMAF has responsible for the marine and fisheries development in Indonesia. Definition of marine and fisheries is described on Indonesia Law No. 45 year 2009 and No.32 year 2014. Based on Law No.32 year 2014, marine is all activities that related to the ocean from the seabed, water column until its surface including the coastal and small islands. Definition of fisheries is all activities that related to the management and utilization of fisheries resources and its environment, starting from pre-production, production, processing, until marketing that all

combined in the one comprehensive business system.Fish in this definition is all the organisms that parts or all of its life cycle were happened in the aquatic environment. With this definition sea weed and coral are also categorized as fish.

Fishery contributes to 25% of total of food agriculture. Within the archipelago, fisheries play an important role in employment and national food security, since fishery products are generally consumed by poor households and other social communities. Based on data from MMAF, marine capture fisheries production in the 2005-2014 period ranges from 4,408,499 tonnes in 2005 to 6,037,654 tonnes in 2014. The catch production in 2014 was :

- 489,920 tonnes in Malacca Strait and Andaman Sea (8.11%),
- 602,148 tonnes in Indian Ocean of Western Sumatera and Sunda Strait (9.97%),
- 459,749 tonnes in Indian Ocean of Southern Java, Southern Nusa Tenggara, Sawu Sea, and Western Timor Sea (7.61%),
- 665.754 tonnes in Karimata Strait, Natuna Sea and South China sea (11.03%),
- 1,081,178 tonnes in Java Sea (17.91%),
- 750,377 tonnes in Makassar Strait, Bone Bay, Flores Sea and Bali Sea (12.43%),
- 604.515 tonnes in Tolo Bay and Banda Sea (10.01%),
- 482.035 tonnes in Tomini Bay, Maluku Sea, Halmahera Sea, Seram Sea and Berau Bay (7.98%),
- 327.364 tonnes in Sulawesi Sea and Northern of Halmahera Island (5.42%),
- 161.496 tonnes in Cendrawasih Bay and Pacific Ocean (2.67%), and
- 413.118 tonnes in Aru Bay, Arafuru Sea and Eastern of Timor Sea (6.84%).

Based on data from MMAF Indonesia in 2014, almost all of the demersal fishes were caught in Java Sea (20.19%) and Karimata Strait, Natuna Sea and South China sea (14.26%) while the highest production of crustacean was found in Java Sea (25.51%). The highest production of big pelagic fish was in Tomini Bay, Maluku Sea, Halmahera Sea, Seram Sea and Berau Bay (13.51%), followed by Java Sea (12.46%), and then Sulawesi Sea and Northern of Halmahera

Island (12.34%). While, the small pelagic fishes mostly caught in Java Sea (19.48%), in Makassar Strait, Bone Bay, Flores Sea and Bali Sea (13.91%), and Tolo Bay and Banda Sea (12.14%). We will discuss further this production related to the oil spill risk analysis on Chapter 4.

2.1.2.2 Marine and fisheries biodiversity

Indonesia is located on the center of region with world's highest marine biodiversity known as the "Coral Triangle" [11]. With this opportunity, the MMAF faces a challenging task. It has to develop the policy that ensuring marine resources are used in a sustainable manner. Meanwhile, the values of the marine and fishery sectors should increase with the main objective to improve the life quality of all Indonesian people.

Based on the marine and fisheries biodiversities, Indonesia divided into twelve ecoregions, namely ; Papua, Banda Sea, Lesser Sundas, Sulawesi Sea, Halmahera, Palawan/North Borneo, Western Sumatra, Tomini Bay, Java Sea, Arafura Sea, Southern Java, and Malacca Strait [12]. The main characteristics of these ecoregions are described below :

1. Papua was ranked as the first ecoregion for marine & biodiversity conservation. Papua has the top coral reef biodiversity, in addition to its particular animals such as endemic fishes, whales, turtles or dugongs. Papua holds many unique genetic species compared to other regions in Indonesia.

2. Banda Sea is the 2nd ranked area for marine & biodiversity conservation. It has high diversities for coral reef species as well. In addition, the location of Banda Sea plays a significant role on the life cycles of sea turtle and blue whales. The latter are still categorized as highly endangered cetaceans.

3. Lesser Sunda plays an important role on migration for large marine mammals like cetaceans. It has an important commercial role on big pelagic fishes. Upwelling in this region provides nutrition to the big pelagic fish.

4. Sulawesi Sea/Makassar Strait has an important role in larval dispersal and habitats for the cetaceans. Sulawesi Sea has very high diversity of species.

5. Halmahera is a region connecting Sulawesi and Papua. Because of its location, Halmahera is the habitat for a unique biodiversity since the fauna in this region is mixed between Asian and Australian continents.

6. North Borneo region is located between Indonesia, Malaysia and Philippines. It has mangrove forests and seagrass which is the habitat for the dolphins, seabirds and sea turtles.

7. Western Sumatra is the habitat for the six sea turtles species that are found in Indonesia. Even the biodiversity data deficient for this region, Western Sumatra were noted having wide range of reef.

8. Tomini Bay in Northeast Sulawesi region particularly in Togean Islands National Marine Park has high biodiversity and endemic taxon.

9. Java Sea has lesser marine species compared to other regions of Indonesia. This region is relatively disturbed with anthropogenic activities. However, this region is a very important habitat for Green and Hawksbill turtles. Mangroves found in this ecoregion are the habitats of seabirds when they migrate to the eastern of Sumatera.

10. Arafura Sea has low degree in reef biodiversity. However, this region holds the largest mangrove in the world, which is in the south of Papua. This mangrove is an important habitat of threatened seabirds, dugongs and sea turtles. Whale sharks, coastal cetaceans and sawfish are found in this ecoregion.

11. Southern Java has less biodiversity compared to the Lesser Sunda and Western Sumatera. With the impact of rough sea condition, there are few coral reefs. Fishing activities are limited. Nonetheless, this region is the nest habitat for sea turtles, and mangroves remain an important habitat for seabirds.

12. Malacca Strait is considered as the lowest priority for marine conservation. Its shallow water characteristic is an important habitat for many seabirds. The coral reef in this region has been highly impacted by human activities such as shipping traffic. Many oil spill accidents and pollutions from ship occurred in this region.

Some marine and coastal environments in Indonesia are in very critical conditions for their sustainable uses and conservations. The protection of this environment is maintained for securing livelihoods, fisheries and food resources, and biodiversity conservation. Marine, coastal, and estuarine protected areas range from small, locally managed and enforced fishery reserves (also known as no-take ecological reserves) to larger national marine parks that are zoned for multiple use. Several types of coastal and marine conservation management exist in Indonesia :

1. Marine National Park, managed by the Ministry of Forestry
2. National Coastal Park managed by the Ministry of Forestry
3. Local Marine Conservation Area managed by the Ministry of Marine and Fisheries
4. Fish Sanctuary managed under co-management of International Donor
5. Marine Protected area managed under community based approach of International Donors
6. "Sasi, awig-awig, panglima laut" managed by communities based of local people

MMAF as a responsible institution in marine together with People's Representative Council have developed some acts and regulations to protect the environment. One of the example is Act no. 7/2007 on Management of Coastal Zone And Small Island. Furthermore, there is the Presidential Decree No.32/1990 that regulates the Conservation Area Management in Indonesia.

Marine Protected Area (MPA) is one of key tools on the national marine and fisheries planning. Development of MPAs is important to support sustainable development on MMAF's national objective. On the development of MPAs, MMAF has been also actively supported by the provincial and regional governments.

In the analysis of oil spill risk later in the Chapter 4, we used this biodiversity data to calculate the cost of oil spill related to its environmental impact. We will analyze the most vulnerable MPAs in the zone of Fisheries Management Area (FMA).

2.1.2.3 The management of marine and fisheries resources is highly complex, becoming a major issue for the country

A comprehensive data collection and information system on key aspects of population, development and resource linkages that have implications for environmental quality must be developed to support planning, implementation and management, and evaluation of, as well as research on, population and sustainable development programs. For this reason, Indonesia government uses Fisheries Management Area (FMA) to support the management of marine and fisheries. The Ministerial Regulations No. PER.18/MEN/14 mentions that the Indonesian marine waters are divided into 11 FMAs, namely : (1) Malacca Strait and Andaman Sea, (2) Indian Ocean of Western Sumatera and Sunda Strait, (3) Indian Ocean of Southern Java, Southern Nusa Tenggara, Sawu Sea, and Western Timor Sea, (4) Karimata Strait, Natuna Sea and South China Sea,

(5) Java Sea, (6) Makassar Strait, Bone Bay, Flores Sea and Bali Sea, (7) Tolo Bay and Banda Sea, (8) Tomini Bay, Maluku Sea, Halmahera Sea, Seram Sea and Berau Bay, (9) Sulawesi Sea and Northern of Halmahera Island, (10) Cendrawasih Bay and Pacific Ocean and (11) Aru Bay, Arafuru Sea and Eastern Timor Sea.

Indonesia has a tropical climate, resulting in multi-species catches. There are various demersal and pelagic fish i.e snappers, tunas like skipjack, yellowfin and bigeye, shrimp, squid, etc. Production of marine capture fisheries in 2014 was 6,037,654 tonnes. The catch production was : 1) 489,920 tonnes in Malacca Strait and Andaman Sea (8.11%), (2) 602,148 tonnes in Indian Ocean of Western Sumatera and Sunda Strait (9.97%), (3) 459,749 tonnes in Indian Ocean of Southern Java, Southern Nusa Tenggara, Sawu Sea, and Western Timor Sea (7.61%), (4) 665.754 tonnes in Karimata Strait, Natuna Sea and South China sea (11.03%), (5) 1,081,178 tonnes in Java Sea (17.91%), (6) 750,377 tonnes in Makassar Strait, Bone Bay, Flores Sea and Bali Sea (12.43%), (7) 604.515 tonnes in Tolo Bay and Banda Sea (10.01%), (8) 482.035 tonnes in Tomini Bay, Maluku Sea, Halmahera Sea, Seram Sea and Berau Bay (7.98%), (9) 327.364 tonnes in Sulawesi Sea and Northern of Halmahera Island (5.42%), (10) 161.496 tonnes in Cendrawasih Bay and Pacific Ocean (2.67%), and (11) 413.118 tonnes in Aru Bay, Arafuru Sea and Eastern of Timor Sea (6.84%)

Indonesia fishermen use various fishing gears, being either traditional with sail boats or modern with mechanized gears like trawls, purse seines and longlines. The number of traditional fisherman with non-motorized vessel is still high. On the other side, the number of modern fishing gears tends to grow. In 2014, there are 165 066 non motorized vessels and 238 010 with outboard motor and 222 557 inboard motor.

We will take in our consideration the number of fish production and the number of fishing vessels in each FMA as factors for potential economic and social losses due to an eventual oil spill.

2.2 Oil spill monitoring as conceived by the INDESO system

INDESO system and oil spill monitoring application shall support Indonesian authorities (MMAF, Ministry of Transportation, and Ministry of Environment) in the field of monitoring marine oil spills. As the application was conceived by the project, it is related to the detection of marine oil spills caused by ships and platforms.

The oil leakage can be accidental (vessel crash or platform blow out) or voluntary (vessel bilge water discharge or production water from a platform).

In INDESO, oil spill monitoring application benefits from satellite radar imagery that can be used for effectively detect oil pollutions at sea. Unlike optical sensors, satellite radar imagery is not weather dependent, has night/day observation capacity and has a high resolution capacity. The satellite radar imagery also offers a wide area monitoring which is suitable for the detection of oil films at the sea surface. In INDESO, the global amount of satellite radar images should be shared by the 2 applications which use Radar imagery as input, Oil Spill monitoring and IUU Fishing.

2.2.1 Operational

Since the greatest amount of oil pollution comes from voluntary discharge from vessels, the standard operational scheme shall be a routine monitoring that will offer the necessary mean for continuous and global monitoring. The continuous routine monitoring shall enable to quantify and monitor the level of pollution activities in the targeted areas of interest. When necessary, a reactive monitoring (less than 3 days) for emergency cases such as vessels accidents or oil rigs blow out shall be put in place. Thanks to the satellite receiving station in Perancak, the application shall provide pollution alerts within 2 hours after satellite acquisition to allow an effective use of the data for follow up activities. Delivery timeliness and quality control of the data and reports bring the guarantee of the best service.

Before the operational phase of the application starts, the monitoring strategy had to be defined addressing the following questions : how to optimize acquisitions plans for both routine and reactive oil spill monitoring ? Where, when and how often shall images be taken ? Based on the key inputs of the application : - the areas of interest and their priority have been defined - the amount of unit scenes dedicated to oil spill monitoring has been validated

Once the INDESO system was declared operational, the application has started operating according to scheme below : - Monitoring requirements are translated into acquisition plans and sent to the satellite operating agency. This task is performed by the INDESO operations team on a quarterly basis. The acquisition plan is then available for application users through INDESO Central Information System (CIS) web portal. - Two hours (at the latest) after the time of each unit scene, application users are notified upon the delivery of the oil spill report that is available through INDESO CIS web portal. - On site verifications activities may be organized with Coast Guards patrol vessels for specific occasions (major oil spill or pollution in or near a sensitive area). - Measurements of the level of pollutions are performed periodically based on the accumulation of oil spill reports.

2.2.2 INDESO sites for the oil spill monitoring

Oil spill activities can be monitored in all areas of the Indonesian waters thanks to the coverage of the INDESO satellite receiving station. The Figure below shows the approximate visibility circle of 2500 km radius. Actual visibility circle was determined during the set-up of the antenna.

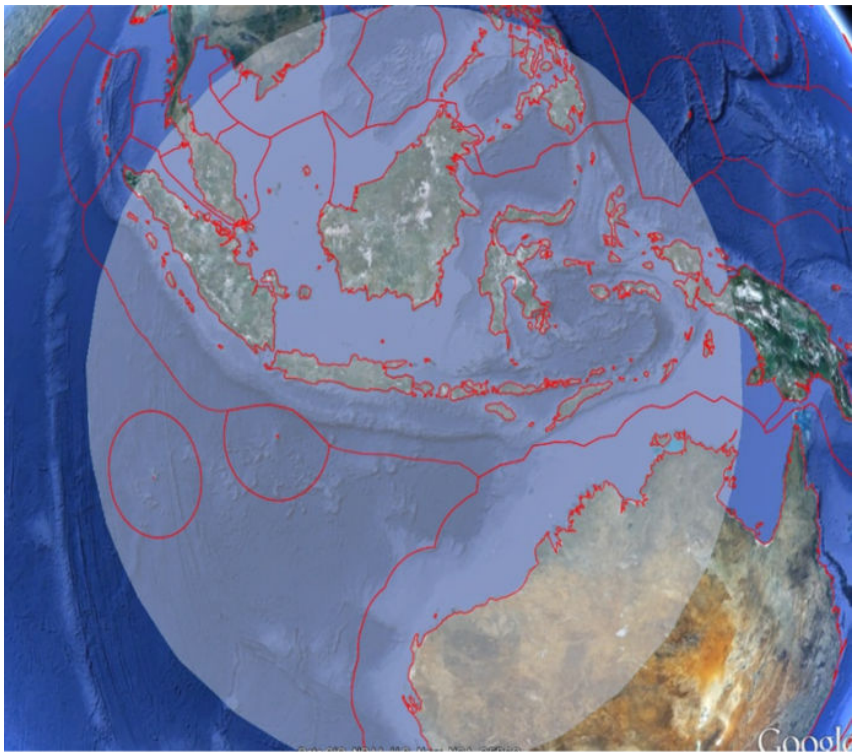

FIGURE 2.1 – Perancak satellite receiving station visibililty circle, Courtesy : INDESO project

Oil Spill monitoring application focus on targeted areas which are heavy density maritime traffic areas and O&G concession areas. On the next figure, primary priority areas are depicted in pink and secondary priority areas are shown in green. Three initial areas of interest were originally defined : Makassar Strait, Malacca Strait and Timor Sea. Some precisions of the areas have been updated during the phase of the project, as follow :

- Primary priority areas : Eastern part of Malacca Strait, Makassar Strait, and Timor Sea
- Secondary priority areas : Western part of Malacca Strait, Natuna Sea, Java Sea

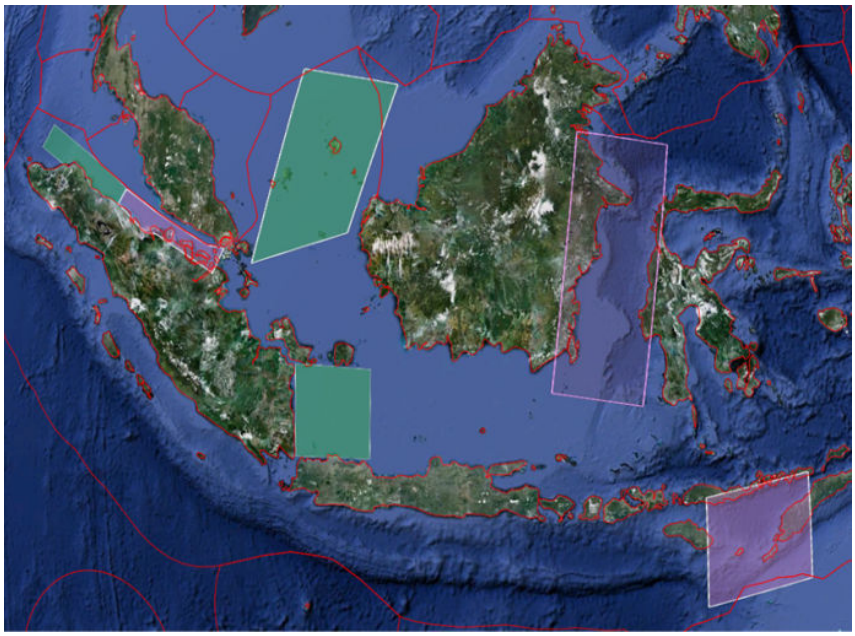

FIGURE 2.2 – Primary priority (purple) and secondary priority (green) priority areas for oil spill monitoring

Area	Priority	Approx. Surface
Eastern Malacca Strait	Primary area	100km x 500km
Makassar Strait	Primary area	960km x 390km
Timor Sea	Primary area	360km x 470km
Western Malacca Strait	Secondary area	100km x 500km
Natuna Sea	Secondary area	750km x 400km
Java Sea	Secondary area	300km x 300km

TABLE 2.1 – Targeted areas for oil spill monitoring

The definition of the areas of interest is a key input for the design of the rationale for the volume of imagery allocated for this application.

2.2.3 System design

The next figure depicts the INDESO sub-systems and the interfaces implemented for the Oil Spill monitoring application : - From the INDESO Core system : the sub-systems of the INDESO Core that are considered are those that interact with the applications users. In this context, the web portal of the CIS (Central Information System) is the only part of the core system that the applications users can see although the Satellite Receiving Station (SRS) and other parts of the CIS are operated by the Perancak team to produce the oil spill reports. - External Data provision : Radar data are provided by satellite operating agency through Radarsat-2 satellite. Meteorological forecast are provided by the National Center for Environmental Prediction (NCEP) - Applications users will interact with the CIS system and more precisely they will use the Maestro web portal to access to the online acquisition planning and to the oil spill report.

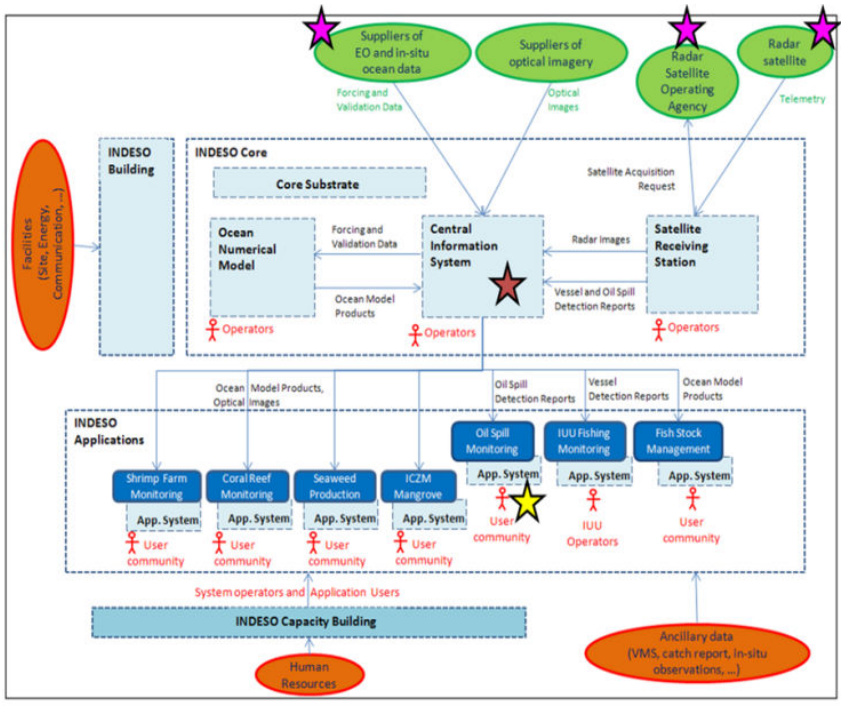

FIGURE 2.3 – Oil Spill monitoring general architecture showing external systems (INDESO Core system with a red star), external interfaces (data providers with a pink star) and applications users (yellow star)

In INDESO system, we can find comprehensive information related to the oil spill. These informations are included metocean data that will be used as input on trajectory modelling to predict the movement of oil spill.

1. **Oil spill detection** : Oil spill detection reports are based on satellite radar imagery and additional processing. If a potential oil spill is detected, the system will provided the following information of geo-referenced polygon of the oil spill with detail in area, length and width of the polygon.

2. **Data radar image level 0 and level 1** : The Radar level 0 is radar raw data product. This raw data is data from sensor on remote sensing satellite, and any auxiliary data that required to produce remote sensing products. All of this data have not been transformed into a remote sensing product. The Radar level 1 is radar product. It is the image generated from the satellite signal.

3. **Optical remote sensing data** : This product is a radiometrically and geometrically corrected high-precision digital imagery product.

4. **Vessel detection** : Using the satellite radar image and continue with additional processing produce the information of all vessel detected, their position, size, speed and heading. All this information are present in the report. This information is important related to detection the source of the oil spill.

5. **Wind radar** : The wind radar product is coming from processing of the roughness of SAR images.

6. **Physical models outputs** : This model outputs includes daily mean fields of atmospheric fluxes, physical parameters (temperature, salinity, currents, sea level...), hourly surface variables (SST, Sea Surface Height-SSH, currents), and also hourly values of all fields at selected mooring sites.

7. **In situ observations** : are real-time and historical, in-situ temperature and salinity profiles, surface velocities, and sea level.

8. **Meteorological data** : consists of a 2 weeks hindcast and a 10-day meteorological forecast for the INDESO area with an ORCA grid at 1/12° and temporal resolution of 3 hours.

9. **Validation files** : There are 4 datasets of validation :

   (a) Daily Ocean volume transports,

(b) Daily Model Sea Surface Temperature (SST) error ratio and error mean time series per region,

(c) Enriched in situ temperature and salinity profiles with physical ocean model,

(d) Enriched UV drifters files with physical ocean model.

In this thesis we will use some informations from INDESO systems to support our analysis in particular oil spill observation from SAR image and data related to the oil spill model trajectory. Figure 2.4 below showed example of information of oil spill SAR detection, vessel position, wind data, and bathymetry data.

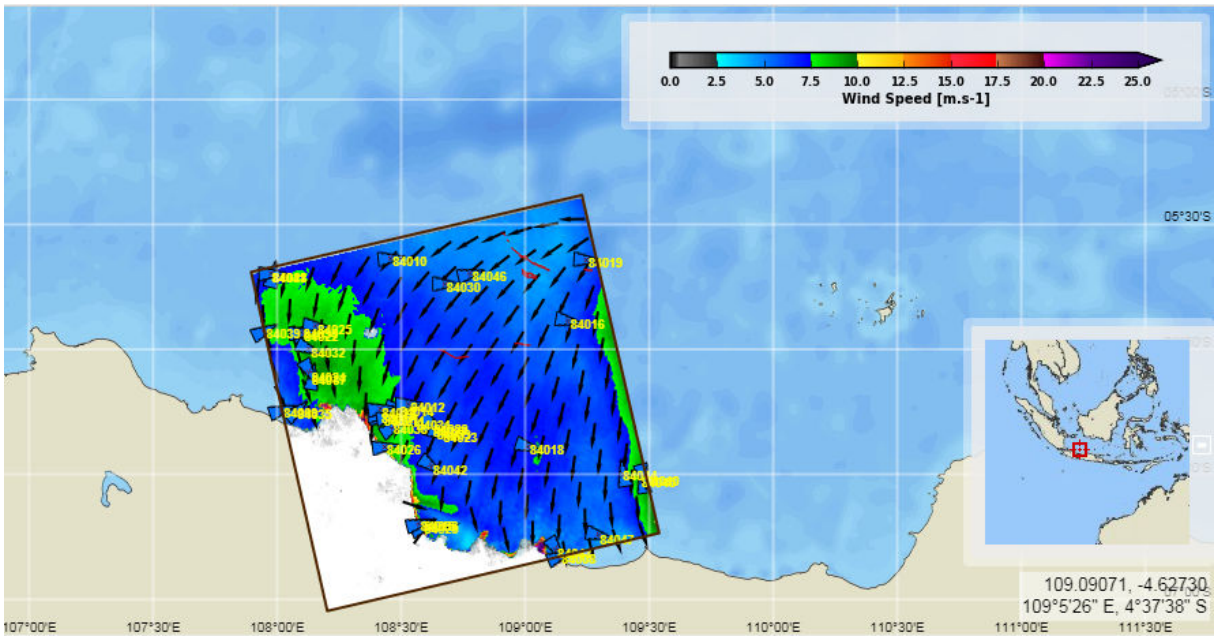

FIGURE 2.4 – Oil spill observation in INDESO system with SAR detection in North of Java on 25 July 2016 (black box), the wind vector (black arrow), the vessel ID and position showed in triangle with yellow number and the contour of oil spill detected in red

2.3 Detection of oil spill using EO-based imagery

Detection of oil spill in ocean can be conducted with airborne and satellite measurements. Airborne detection carried out with simple still or video photography [13]. Nowadays, small remote-controlled aircraft can be equipped with visible and infrared cameras [14]. Satellite detection provides more advantages because it can produce regularly images in remote locations. In this section, we will review the-state-of-the-art of oil spill detection, based on Earth Observation (EO) data and in particular SAR-based detection.

2.3.1 Spaceborne/airborne remote sensing

There are mainly two types of remote sensing sensors, optical and infrared sensors and microwaves sensors. Meanwhile, there are two methods of sensors, active sensors and passive sensors.

EO-based system with passive optical sensors is using the sun's energy reflected to the sensors. These sensors can only be used when the energy from the sun is available, meaning at daytime. It is possible to detect the energy from the Thermal Infra Red (TIR) at day/night time when the amount of this energy is sufficient to be detected. Active sensors like laser fluorosensor and SAR have their own energy emitting source. They produce their own radiation with large amount of energy and emit directly toward their targets. The targeted object will reflect this radiation back to the sensors. The active sensors have advantages in their capabilities to work days and nights, independently on the sun condition. They can also detect the object that not sufficiently radiated by the sun, for example in case of cloud coverage. Below is the list of advantages and disadvantages of both type of sensors for oil spill monitoring.

1. Optical remote sensing

Optical remote sensing can be used to get a timely and initial map for the oil spill but it has limitation because it is weather dependent. In optical remote sensing, measurement can be conducted by visible, InfraRed (IR), and UltraViolet (UV). In the case of the Montara event, when the uncontrolled release of hydrocarbon happened on 21 August 2009, AQUA, a multinational NASA scientific research satellite launched in 2002, showed no oil slick nearby the wellhead (Figure 2.5). This is due to the important cloudiness. Figure 2.6 showed the detection using TERRA (NASA satellite launched in 1999). In this optical image, oil slick was detected more than 200 km long and its contour is showed in red line.

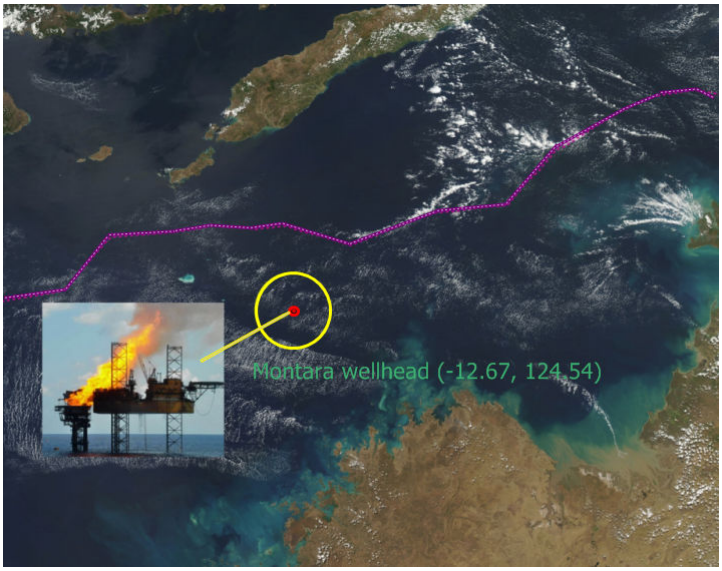

FIGURE 2.5 – Image AQUA on Montara wellhead location (red dot) on 21 August 2009, no oil slick detected, the purple line is the border of Indonesia territory

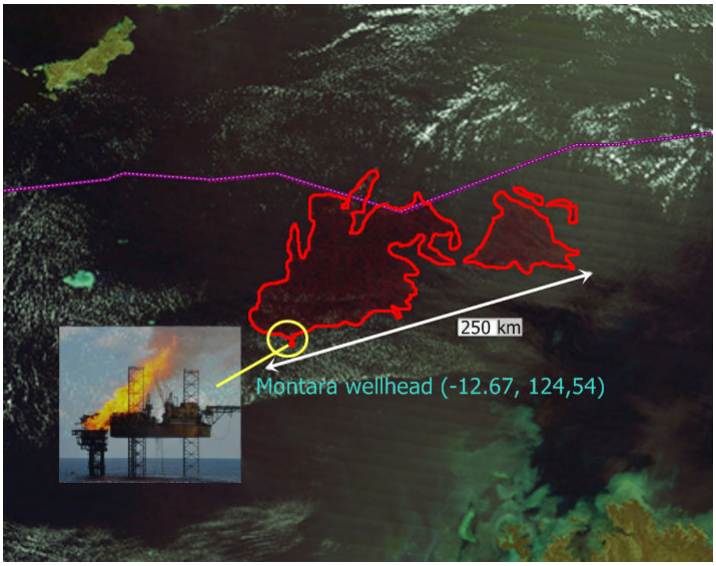

FIGURE 2.6 – Image TERRA on Montara wellhead location on 03 September 2009, oil slick polygon detected in red line, the purple line is the border of Indonesia territory

Oil has higher surface reflectance than water in the visible region of electromagnetic spectrum thus oil will show up silvery and reflects light [15].

Detection with IR is relatively inexpensive. It uses scanner with infra red detectors in application. In infra red images, thick oil slick appears hot, intermediate thick oil is cool, and thin oil not detected [16] [17].

Oil can be detected with Ultra Violet because oil has stronger reflectivity than water in the UV region. This measurement is relatively inexpensive and can detect thin layers of oil slicks [18] [17].

2. Laser fluorosensors

Laser fluorosensors has capability to differentiate oil and non-oil substances backgrounds (e.g., seaweeds, kelp), detect oil in certain ice and snow situations and detect oil in the water column but it is relatively expensive with potential interferences from cloud and fog [19], [20]. Currently, it is essentially available in airborne system.

3. Microwaves sensors

Microwaves sensors has the advantage in its adaptable to different weather and all-day detection. It is commonly used and generally preferable than optical sensors [21].

A microwave radiometer is categorized as passive device which records the natural microwave emission from the earth. Passive microwave radiometers detect the presence of an oil film on water by measuring the reflection of the surface as excited by the radiation from space. Some researchers have focused on using passive microwave to image oil slicks as a remote sensing tool [22], [23], and [24]. Radiometers is used in aircraft oil spill monitoring. Passive microwave radiometers detect the oil-water emissivity difference, with its signals indicating oil thickness. Even if it is all weather oil sensors, its relatively expensive in operation [25], [26].

There are two types of radar, Synthetic Aperture Radar (SAR) and Side-Looking Airborne Radar (SLAR). They can be used in large area monitoring because they have wide area coverages. They are more reliable in operation since they are applicable at night and in all weather condition. The basic concept of radar oil spill monitoring is using capillary waves on the ocean that reflect radar energy and produce a bright image, known as the sea clutter. Surface oil partially reduces the roughness of capillary waves and gives a darker image. With this concept, it has limitation by wind speeds. In low sea state situation, it does not produce any sea clutters, hence the differentiation between oil and water is difficult.

Currently many different SAR systems exist, giving scientists and end-users a choice of configurations, bands and polarizations. Several different polarizations exist based on vertical (V) and horizontal (H) electromagnetic wave propagation. Typically transmission and reception can be in the same polarization, i.e. VV or HH. Emitting and receiving in different polarizations

results in the possibility to get 4 different channels : HH, VV, HV and VH. The use of these 4 polarizations is the so-called Polarimetry SAR. Most radar satellites have a variety of coverages, a variety of resolutions and polarizations. Table 2.2 lists some of the current and future SAR satellites.

TABLE 2.2 – List of satellite-borne SAR sensors

Satellite	Launch Date	Owner/Operator	Band
RADARSAT-2	2007	Canadian Space Agency	C (quad)
TerraSAR-X	2007	German Aerospace Centre	X (quad)
Tandem -X	2010	German Aerospace Centre	X (quad)
Cosmo Skymed-1/2	2007, 2010	Italian Space Agency	X (dual)
Risat1	2012	India Space Agency	C (quad)
Kompsat-5	2013	Korean Space Agency	X (dual)
Sentinel-1	2014	European Space Agency	C (dual)
RADARSAT-Constellation (3-satellites)	2018	Canadian Space Agency	C (dual)

2.3.2 Detection of oil spill based on SAR imagery

Detection of oil spill is not merely when the accident of oil spill happened but in the operational level the detection of oil spill is to monitor the oil spill that coming from the intentional release from the ship. In this thesis we use the detection of SAR in the case of oil accident in Chapter 3. In Chapter 4 our assessment of oil spill risk include the oil spill coming from intentional release as capture in the Indeso oil spill detection systems and the position of ship based on the AIS data. This subsection discuss the detection of oil spill in Indeso based on SAR imagery and it's relation to the position of ship.

2.3.2.1 SAR sensors

In SAR imaging, microwave pulses are transmitted by an antenna to the earth surface. The energy that scattered back is then measured. It calculates the time delay of the scattered and backscattered signals. Working with different frequency bands, SAR can be used in many applications. L-band in the frequency 1 GHz - 2 GHz can be applied in agriculture, forestry, soil moisture, C-Band (4 GHz - 8 GHz) in ocean, agriculture and X-band (8 GHz - 12 GHz) agriculture, ocean, high resolution radar. Experimental work on oil spills has shown that X-band radar yields better data than L- or C-band radar ([27], [28], [29]).

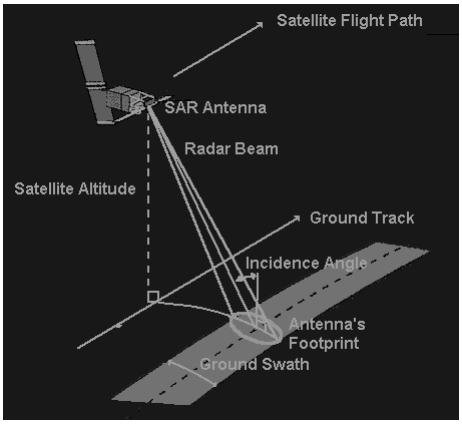

FIGURE 2.7 – Synthetic aperture radar imaging system basic principle

Due to the capability to penetrating cloud, SAR can acquire images in all weather. This is important factor that consider in operational on the tropical regions like Indonesia which are frequently covered by cloud throughout the year. Other advantage of an active remote sensing device, it is also capable to operate at night.

2.3.2.2 SAR processing

The detection of oil slick is limited by wind speeds. When there is not enough wind, capillary waves are not created, radar backscattering becomes weak, and the contrast becomes insufficient. Some phenomena like fresh water slicks, wind slicks, wave shadows behind land or structures, seaweed beds that calm the water just above them, glacial flour and biogenic oils can interfere. It could produce false alarms or look-alikes. Much work has taken place on means to differentiate oil slicks and false targets as well as methods to automate the analysis process [30]. To solve this problem, some researches have been developed in the method of edge detection [31], [32], texture analysis [33], [34], shape analysis [35], [36], fuzzy logics [37], [38], [39], and neural networks [40], [41], [42], [43], [44], [45].

In INDESO systems, the oil spill detection process is conducted with a semi-automated process. It means that the system requires supervision from the Radar Analyst and utilize the SARTool Oil module of SARTool application in the process. SARTool is designed by a CLS team of radar experts. SARTool has proven high level performance. It has been used to detect sharp features of interest in the radar scene and capable to produce user-friendly reports for end users.

On the detection of oil spill, there are 4 process. The description of each step is as follows :

- Detection of all suspicious slicks

Using SARTool software, radar analyst analyzes SAR level-1 products. In this process, the full resolution capacity and the best dynamic range of pixel is used. Radar analyst visually identified all the suspicious slicks directly on the SAR image with its native geometry and projection. If the inspection result is that no suspicious slick is detected, then the analysis is completed. In this case no Oil Spill Detection Report is generated.

- Determination of look-alikes

On the process of SAR images analyzing, the operators in charge play an important role. They have to analyze SAR images using a set of ancillary information about the situation at sea. Using the supplementary information (in particular Wind product), the Radar Analysts then attempt to discriminate all detected suspicious slicks. Some of the suspicious slicks can be categorized as look-alikes. This look-alikes are typically caused by low wind situations, wave-current interactions that dampen the short gravity waves, rain cells, cold upwelling areas and algae blooms or suspended matters. When the cause of the look-alikes is unknown, the detected feature will be kept and labeled as "look-alike" in the Oil spill detection report.

- Define of possible oil spills

Using the SARTool Graphical User Interface (GUI), the Radar Analyst create annotation of possible oil spills. The SARTool GUI is very easy to used to navigate within the SAR image. It can be used by the Radar Analyst to create Oil Spill Detection Reports as necessary. In each Report, we can find an overview of a specific pollution that composed of one or many slicks.

- Production of Oil spill detection report

Oil spill detection report produced by the radar analyst is then indexed in INDESO Maestro module. The report will be available on the CIS Web Interface in Oil Spill Monitoring session. Example of INDESO oil spill report is showed in Figure 2.8.

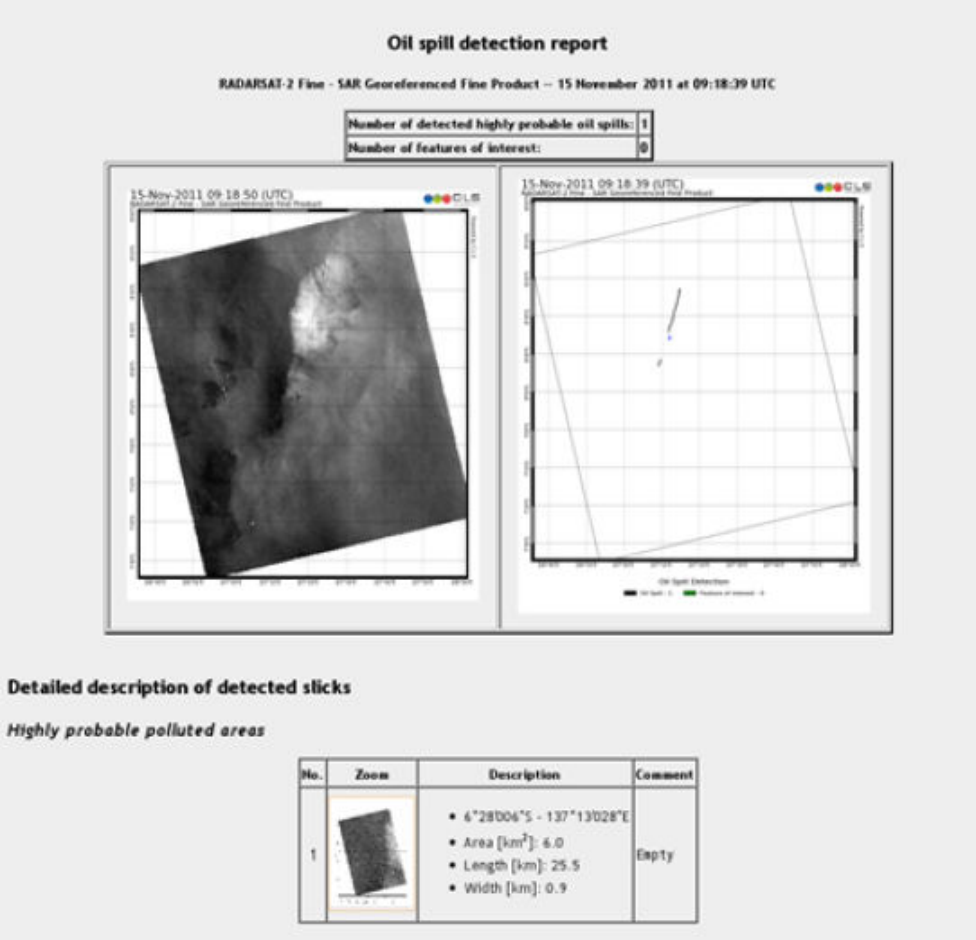

Oil spill detection report

RADARSAT-2 Fine - SAR Georeferenced Fine Product -- 15 November 2011 at 09:18:39 UTC

Number of detected highly probable oil spills:	1
Number of features of interest:	0

Detailed description of detected slicks

Highly probable polluted areas

No.	Zoom	Description	Comment
1		• 6°28'006"S - 137°13'028"E • Area [km²]: 6.0 • Length [km]: 25.5 • Width [km]: 0.9	Empty

FIGURE 2.8 – INDESO oil spill report

2.4 Oil spill transport model

2.4.1 Introduction

The development of mathematical models to predict and forecast the fate and transport of oil spill in marine environment has become an interesting research topic over the last decades. It is related to the needs to mitigate the effects of oil spill to the environment. It is a challenging topic since extremely complex phenomena may affect the fate and transport oil spill. It concerns not only physical but also chemical processes.

Since the early sixties, a number of oil spill models have been developed. There are three types of model. First models are essentially transport models with limited fate analysis. Second models are oil spill model with two dimensional hydrodynamics and fate analysis. And the third models are comprehensive oil spill model that consists of fate and transport in 3-dimensions. Comprehensive oil spill models generally include the processes of evaporation, emulsification, dissolution, dispersion, spreading, biodegradation, photolysis, sedimentation, advection, and oil-shoreline interactions. In the weathering processes, the most important processes is evaporation and emulsification [46].

Evaporation is the most important weathering process because most parts of the oil spills evaporate within the initial stage of spill. This process is influenced by the composition of oil, air and sea temperature, wind speed, solar radiation and slick thickness. Relative reference on the formulation of evaporation process can be found on the research by [47], [48], [49], [50], [51], [52], [53]. On the emulsification process, spilled oil is broken into small droplets and enters the water column due to wave or turbulence. Light oil is usually not emulsified which is not the case for crude oil. The emulsification significantly changes the physic and chemical properties of oil (i.e., density and viscosity). Some researches of this process can be found on [47], [49], [50], [54], [52], [55], and [53].

Many integrated models have been developed for the oil spill transport and fate based on trajectory method. Some of them focus on the surface movement of spilled oil [56], [57], [58], [59]. Some commercial versions have been developed, *inter alia* COZOIL [60], OILMAP [61] or WOSM [62].

In general, the requirements of oil spill model are :

- Rapid response

- Accuracy of predictions for forecasting
- Capability to adjust predictions considering data observation
- User friendly

If rapid response is required, the model cannot have complex computational procedures. In rapid response, the model provides short-term forecast when meteorological data are available and reliable. Rapidity and accuracy prediction is important to minimize environmental damage caused by oil spill. To assure the accuracy, the model has to have capability to adjust predictions considering the input data. And the user-friendliness is yet another consideration to support the rapid response.

Related to the INDESO project, our focus is on the operational level. In this case, the rapid response and accuracy are the most important factors considered. The oil spill model has to have the capability to use the meteorological and oceanography data from INDESO system as an input data.

Ideally, a model is calibrated during actual oil spill. This concept requires the assimilation of observed data (location of spill, winds and currents) into the model. We can then compare with the feedback from the field to ensure the accuracy of the forecast. Linkage between the oil spill model and satellite data or field observation should be established and used to tune and calibrate the model. In our thesis, we will calibrate the model using the SAR-detected oil spill and test our model in the case of Montara.

2.4.2 Lagrangian 2D Trajectory Model

In pollutant fate and transport models, the fundamental principle is the rate of change mass concentration of pollutant within a given control volume. It is equal to the sum of the net advective flux of pollutant into the control volume, the net diffusive flux of pollutant into the control volume and the net rate of production of pollution within the control volume. In mathematically, that principle stated as advection-diffusion equation :

$$\frac{\partial C}{\partial t} = -V_a \cdot \nabla C + \nabla \cdot (D \nabla C) + S \tag{2.1}$$

where :

C = mass concentration of the pollutant

V_a = advective velocity of the surrounding medium

D = the diffusivity coefficient

S = external fluxes

The advective velocity depends on the currents and wind velocity, and the sea state. The diffusive velocity depends on the sea turbulence characteristics. Usually, the latter is simulated as a Brownian motion of particles by means of a random walk procedure [58].

2.4.3 Mobidrift

Mobidrift is the numerical model implemented by CLS that simulates the trajectory of various objects in the sea. The objects can be icebergs, oil spill slick, Search and Rescue object and containers. In the calculation of trajectory of the object, Mobidrift uses a forward approach. The simulation in this model is based on a 2D Lagrangian advection scheme as we mentioned in the subsection 2.4.2. Wind and/or current velocities are used as input for the advective component.

As input data, we used outputs of the INDESO CIS system. In the next paragraph, we will further discuss the wind and current data of INDESO system used in simulation. Within Mobidrift, there are three different manner to model the presence of oil spill particles, the so-called "slick", "outline" and "trajectory" modes. In the "Slick" mode, the oil spill is modeled as location point or list of location points. In the "Outline" mode, the geographical coordinates of the oil spill contour are given. The "trajectory" mode can be used when trajectory positions of ship from AIS data are available. Mobidrift has many output formats. Standard format is XML. In addition, Mobidrift can produce many graphics of simulated oil spills.

As input of Mobidrift, the zonal and meridian components of 10-m wind come from meteorological data products provided by the INDESO CIS. Those datasets are delivered in Network Common Data Form (NetCDF) format. The meteorological data products is provided by the ECMWF (European Centre for Medium Range Weather Forecasting) meteorological analysis and forecast over the INDESO area on a 1/8° horizontal grid and a 3-hour temporal resolution up to 6 days and 6-hour temporal resolution after (10 days). The results of post-processed of this fields are able to be read on the ocean model with an ORCA grid at 1/12° [63].

Our Mobidrift input of ocean current data is provided by INDESO physical model outputs. INDESO produce daily mean fields of atmospheric fluxes, physical parameters (temperature, salinity, currents, sea level...), hourly surface variables (SST, SSH, currents), as well as hourly values of all fields at selected mooring sites and validation metrics. The regional ocean physical model provides physical fields for the past two weeks (forced by a global 2-weeks analysis) and ocean forecasts (forced by a global 10-day forecast) for the next 10 days. INDESO physical ocean model has a horizontal resolution of 1/12° and 50 vertical layers. The resolutions are increased near the surface. Meanwhile on the horizontal grids are provided on a regular 1/12°.

In our Mobidrift simulation, we used the bathymetry data based on ETOPO2V2g (2-minute grid) and GEBCO (1-minute grid). This bathymetry has been locally modified by a hand editing mainly on the straits with a threshold value of 7m.

2.4.4 Application of Mobidrift in Indonesia's Oil Spill Trajectory

In this thesis, we use the CLS Mobidrift to simulate the drift of oil slick in two applications, both of them is to support mitigation planning and development of marine and fisheries. First application is on the case of Montara oil spill. In this application, Mobidrift is used to simulate the drift of oil spilled from the Montara oil platform. There are three data that we used as an input to Mobidrift from INDESO system output i.e bathymetry, wind velocity and current velocity. An illustration of these data is showed in Figure 2.9, 2.11 and 2.10. Then we will compare this simulation with the detection of SAR. We will discuss in more details application of Mobidrift in Montara oil spill in Chapter 3. The second application is on the assessment of oil spill risk in the Indonesian FMA.

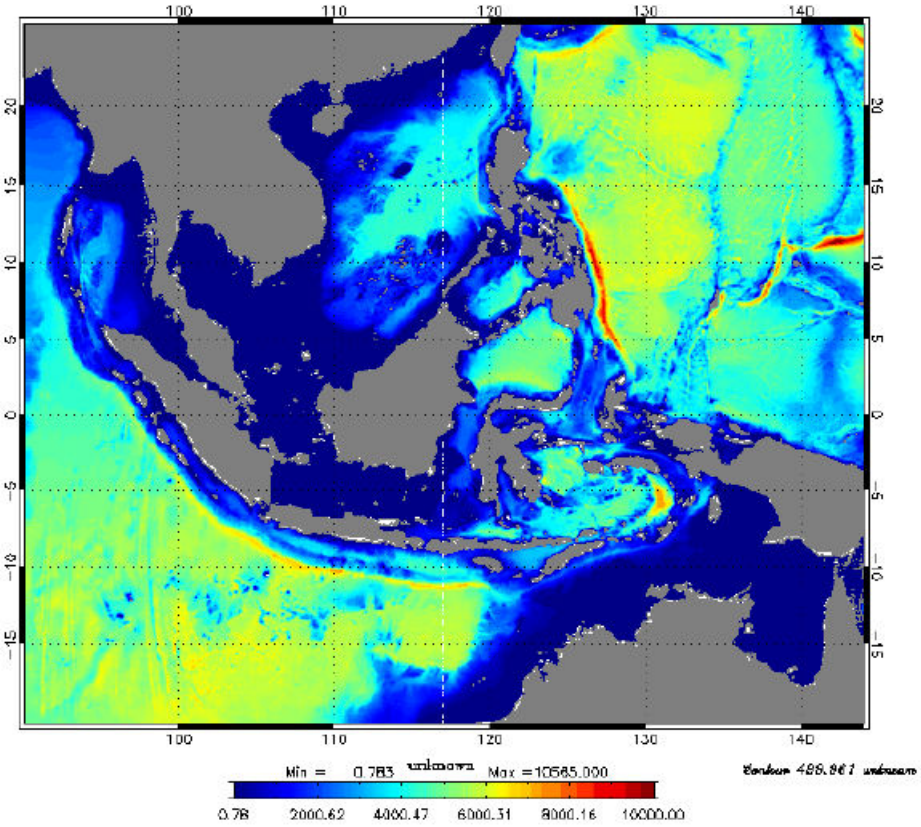

FIGURE 2.9 – Bathymetry (meter) of the INDESO configuration. (ETOPOV2g/GEBCO1 + in-house adjustments in straits of major interest)

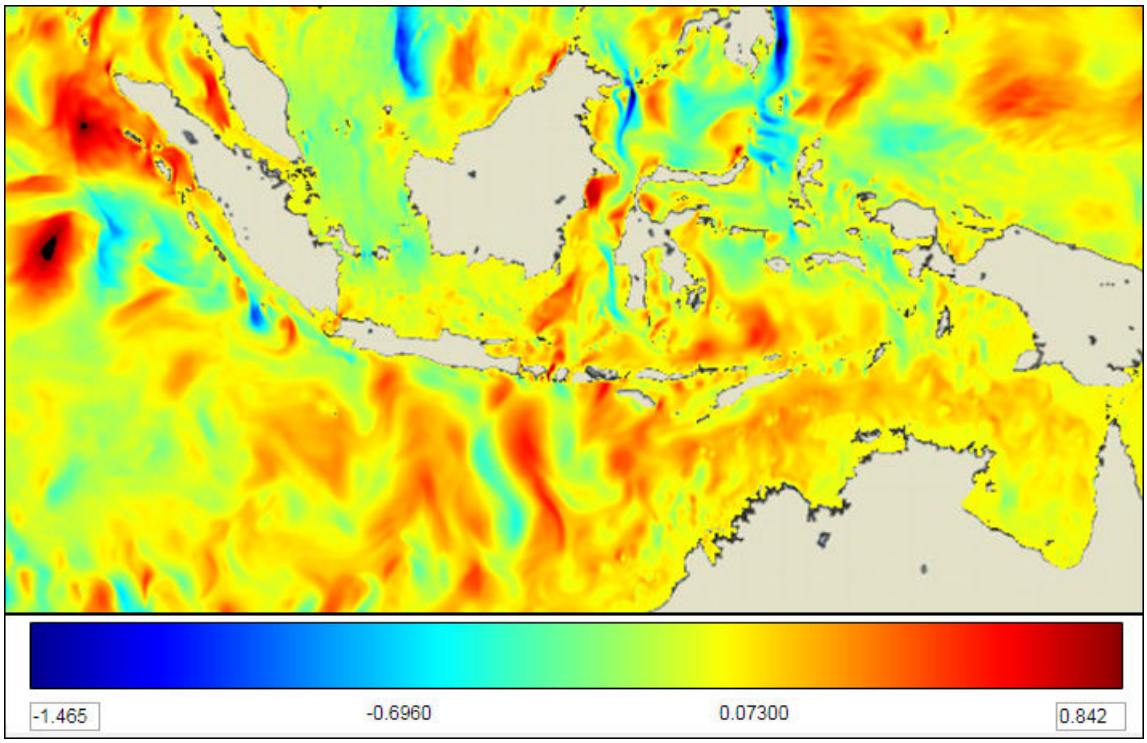

FIGURE 2.10 – Sea surface current velocity (m/s) on 01 January 2015 data from the INDESO system

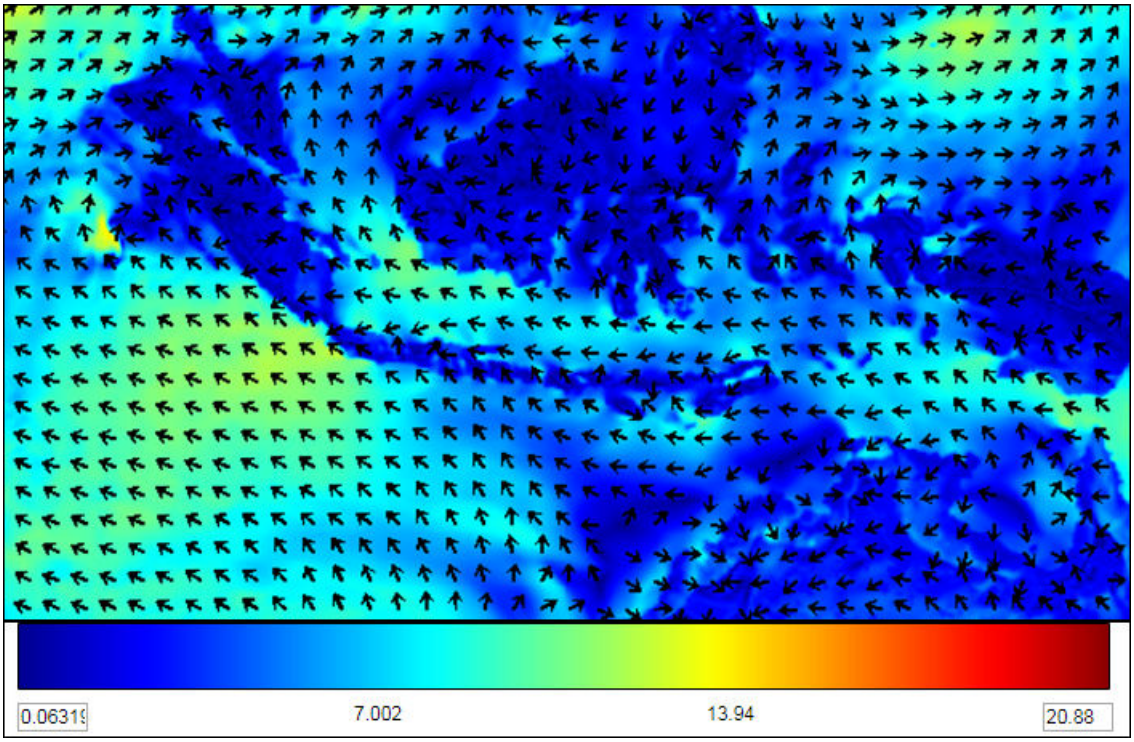

FIGURE 2.11 – Wind velocity data (m/s) and its direction (black arrow) on 01 January 2015 data from the INDESO system

2.5 Conclusion

This chapter has discussed the current oil spill monitoring system in Indonesia. We began with the description of Indonesia waters that give brief illustration of general aspects of ocean circulation and main issues of Indonesia marine and fisheries related with oil spill. Then we explain the oil spill monitoring as conceived by the INDESO system. In this subsection, we showed the system design of INDESO. Further, we discussed the detection of oil spill using SAR imagery as used in INDESO systems. The state-of-the-art of SAR detection was presented. And finally, the oil spill transport model was discussed. First we reviewed the state-of-the-art of oil transport model and we discussed the Lagrangian 2D model trajectory model. In this research, we use the Lagrangian-based CLS Mobidrift model to simulate the oil slick transport in the ocean. Using the output data from INDESO CIS as the input for Mobidrift, we will analyze the Montara study case and will calculate the risk and cost of oil spill in Indonesia. These applications are presented in the following two Chapters.

Chapitre 3

Oil spill parameter retrieval

3.1 Introduction 40
3.2 Proposed approach 42
3.3 Montara SAR based oil detection 44
3.4 Similarity between SAR oil spill detection and model 47
3.5 Estimation of oil leakage parameters assimilation of SAR images 49
3.6 Application to Montara case study 52
3.7 Conclusion 59

3.1 Introduction

Oil spill is one of the most serious threat for all marine and coastal environments. Oil spill can cause high economical and ecological damages in marine and coastal ecosystems. Indonesia, as an archipelago country, is particularly vulnerable to oil spill since national waters, which account more than 70% of its territory, involve a very active maritime traffic and a large number of onshore and offshore oil platforms. The accidental or intentional releases of petroleum products are the two sources of oil pollution into the marine environment. Even though the pollution from voluntary rejection of waste oil and residual fuel are of high importance, for instance the equivalent of 50 Erika or 15 Prestige per year in the Mediterranean Sea [64], major oil spill accidental disasters such as Deepwater Horizon or Torrey Canyon oil spills still have devastating long-term consequences for society, economically, environmentally, and socially [65]. Montara oil spill in 2009 stressed the urgent needs for the operational monitoring of oil spill in Indonesian waters. The operator, PTTEP Australasia (Ashmore Cartier) Proprietary Limited (PTTEP AA), initially estimated the oil leakage to 400 barrels (or approximately 64 tonnes) of crude oil lost per day [66]. The uncontrolled release started on 21 August 2009 and crude oil continued to be released until 3 November 2009 when the well brought under control. Montara wellhead platform is located in Australian waters at coordinate latitude 12°40′20.5″N and longitude 124°32′22.2″E. The depth of water was approximately 250 ft (76 m) as show in Figure 3.1. It is very close to Indonesian waters, only 310km from Timor island. This south-most island Indonesia archipelago has an important ecological and economical value. There are 3,355,352.82 hectare of marine protected areas in Sawu seas. Its coral ecosystems with 532 coral reef species and 11 species endemic with total area 633.39km^2 [67] is a peculiar example. Following Montara oil spill, the Indonesian Ministry of Marine and Fisheries Affairs initiated the development of ocean monitoring systems, in combination with operational oceanography, especially within the framework of Infrastructure Development Space Oceanography (INDESO) project. In this context, the present study addresses the assimilation of satellite-based Synthetic Aperture Radar (SAR) observations of oil spills into an oil trajectory model. It relies on Lagrangian-based simulations of the transport of particles at sea surface and on the comparison of transport simulations and detected oil spills from implicit level-set-based representations. Using Montara oil spill as a case study, we demonstrate the relevance of the proposed model and associated

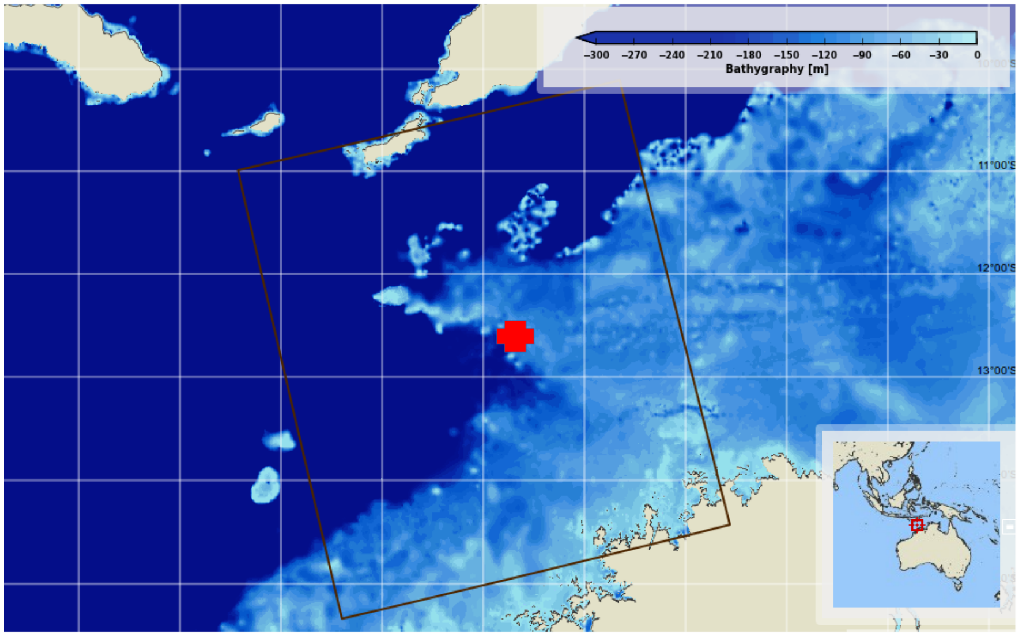

FIGURE 3.1 – Position of the Montara oil platform on the map of bathymetry, the red sign is Montara wellhead position and the black box is our boundary box for oil trajectory simulation.

numerical scheme for the optimization of oil leakage parameters (namely the starting date of the leakage, its duration, the mean wind-related and current-related drift coefficients). This work is organized as follows, in Section 3.2 describes the proposed approach. We report numerical experiments in Section 3.3. Section 3.4 further discusses the key features of the proposed model.

3.2 Proposed approach

We report in Figure 3.2 the synoptic sketch of the proposed approach for the assimilation of oil leakage parameters from satellite-based SAR observations. Our approach involves three main components :

- A Lagrangian-based 2D transport model, which simulates the advection of particles at sea surface under given wind and current conditions. This component is detailed in Section 3.3 ;
- The detection of oil spills from satellite-based SAR observations in Section 3.4 ;
- The definition of a similarity measure between simulated particle sets and oil spill detection from satellite-based SAR observations as detailed in Section 3.5.

These three components are combined within an assimilation model and applied in Montara case detailed in Section 3.6 along with the associated numerical resolution.

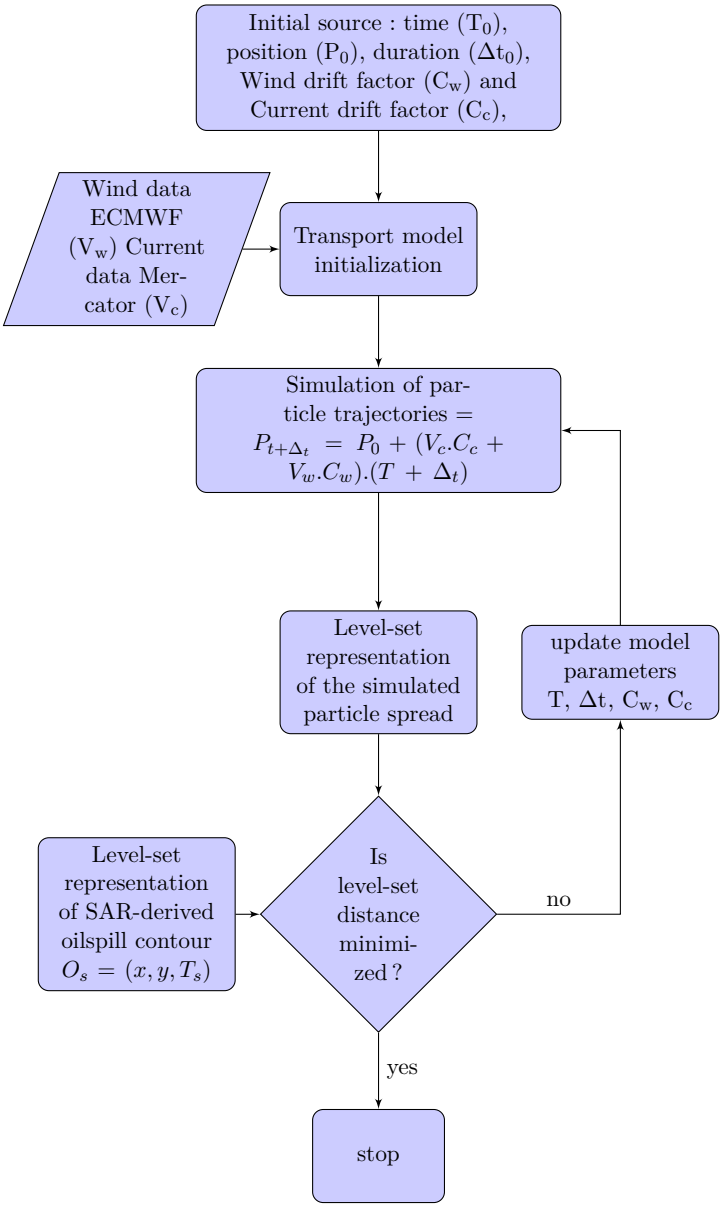

FIGURE 3.2 – Flowchart of the proposed approach for the assimilation of oil leakage parameters from satellite-based SAR observations

3.3 Montara SAR based oil detection

The analysis of oil spill dynamics is an active research topics [68]. The considered models range from 2D surface trajectory to 3D+t space-time dynamics and fate analysis. In general, an oil spill model combines a description of the oil spill, which may include the space-time extension of the oil spill as well as geochemical characteristics, and the undergoing weather conditions, typically wind and current conditions. In general, commonly used operational oil spill models include GNOME (General NOAA Operational Modeling Environment, `http://response.restoration.noaa.gov/`), MOTHY (French operational oil spill drift forecast system, `http://www.meteorologie.eu.org/mothy/`), OSCAR (Oil Spill Contingency and Response, `http://www.sintef.no`), ADIOS2 (Automated Data Inquiry for Oil Spills, `http://response.restoration.noaa.gov`), OILMAP (Oil Spill Model and Response System, `http://www.aims.gov.au/pages/research/oil-map/oil-map01.html`) and OSIS (Oil Spill Identification System, `http://www.osis.biz/ss2.asp`) [69]. In the Deepwater Horizon, as one of the biggest oil platform leakage accident, the efforts of observation to detecting the existence of oil on the ocean surface and modeling of the oil spill trajectory are well documented [70]. One of the study that was conducted for this accident is an assimilation of modeling and satellite-observed surface oil locations where models were seeded with oil location inferred from satellite images with virtual particles and then these particles were advected with the surface velocity fields as forecast by numerical ocean circulation models [71]. The simulated surface oil trajectories were compared to the satellite observations in subsequent forecast cycles for veracity testing [72]. We consider some study application on case of the oil spill accident i.e two oil platforms in the Bohai Sea, China [73] and The Shell North Sea Gannet Alpha platform [74].

Here, our focus is on the assimilation of oil leakage parameters and we consider a computationally-tractable surface transport model. The oil spill leakage is characterized by the location of the source of the leakage, the type and quantity of oil. The considered transport model, namely Mobidrift model [75] developed by Collecte Localisation Satellite (CLS), simulates Lagrangian trajectories of particles at sea surface for given wind and current conditions. In Mobidrift model, fluids are modeled by a set of deterministic particles. For a source defined by a fixed oil platform, we provide to Mobidrift model the location of the source, the starting time for the release of particles and the duration of the leakage. For each particle released from the initial

position, we apply the considered 2D transport model to derive its trajectory up to the final date of the simulation. In our simulations, we typically consider about 500 particles released on a daily basis. Formally, Mobidrift model relies on the two-dimensional advection of particles by a surface displacement given by a weighted sum of tidal current and wind-induced current velocities

$$u_p^{adv} = C_c \cdot V_c + C_w \cdot V_w \tag{3.1}$$

where u_p^{adv} is the advection velocity, V_c the sea surface current and V_w the sea surface wind speed at a height of 10m. Coefficients C_c and C_w are the current and wind drift factors. In our study, as sea surface wind and current data, we use PSY4V2 MERCATOR system (1/12° horizontal resolution) with daily forecast production [76], and 10-meter wind field provided by the analysis of the European Centre for Medium-Range Weather Forecasts (ECMWF) at a 0.140° spatial and 6-hour temporal resolution [77].

The transport model is complemented with a diffusion component. Neglecting viscous effects, the total velocity of a transported particle can be decomposed as

$$\frac{\mathrm{d}x}{\mathrm{d}t} = u_p^{adv}(x,t) + u_p^{dif}(x,t) \tag{3.2}$$

where $u_p^{\mathrm{dif}}(x,t)$ is the diffusive component, which amounts to an isotropic Gaussian velocity, parameterized by standard deviation σ.

The simulation of the displacement of a particle between time t and time $t+\delta t$ resorts to the integration of Eq. (3.2) :

$$x_p(t+\delta t) = x_p(t) + \int_t^{t+\delta t} u_p^{\mathrm{adv}}(x_p,t)\,dt + \int_t^{t+\delta t} u_p^{\mathrm{dif}}(x_p,t)\,dt. \tag{3.3}$$

It should be stressed that, through the stochastic diffusive component, the numerical integration results in a randomized simulation of trajectories. As a result, from multiple numerical integration, this transport model results in the simulation of the spread of an oil spill.

Wind drift factor C_w in eq. (3.1) typically ranges from 0.01 to 0.06 [78–80]. In many applications of oil movement forecast, wind drift factor C_w is set to 0.03 [59], [81]. Regarding sea surface current, drift factor C_c typically ranges from 1.0 to 1.5 [79]. In this study, factors C_w

and C_c are among the oil leakage parameters estimated to assimilate the satellite-based SAR observations and the simulated oil particles from trajectory models.

3.4 Similarity between SAR oil spill detection and model

Remote sensing can provide substantial support to routine surveillance in open-ocean and coastal areas and has the advantage of being able to observe oil spill events in remote and often inaccessible areas. The high resolution radar technology (the so called Synthetic Aperture Radar - hereafter SAR) on board satellites is widely used for operational oil spill surveillance [82], [83].

The information that is present in these data can be useful for extracting important indications for risk assessment, emergency management, and damage inventory [84].

Thanks to its very wide area coverage and its capability to work day/night independently of the cloud coverage, space-borne SAR technology provide cost-efficient means. Flying at about 800km altitude, SAR sensors emit electromagnetic (EM) waves with frequency ranging from 1 to 10GHz. At these EM wavelengths, the sea surface back-scatters the EM waves back to the sensor, depending on the sea state and radar acquisition geometry following Bragg theory. An oil spill dampens the sea surface roughness, and basically induces a decrease of this EM back-scattering compared to the surrounding clean water. Hence, the oil spill appears darker on the SAR image (see red contour in Figure 3.3). It is well established that reliable slick detection's are performed for wind speeds in the approximate range of 2.5 to 12.5m/s. In the case of low winds situation (below 2.5m/s), the clean sea-surface and the slick show similar radar backscattering and cannot be distinguished automatically. The operators in charge of analyzing SAR images shall make the best use of any available contextual information such as ancillary data (Sea Surface Temperature, wind field, chlorophyll-A concentration, etc.) in order to assess in the most efficient manner the situation at sea such as captured by the SAR sensor. Some method was developed using μ as a logical scalar descriptor to map oil slicks under low to moderate wind conditions [85].

The oil properties at the sea surface are affected by weathering processes (evaporation, emulsification, photo-oxidation). The weathering of hydrocarbons is complex as it combines the diversity of petroleum products, which have very variable physical-chemical characteristics, with the variety of environmental conditions (wind and waves, sea temperature, etc.) As the SAR sensor is mostly sensitive to sea surface roughness, slick with low viscosity or into the sea subsurface may not be detected.

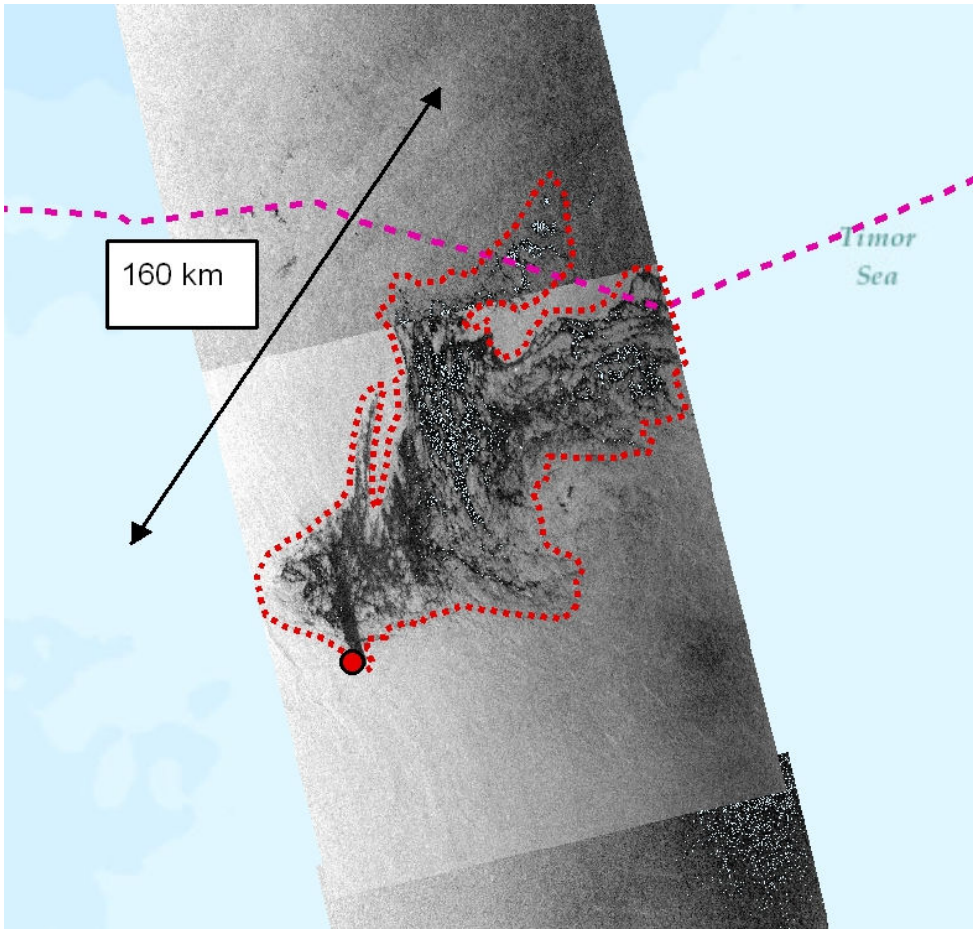

FIGURE 3.3 – SAR Observation on September 02, 2009 by ENVISAT, red contour outlines the main patches of weathered oil on the sea surface, the red dot is Montara wellhead position and the purple outlines the border of Indonesia (above the line) and Australia water territory (below the line).

In this study, the first SAR image covering the Montara event is used. It was observed on September 02, 2009 at 10 :07 UTC by the European ENVISAT mission (see Figure 3.3). The spatial resolution is 75×75 meters with swath width of 400km. Since the blowout from the Montara wellhead platform first occurred on the 21st of August 2009, this image was taken 12 days after the accident. As seen by the SAR sensor, the oil slick is still connected to the wellhead platform, with estimated 160km long.

It is worth noting that the resolution of SAR observation does not induce a dramatic evolution of the detection quality [86], nevertheless, spatial resolution of auxiliary data has a significant impact on the drift simulation and oil slick deformation. So that, the quality of auxiliary data impacts the quality of oil leakage parameters estimation.

3.5 Estimation of oil leakage parameters assimilation of SAR images

A key component of our approach is the definition of a measure of the goodness of the match between the detected oil spill and the simulation of transport model trajectories. This amounts to defining a similarity measure between a set of particles and a contour within a two-dimensional plane. We exploit implicit level-set representations of contours as introduced by Osher and Sethian [1]. As illustrated in Fig.3.4, the level-set representation comes to define a two-dimensional contour Γ as the zero-level-set of a function ϕ, that is to say the set of points of the plane at which the value of function ϕ is zero :

$$\Gamma = \{p \in \Omega \text{ such that } \phi(p) = 0\} \tag{3.4}$$

where Ω is the considered spatial region. As illustrated in Fig. 3.4, the level-set function ϕ is positive inside contour Γ and negative outside. Given function ϕ, the extraction of contour Γ simply comes to extract the contour of a thresholded version of function ϕ at zero. Conversely, one can build the level-set representation of any contour in the plane as the solution of partial differential equation [1] using efficient numerical algorithms. A key interest of this level-set representation is its ability to represent non-connected objects.

Level-set functions also provide a simple mean, without any topological constraint, to evaluate the similarity between any two contours Γ_1 and Γ_2 from a distance between their level-set representations [1] :

$$d(\Gamma_1, \Gamma_2) = \int_\Omega \|\phi_1(p) - \phi_2(p)\|^2 dp. \tag{3.5}$$

This level-set representation directly applies to the contour of the satellite-based SAR detection of the oil spill. We also derive a level-set representation of the spread of the particle sets simulated by the considered Lagrangian transport model. Given a set of particles, we first derive the associated spatial density distribution $\mathcal{D}_S$ using a kernel-based estimation [87]. We then extract the contour Γ_S of the level-set of density distribution $\mathcal{D}_S$, which accounts for a predefined percentage of particles. Let us denote by λ this percentage and $\mathcal{LL}_S(\nu)$ the level-set of $\mathcal{D}_S$ with respect to level ν

$$\mathcal{LL}_S(\nu) = \{p \in \Omega \text{ such that } \mathcal{D}_S(p) > \nu\}. \tag{3.6}$$

Contour $\Gamma_S(\lambda)$ is then extracted as the contour of level-set $\mathcal{LL}_S(\nu^*)$ such that $|\mathcal{LL}_S(\nu^*)|/|\Omega| = \lambda$. We typically set λ to 0.85, such that the contour extracted to represent a particle set accounts for 85% of the simulated particles according to transport model defined by Eq. (3.3). As illustration, we show on Fig. (3.5) the contours of the kernel-based estimate created with different values for spatial density of simulated particles from Lagrangian transport model.

Using the standard Euclidean distance between level-set functions, we define a distance between transport model simulations, characterized by density function $\mathcal{D}_S$ and associated reference contour $\Gamma_S(\lambda)$, and the detected oil spill Γ_{SAR} from the distance between their respective level-set functions $\phi_S(\lambda)$ and ϕ_{SAR} :

$$d\left(\Gamma_S(\lambda), \Gamma_{SAR}\right) = \int_\Omega \|\phi_S(\lambda)(p) - \phi_{SAR}(p)\|^2 dp. \tag{3.7}$$

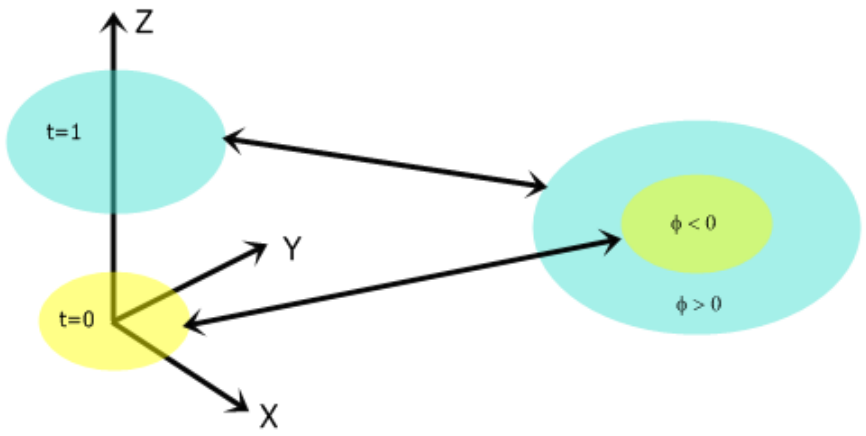

FIGURE 3.4 – Level-set [1] representation of closed contours in a two-dimensional plane : when the contours t=0 (yellow,-) with the value $\phi < 0$ moving forward on t=1 (blue,-) with the value $\phi > 0$

Let us denote by θ the parameters to be estimated, namely leakage date d_L and duration Δ_L, and the mean surface current and wind drifts, respectively C_c and C_w. Let us denote by

Γ_{SAR} the contour of the detected oil spill from the SAR observation. We state the estimation of leakage parameters θ as the maximization of the similarity between the detected oil spill and the simulated particle set from the Lagrangian transport model of eq. (3.3) with respect to parameters θ. Numerically, it comes to solve for the following minimization :

$$\widehat{\theta} = \arg\min_{\theta} d\left(\Gamma_S(\lambda|\theta), \Gamma_{SAR}\right), \tag{3.8}$$

where contour $\Gamma_S(\lambda|\theta)$ refers to the simulation of the Lagrangian transport model of eq. (3.3) from the known leakage source with respect to parameter θ.

The numerical resolution of this minimization exploits Powell's method [88] as we cannot derive the first-order derivatives of the considered function with respect to parameter θ. Powell's method iterates until convergence one-dimensional searches along conjugate directions, initialized as the basis vectors of the considered n-dimensional parameter space. Our implementation uses the scipy optimization package under Python environment.

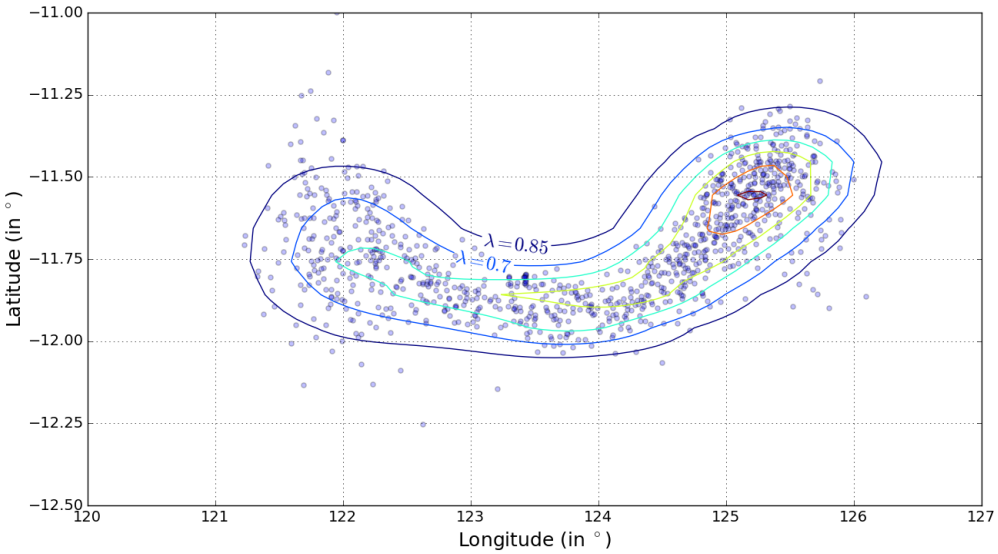

FIGURE 3.5 – Spatial density of a set of particles simulated from Lagrangian transport model (3.2). The simulated particle set is depicted as a set of blue dots. We also display the contour of the kernel-based estimate of the spatial density of the simulated particle set.

3.6 Application to Montara case study

As a mean to investigate the sensitivity of transport model simulations with respect to oil leakage parameters, we first report assimilation results for one-day oil leakage ranging from August 21 to September 02. This first simulation uses different dates of source of leakage with one day duration.

The result is given in Fig. 3.6-above, showing that the first five days of leakage give the minimum value of RMSE. For each date, we solve for minimization Eq. (3.8) to estimate wind and current drift factors C_w and C_C. We report in Fig. 3.7 and 3.8 the series of the optimal parameters C_w and C_C related to the simulations on the Fig. 3.6-above. For the source of leakage August 21, 2009 with one-day duration, the minimum RMSE was reached for the optimal drift factors $C_w = 0.0493$ and $C_C = 1.221$ The values of optimal current drift factor range from 1.2 to 1.3 (boundary given to the Powell's method being $[0.1, 2]$). The retrieved optimal wind drift factors range from about 0.037 to 0.049 (boundary for the optimization scheme being $[0.01, 0.06]$). Overall, these initial experiments point the greater contribution of the oil leakage, which occurred from the first five days, to the oil spill detected from the SAR observation on September 02, 2009.

Then we try to simulate the leakage with different duration. The result for simulation from a leakage start on August 21,2009 with different duration is given in Fig. 3.6-below. This simulation shows that the RMS error decreases as the duration increases. The minimum RMS error was reached for the source of leakage August 21, 2009 with duration 12 days. Most of the surface of the detected oil spill is actually explained by the leakage occurring on the first 5 days was happened for its duration maximum (12 days for source of leakage 21 August, 2009, 11 days for source of leakage 22 August, 2009, 10 days for 23 August, 2009, etc.) We will see the proof of this hypothesis later in Fig. 3.11.

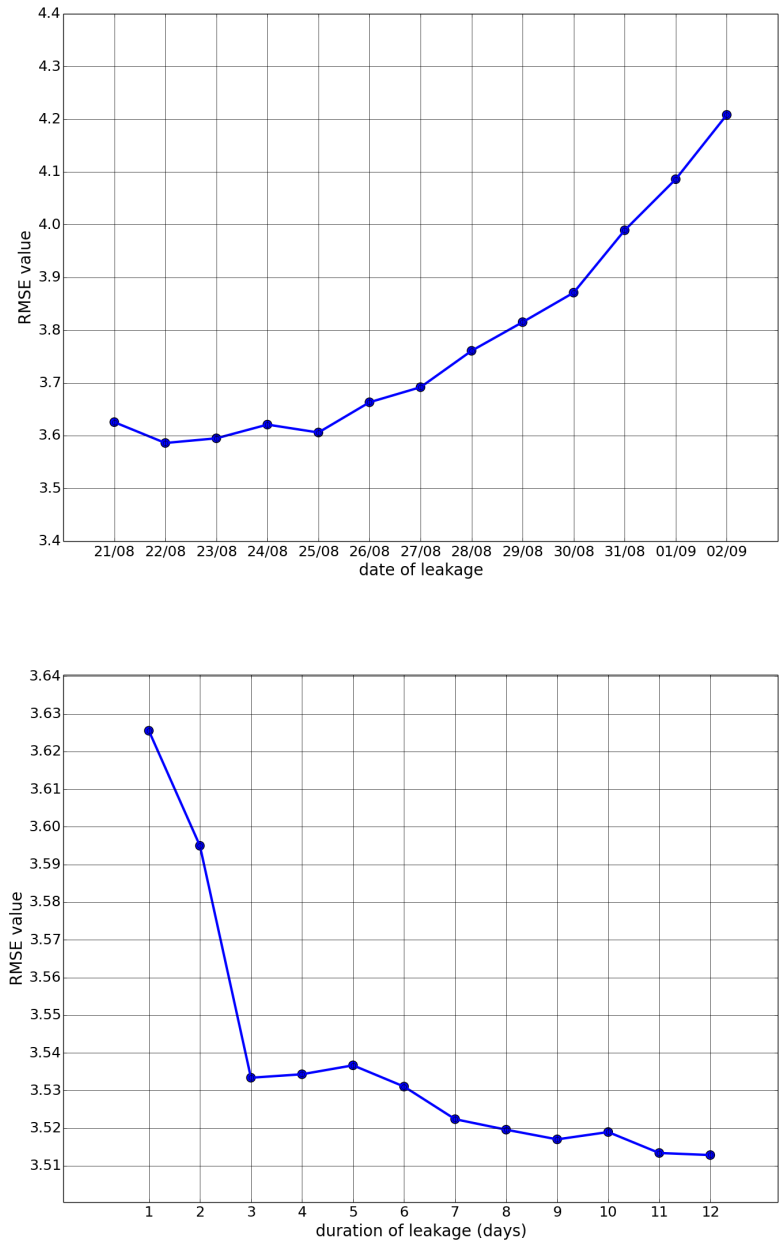

FIGURE 3.6 – Minimum RMSE of level set value of images SAR on September 02, 2009 with simulations of one-day oil leakage from August 21, 2009 to August 02, 2009 (a) and oil leakage started on 21 August,2009 with different duration (b) from Montara wellhead platform.

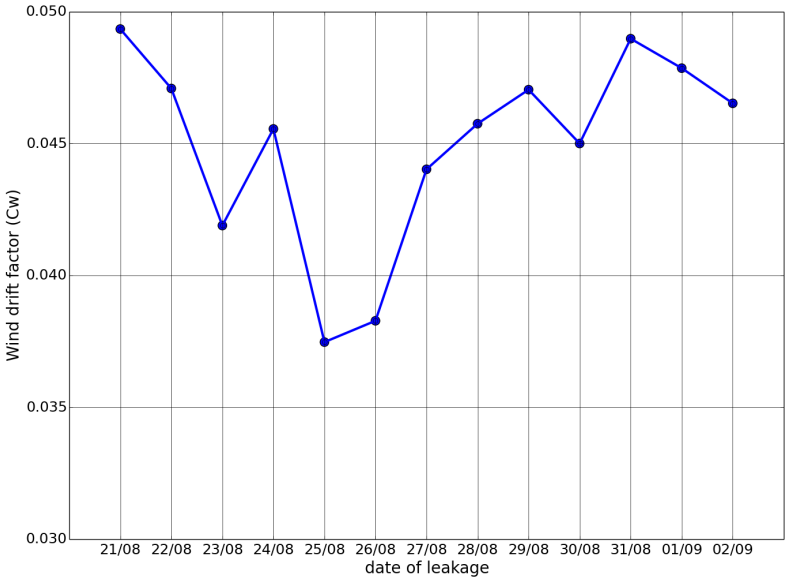

FIGURE 3.7 – Optimum value of wind drift factor C_w from simulations of one-day oil leakage from Montara wellhead platform from August 21, 2009 to September 02, 2009.

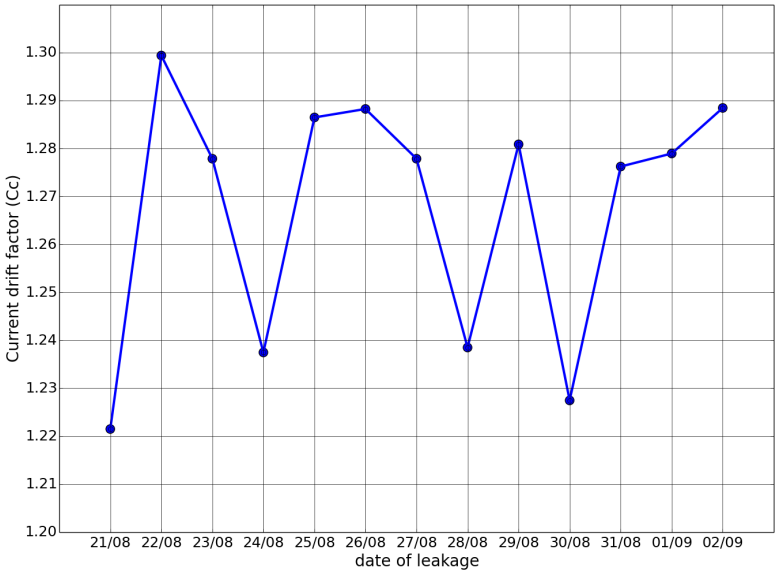

FIGURE 3.8 – Optimum value of current drift factor C_c from simulations of one-day oil leakage from Montara wellhead platform from August 21, 2009 to September 02, 2009

As an illustration of Powell's optimization procedure, we illustrate in Fig. 3.9 the minimized cost function landscape and the points at which the cost function is actually evaluated for

a twelve-days leakage started on August 21, 2009. The contribution of the wind is of minor importance compared to the current as the impact of C_w values is negligible.

We also report the level-set representations of the SAR-detected oil spill contour and of the transport model simulations for optimal drift factors $C_w = 0.0493$ and $C_C = 1.221$ with one-day duration in Fig. 3.10-above, as well as a comparison to the transport model simulations for optimal drift factors on simulations with 12 days duration $C_w = 0.0493$ and $C_C = 1.285$ Fig. 3.10-below. Optimal drift factors with twelve-days duration lead to a visually-better match between model simulations and the SAR detection. Besides, such one-day leakage hypothesis only provides a partial match to the observed oil spill spread.

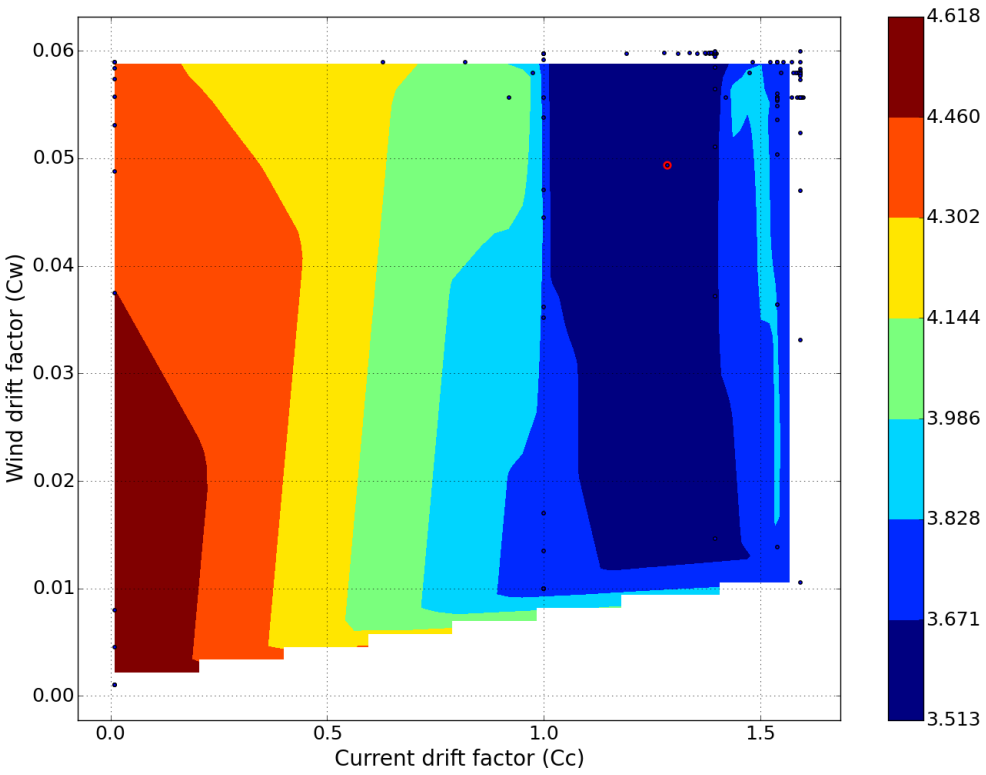

FIGURE 3.9 – Level-set-based distances between the SAR observation of the oil spill on September, 02 2009, and Lagrangian-based drift simulations of twelve-day oil leakage, started on August 21, 2009, within Powell's optimization scheme for wind and current drift coefficients. Red dot show the minimum RMSE value founded (3.513) with the value of $C_C = 1.285$ and $C_w = 0.0493$.

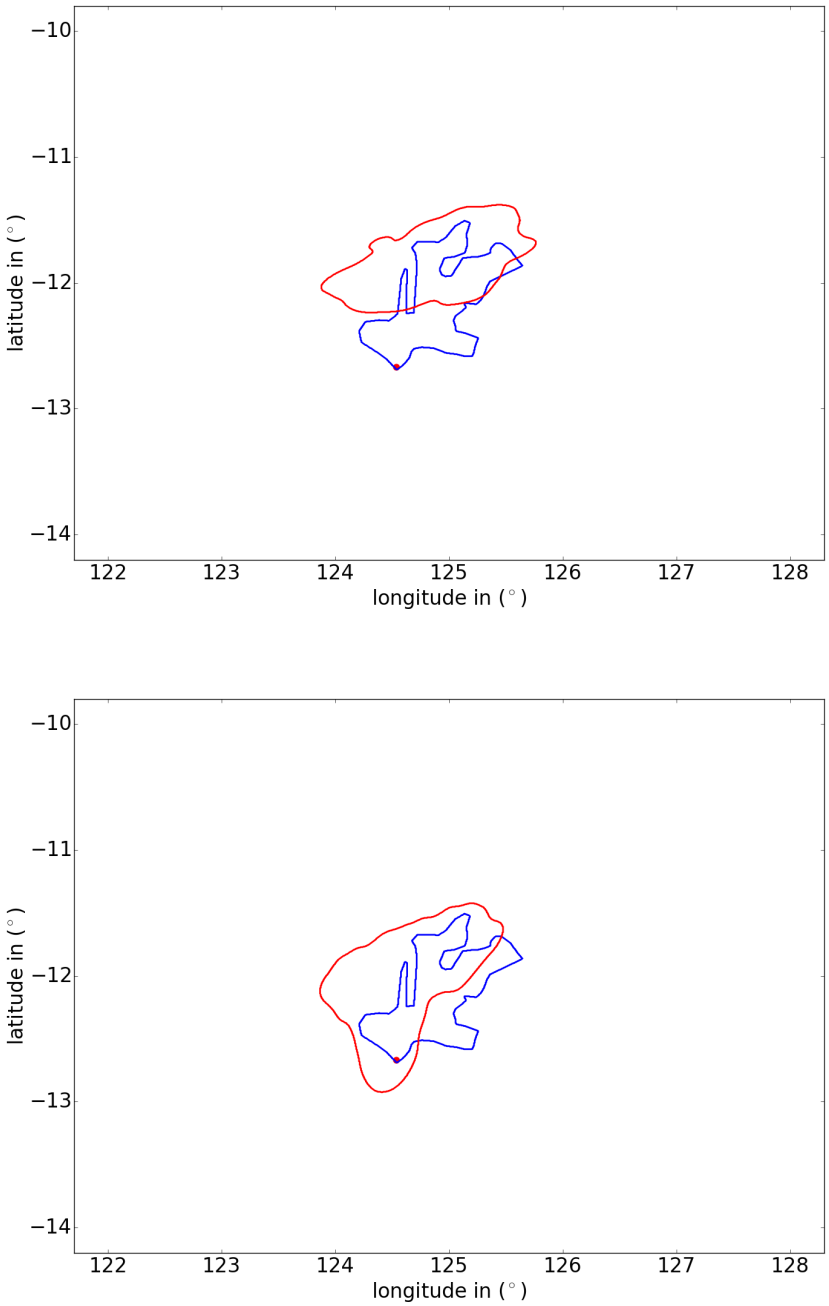

FIGURE 3.10 – Level-set-based representation of the SAR-derived detection of the oil spill on September 02, 2009, and Lagrangian-based drift simulations for a one-day oil leakage on August 21, 2009, with optimal wind and current drift coefficients, $C_w = 49.3\%$ and $C_C = 122.1\%$ (a) and Lagrangian-based drift simulations for a twelve-days oil leakage started on August 21, 2009 with optimal wind and current drift coefficients, $C_w = 49.3\%$ and $C_C = 128.5\%$ (b). The SAR detection and simulation contours are shows in blue and red line respectively and red dot is the position of Montara oil platform

We then carry out to the joint assimilation of both the oil leakage starting date, its duration and drift factors C_w and C_C. For each starting date and duration configuration, we proceed to

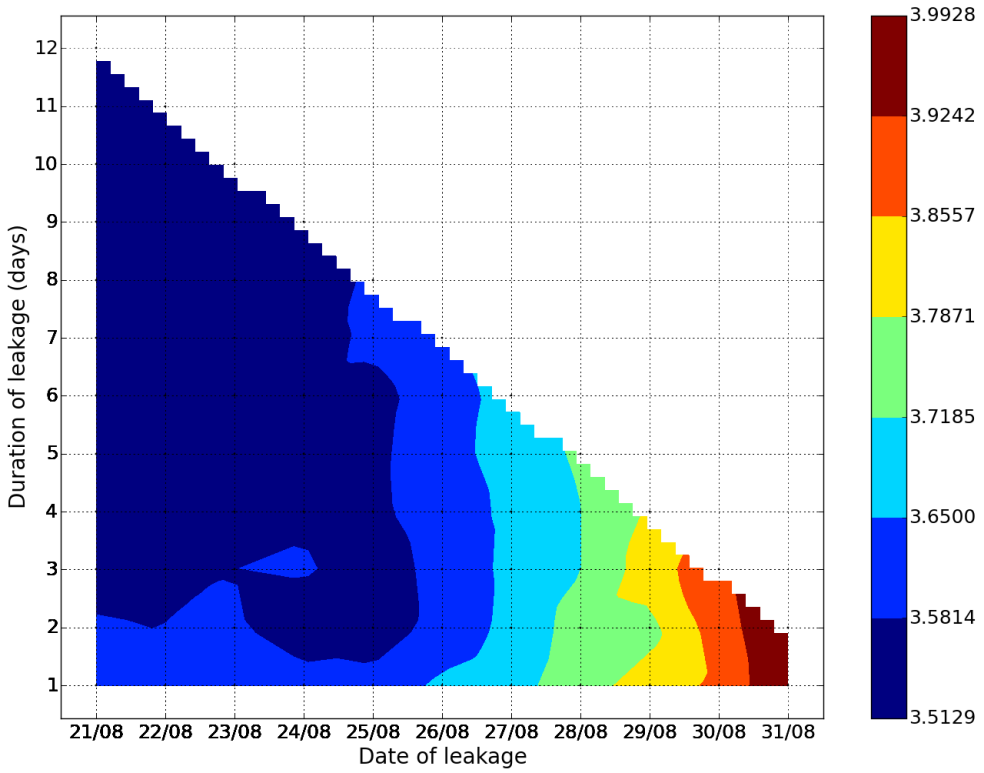

FIGURE 3.11 – Optimal level-set-based distances between the SAR observation of the oil spill on September 02, 2009, and Lagrangian-based drift simulations of oil leakage with respect to leakage starting date (x-axis) and duration (y-xis). The optimal level-set-based distances are issued from Powell's optimization of wind and current drift coefficients.

minimization of Eq. (3.8). We report in Fig. 3.11 the resulting optimal level-set-based distances between the detected oil spill and transport model simulations as a function of the starting date of the oil leakage and of its duration. The series of the level-set-based distance depict a clear increasing trend, which stresses the impact of the initial oil leakage on August 21. These results clearly support the existence of a continuous oil leakage for at least 5 days starting on August 21, 2009 with the minimum RMSE reached for oil leakage from oil leakage on August 21,2009 with duration 12 days. Estimated optimal drift factors, respectively $C_w = 0.0493$ and $C_C = 1.285$, are realistic and in agreement with the experiments reported above and previous work [78–80]. In Figure 3.11, the comparison between transport model simulations and the SAR-derived oil spill detection on September 02, 2009 points out the improved match associated to the five first-day with duration until the September 02 leakage hypothesis compared with the one-day leakage hypothesis with nominal and optimized wind and current drift factors. It is worth noting

that the Mobidrift simulations does not account for concentration effect of the particles in the diffusion process so that it yields a similar level-set shape with the duration of leakage. That explains the flatness of the level-set distances of Fig. 3.11 with duration leakage between 2 and 12 days.

3.7 Conclusion

We developed a novel framework for the assimilation of oil leakage parameters, including leakage starting data and duration along with wind and current drift factors, from a SAR-derived detection of an oil spill. This framework states the assimilation as the minimization of a level-set representations of the SAR-derived oil spill detection and of 2D transport model simulations. We illustrated its relevance on Montara oil spill case study. We showed that the observed oil spill on September 02, 2009 was mainly due to the oil leakage from August 21 until September 02 with majority of slick is coming from five first days of leakage (August 21-25, 2009). The estimated wind and current drift factors were in agreement with values previously reported in the literature. They were however significantly different from nominal parameters and shown to affect the match between the observed oil spill and transport model simulations.

This study opens new research avenues for the satellite-based operational monitoring of oil spills. Future work will further investigate the assimilation of oil leakage parameters from multi-date observations as well as other oil leakage configurations, such as illegal oil discharges from vessels or natural oil seeps.

Chapitre 4

Oil spill risk assessment in Indonesian Fisheries Management Area

4.1 Introduction . . . 62
4.2 Data and Study area . . . 65
4.2.1 Study Area . . . 65
4.2.2 Data Collection . . . 66
4.2.3 Marine Protected Area Data . . . 71
4.2.4 Marine fisheries data . . . 74
4.2.5 Socio-economic data for fishing activities, tourism services and salt ponds 75
4.3 Proposed methodology . . . 77
4.3.1 Oil spill risk indices . . . 77
4.3.2 Environmental and socio-economical vulnerability indices . . . 80
4.3.3 Global FMA-level risk index . . . 83
4.3.4 MPA-level vulnerability analysis . . . 84
4.4 Results and Discussion . . . 87
4.5 MPA-level risk assessment . . . 89
4.6 Conclusion and Discussion . . . 101

4.1 Introduction

Oil spill is one of the most destructive marine pollution with high impact on marine environments. Its negative impacts are not limited to wildlife, fisheries and coastal habitats but also affect human activities. Oil spill source coming from natural events and mostly from anthropogenic activities. Even though the number of marine accidents and the volume of oil released accidentally have declined, major oil spill accidental disasters such as Deepwater Horizon [89] Torrey Canyon oil spills [90] still have devastating long-term consequences. In addition, the still-growing activity of maritime transportation increases the risk of illegal oil discharges as well as accident-related pollutions. For instance, oil tankers are often among the ships suspected of illegal discharges. Routine tanker operations can lead to the release of oily ballast water and tank washing residues. Other oil-related waste produced by all types of ships such as fuel oil sludge, engine room wastes and foul bilge water, may also be released in the sea.

Indonesia is one of the largest maritime country in the world. It covers a 5.8 million km^2 water territory that consists of 2.7 million km^2 of exclusive economic zone and a 3.1 million km^2 territorial sea [91]. As three international sea lanes go across Indonesia waters, they involve a dense maritime traffic. From [92], the main sources of marine pollution in Indonesia are wastes from oil refineries, offshore exploration and shipping. The increase of maritime transportation, oil refineries and offshore exploration increases the threat of oil spill in Indonesian seas, the Montara oil spill in 2009 being a striking example [93]. In several regions oil spill is still a recurrence problem with unidentified source.

Marine and coastal resources are of key importance for Indonesia. Marine capture fisheries is one of the most important food resources which production from 2005 to 2014 increased on average of 3.58% per year. From 4 408 499 tonnes in 2005, fish production increased to 6 037 654 tonnes, with a commercial value of more than 7.5 billion dollars in 2014 [94]. The fish production consists of large and small pelagic species and demersal fish stocks as well as crustaceans, molluscs, and seaweeds. To enhance the management of marine and fisheries resources, the Ministry of Marine and Fisheries Indonesia divided marine waters into 11 Fisheries Management Areas (FMA). Indonesia also involves a very high biodiversity of species with a variety of important species such as coral reef fish, cetaceans, sea turtles, mangroves, sea grass,

dugongs, and seabirds. In some specific regions, the Government of Indonesia created in 2013 Marine Protected Areas (MPA) for a total surface area of 17 144 702 ha [95].

One of important biodiversities in the coastal zone is coral reef . A literature has mentioned the destructive influence of oil spill on coral reef. The oil will agitate the colony viability, damage the reproductive systems, lower growth rates and so on [96]. coral reef fish is the habitat for the coral reef fish. There is a positive relation between the live coral cover and the number of coral fish species as mentioned in the research conducted in the lagoon of Mataiva Atool, Tuamotu Archipelago [97]. Oil spill that destruct the coral reef will certainly impacted the coral reef fish. As reported from Directorate General Aquaculture MMAF, coral reef fish is one of contributor to Indonesia export product with value in 2014 more than US$ 20 million. In our work, we consider the coral reef fish as one of component that will be used on the risk assessment of oil spill that will be discussed later. Due to the increasing awareness of oil spill threat, the Indonesian government in cooperation with France has been developing ocean observation systems, oil spill monitoring being one of the targeted applications. This system is integrated with the spatial oceanography systems in the framework of INDESO project (Infrastructure of Development Space Oceanography). Using Synthetic Aperture Radar (SAR) sensors on-board satellites, one can monitor and detect oil spill at sea surface. The combination of such oil spill detection to Lagrangian drift models provides means to predict the drift of detected oil spills and their potential impact [93]. Many government institutions, such as the Ministry of Transport, the Ministry of Environment and Forestry, the Ministry of Marine and Fisheries, the Ministry of Energy and Mineral Resources, the National Disaster Management Authority, the Maritime Security Coordinating Agency, etc., have developed specific policies regarding intentional and unintentional oil spills. To implement such policies, especially monitoring and surveillance efforts, the assessment of a risk level that vulnerable areas may be impacted by oil spill sources is of high interest. For instance, in the North of Java and in Batam Island, recurrent oil spill occurrences are reported. Information onto their impacts on the coastal and marine ecosystems would be of key interest to implement adequate mitigation plans.

Recent studies have addressed similar issues in other regions. Several studies have analyzed oil spill pollutions in terms of ecological damage and of vulnerability for coastal area and coastal zone management [98], [99]. Fewer studies have targeted both environmental and socio-economic vulnerability to oil spill pollution. We may cite the combination of environmental and socioe-

conomic factor in Noirmoutier Island (France) [100], the determination of oil spill risk levels in coastal waters of Thailand [101], or the assessment of oil spill risk levels in the Chinese Bohai Sea [102]. The later analyzes different oil spill sources, namely ship and platform pollutions.

In this context, the objective of this study is to provide practical information for improving oil spill prevention and management policies for the Indonesia government, with a focus on Fisheries Management Areas. The proposed methodology involves two main steps : i) the assessment of global oil spill risk levels at the scale of fisheries management areas, ii) for high-risk areas, a further analysis at finer space-time scales using oil spill drift simulations. For these two levels, the vulnerability of a given area is evaluated both in terms of ecological and economical impacts. The ecological impact is evaluated with respect to a biodiversity index and the surface of MPA (Marine Protected Areas), whereas the economical impacts takes into account the economic value of exploited resources as well as the direct and indirect employment level of fisheries activities and maritime services. Our study clearly highlights strong discrepancies in the vulnerability to oil spill threat over the considered fisheries management areas. Such knowledge is of key interest to implement appropriate spatialized monitoring and prevention plans.

This Chapter is organized as follows. In Section II, we describe the characteristics of our study area. Section III presents the proposed methodology for the assessment of the vulnerability to oil spill pollution. We report the application of this methodology to the considered case study are in Section IV. Section V further discusses the key features of the proposed study.

4.2 Data and Study area

4.2.1 Study Area

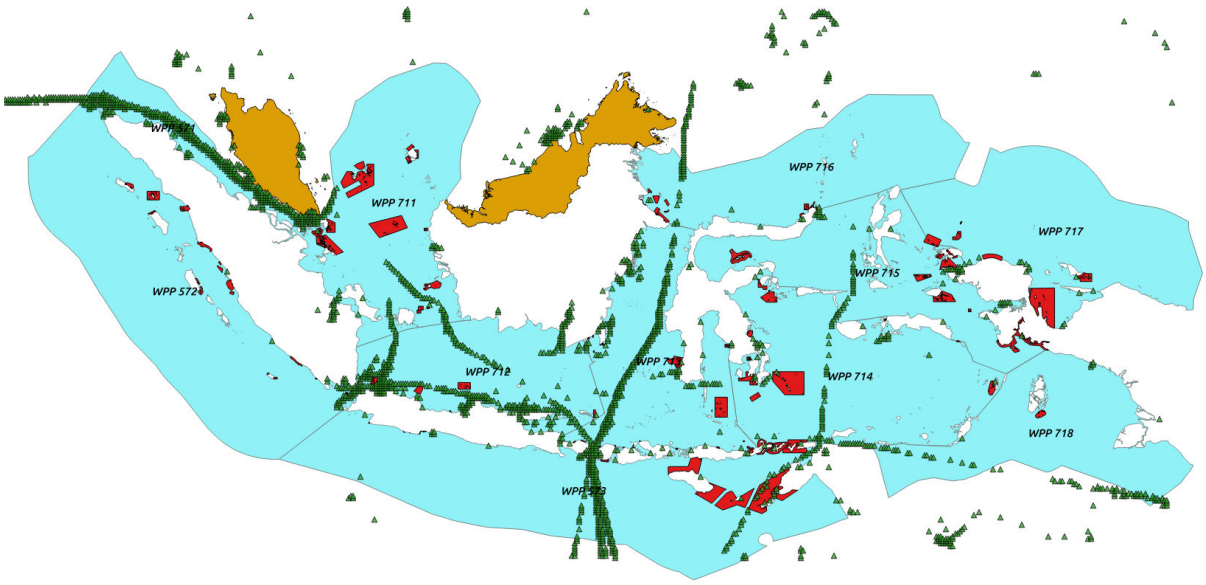

FIGURE 4.1 – Map of the study area with Indonesian Fisheries Management areas in blue, Indonesian land territory (in white) and its neighboring country (in brown), Marine Protected Area (in red) and ship density map estimated from AIS data to be used as potential source of unintentional and intentional oil spills (in green triangle)

Our study area comprise the Indonesian marine waters. From Ministerial Decree Number 18 on 2014, they were divided into 11 Fisheiries Management Areas (FMA), namely : (1) FMA 571 for Malacca Strait and Andaman Sea, (2) FMA 572 for Indian Ocean of Western Sumatera and Sunda Strait, (3) FMA 573 for Indian Ocean of Southern Java, Southern Nusa Tenggara, Savu Sea, and Western Timor Sea, (4) FMA 711 for Karimata Strait, Natuna Sea and South China Sea, (5) FMA 712 for Java Sea, (6) FMA 713 for Makassar Strait, Bone Bay, Flores Sea and Bali Sea, (7) FMA 714 for Tolo Bay and Banda Sea, (8) FMA 715 for Tomini Bay, Maluku Sea, Halmahera Sea, Seram Sea and Berau Bay, (9) FMA 716 for Sulawesi Sea and Northern of Halmahera Island, (10) FMA 717 for Cendrawasih Bay and Pacific Ocean and (11) FMA 718 for Aru Bay, Arafuru Sea and Eastern Timor Sea. Each FMA comprises Marine Protected Areas (MPA). The 11 FMA and the associated MPA are shown in Figure.4.1.

4.2.2 Data Collection

Oil spills can cause damage to fishing and aquaculture resources by physical contamination, toxic effects. They may also alter business activities. We collected and synthesized documents and reports from various institutions in Indonesia to assessment the vulnerability to oil spill pollution of the 11 FMA. The following factors regarded as possible proxies for oil spill occurrences were considered :

- the number of ship accidents (Section 4.3.1.1) ;
- the number of ships (Section 4.3.1.3) ;
- the location of all oil platforms in Indonesian waters (Section 4.3.1.2) ;
- the location of oil refinery facilities in Indonesia (Section 4.3.1.2) ;
- the list of Indonesian ports with oil distribution activities (Section 4.3.1.2) ;
- the total area of SAR-derived oil spill detection (Section 4.3.1.4).

With a view to evaluating the impact of oil spill pollutions in terms of environmental, social and economical impact, we collected the following information for each FMA and MPA :

- the number of species for important species groups (i.e. coral reef fish, cetaceans, sea turtles, mangroves, sea grass, dugongs, and sea birds) ;
- the number of MPA and the associated area ;
- total fish productions and associated economic values ;
- the number of water tourism services ;
- the number of salt pond centers ;
- the number of operating fishing vessels ;

4.2.2.1 Ship accident data

According to the International Tanker Owners Pollution Federation, there are three tiers of spills : tier 1 : $x \leqslant 7$ where x = amount of oil leak in tonnes categorized as small spills ; tier 2 : $7 \leqslant x \leqslant 700$ categorized as medium spills ; and tier 3 : $x \geqslant 700$ categorized as large spills. We

collected from the Indonesian Ministry of Environment, the Japan International Cooperation Agency (JICA) in Indonesia in cooperation with the Indonesian Ministry of Transport, ship accident statistics from 1975 until 2010 [92], [103] and [104]. Table 4.1 shows oil spill occurrences caused by ships in each FMA and their category. Natuna Sea (FMA 711) involved the greatest number of ship accidents which caused oil spills. Malacca Strait (FMA 571) was the region with the second greatest number of such accidents. Using the criteria from ITOPF, we assigned weights to each tiers of the ship-accident-related oil spill as follows : (w_i), $w_1 = (7 \div 700) = 0.01$, $w_2 = ((7 + 700) \div (2 \times 700) = 0.51$, and $w_3 = 1$.

TABLE 4.1 – Oil spills caused by ships in Indonesia FMA between 1975 and 2010

Year	Location	FMA	Ship type	Category of accident based on volume of oil spilled
1975	Malaka Strait	571	Oil tanker	3
1975	Malaka Strait	571	Oil tanker	1
1979	Lhokseumawe/North Sumatera	571	Oil tanker	3
1979	North Bali	713	Oil tanker	2
1992	Malaka Strait	571	Oil tanker	3
1993	Malaka Strait	571	Oil tanker	1
1994	Cilacap/South Java	573	Oil tanker	1
1996	Natuna	711	Oil tanker	1
1996	Riau Islands	711	Oil tanker	1
1996	Belawan	711	Oil tanker	1
1997	Malaka Strait	571	Oil tanker	3
1999	Batam	711	Oil tanker	1
2000	Cilacap/South Java	573	Oil tanker	3
2000	Riau/Batam Island	711	Oil tanker	3
2001	North Java	712	Oil tanker	3
2002	Riau/Bengkalis	711	Bulk carrier	1
2004	Riau	711	Oil tanker	2
2004	South Java/Cilacap	573	Oil tanker	3
2004	Malacca Strait	571	Cargo ship	1
2004	Riau/Pekanbaru	711	Oil tanker	1
2004	Riau/BatuAmpar	711	Cargo ship	1
2008	Semarang	712	Oil tanker	2
2010	Surabaya	712	Oil tanker	2
2010	Cilacap	573	Oil tanker	1

4.2.2.2 Oil platforms, oil refineries and oil distribution port

We synthesized the 2014 annual report of the Special Task Force for Upstream Oil and Gas Business Activities Indonesia [105] for the number of oil platforms, oil refineries and oil distribution ports. In each offshore and onshore block operated by oil and gas contractor we assumed there is one oil platform. We categorized the number of oil platforms, oil refineries and oil distribution ports in the zone of FMA as showed in the Table 4.2. That table shows that the greatest numbers of oil platforms were observed in Makassar Strait (FMA 713) followed by Natuna Sea (FMA 711). Meanwhile oil refineries and oil distribution ports were mostly observed in Java (Java Sea

in the North (FMA 712) and Indian Ocean in the South (FMA 573)) to support oil needs of Java Island, the island with the highest population in Indonesia.

TABLE 4.2 – Number of potential oil spill source considered in each FMA

FMA	Number of oil platforms	Number of oil refineries	Number of oil distribution ports	Number of point of potential source of unintentional spills from AIS detection	Area of oil spill polygon detected from SAR observation in km^2
571	9	3	0	348	358.92
572	2	0	0	57	45.39
573	1	2	3	217	112.37
711	16	4	2	107	1230.91
712	30	8	7	357	273.46
713	35	2	3	275	517.37
714	5	0	2	108	1.89
715	22	1	0	108	0
716	10	0	0	28	27.17
717	5	0	0	13	0
718	8	0	0	36	0

4.2.2.3 Maritime traffic density from AIS data

As a proxy of maritime traffic density, we extracted data from satellite-based Automatic Identification System (AIS) over a month on Indonesia marine waters. From this AIS dataset, we computed ship density maps as shown in Figure 4.2. We proceeded as follows. We computed the number of AIS messages received on average daily using a resolution cell of 0,01° x 0,01°. On the main sea line, the minimum density equals 10. We extracted the geographical region where this density is higher than 10. This region will be used as possible source of oil spill from ships. We used it as input data for the computation of oil spill risk levels both at the FMA and MPA scales. We synthesized in Table 4.2 the total number of ship-derived oil spill source points.

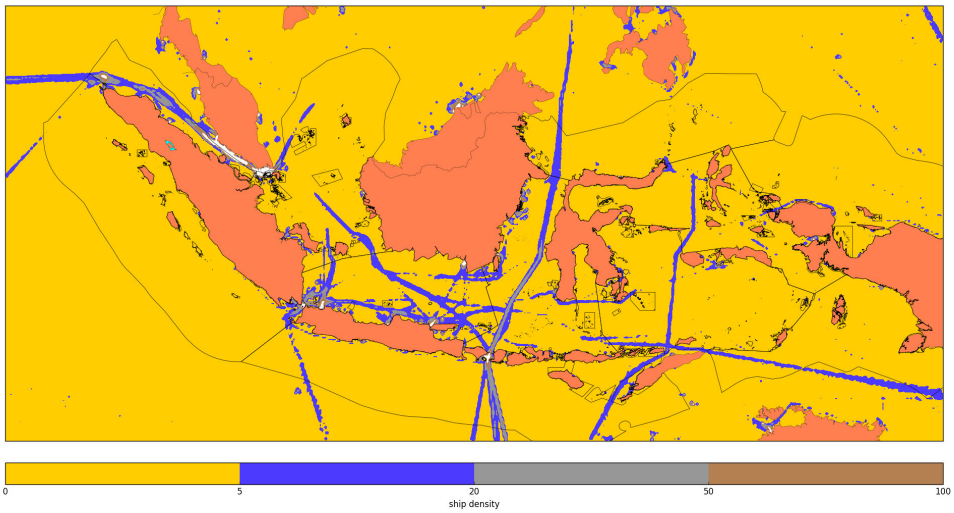

FIGURE 4.2 – Ship density on Indonesia marine waters based on the AIS data

4.2.2.4 Oil spill detection from SAR observation

We used oil spill detections extracted from SAR imagery within the framework of INDESO system from July 2014 until January 2017. There are 271 scenes collected on that period as seen in Figure 4.3. Overall 734 oil spill regions were detected corresponding to a total surface area of 2567.47 km^2. We report one example of SAR-based oil spill detection from a RADARSAT2 images on 25 July 2016 11 :07 :27 (UTC) in the Java Sea in Figure 4.4. We calculate the total surface area of the detected oil spills for each FMA zone as shown in Table 4.2.

To evaluate a risk level from SAR-derived oil spill detections, we used weighting factors. The weighing factor is the surface area of the detected oil spill divided by the coverage of the SAR image in the FMA. We report the area covered by SAR observations and the corresponding percentage w.r.t. the associated FMA area in Table 4.3.

In operational of Indeso system, everyday the chief of operation decided which area and the resolution of image SAR will be taken from the satellite. In the sake of efficient and effective, everyday normally only one scene SAR taken. This image will be processed and analyzed for many applications including for the detection of oil spill. In this relation there will be no overlap in one region in two scene different because one scene is for one day. If there are two scene was taken for the same area that will be for two different time.

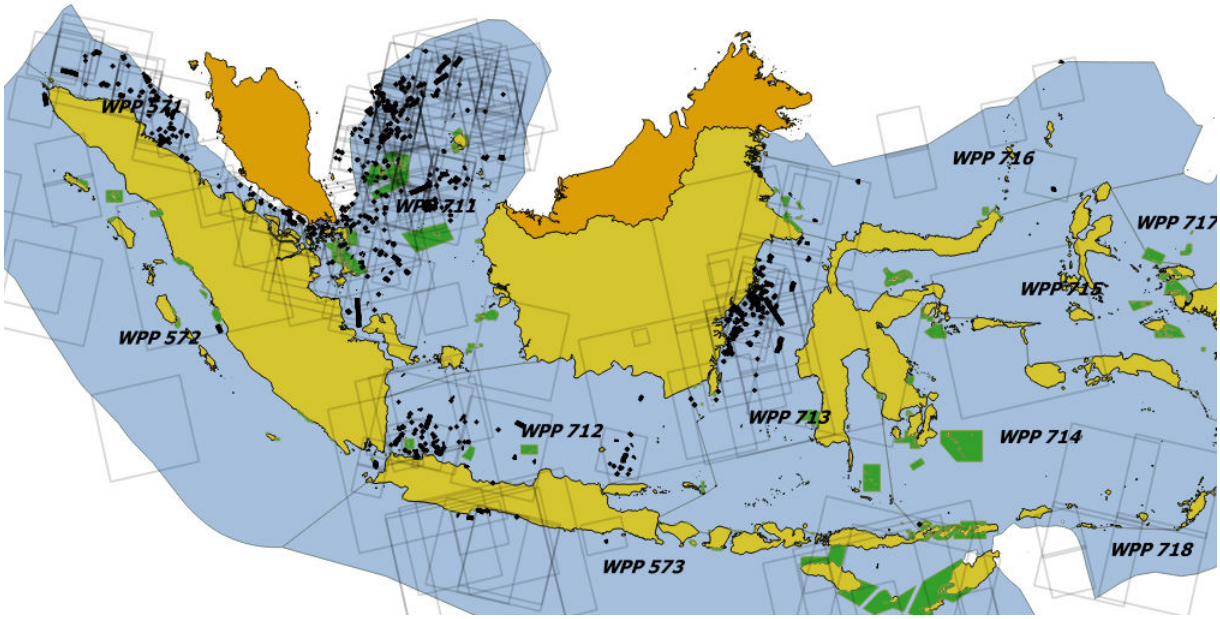

FIGURE 4.3 – SAR-based Detection of oil spills in the framework of INDESO system in Indonesia sea water territory (FMA are depicted in green) from 27 July 2014 until 16 January 2017), the boxes refer to the scene of the SAR images (271 scenes). We report the contours of oil spill detections in black.

TABLE 4.3 – Coverage area of SAR images within each FMA and associated percentage with respect to the total surface area of each FMA

Zone	Area of SAR detection coverage (km^2)	Area of FMA (km^2)	Coverage of SAR (%)
571	147 129.53	151 679.93	0.97
572	441 010.56	980 023.47	0.45
573	631 994.95	987 492.11	0.64
711	592 274.22	696 793.20	0.85
712	314 904.82	431 376.47	0.73
713	318 255.47	497 274.17	0.64
714	308 624.27	685 831.71	0.45
715	157 873.15	526 243.83	0.30
716	182 857.67	554 114.15	0.33
717	4092.69	409 269	0.01
718	7402.54	370 127	0.02

Table 4.3 showed that in FMA 711 and 712 the SAR coverage from 27 July 2014 until 16 January 2017 amounts to more than 70% and 81% of the total surface area of the FMA. FMA 571 has the highest coverage area of almost 100%. Meanwhile FMA 717 and 718 involves a low coverage only around 1% and 2%. This related to the low ship traffic in that zone. From our analysis of ship traffic density, the highest densities were found FMA 571, FMA 711 and FMA

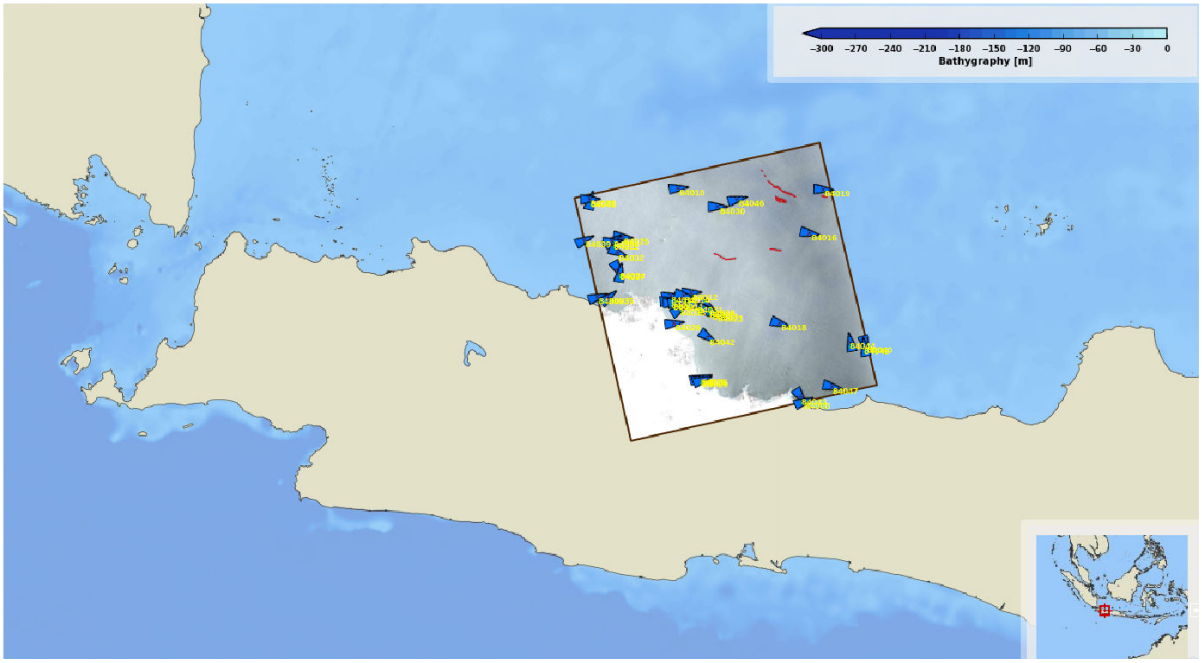

FIGURE 4.4 – Detection of oil spill on the Java Sea using SAR observation (using RADARSAT2 on INDESO system on 25 July 2016 11 :07 :27 (UTC), there are 14 detected oil spill contours (in red) and 40 neighboring ships (in blue) with their ID reference number (in yellow)

712 and the lowest ones in FMA 717 and 718. As shown in Table 4.2, the largest total surface area of oil spill was found in FMA 712 with 1230.91 km^2.

4.2.3 Marine Protected Area Data

To ensure the sustainability of fisheries production, the Government of Indonesia established Marine Protected Areas. The management of Marine Protected Areas (MPA) in Indonesia involves two types of MPA. A the first category of MPA was established and managed by the Central Government i.e Marine National Park, Marine Eco-tourism Park, Marine Nature Recreation Park, Marine Wildlife Sanctuary, and Marine Natural Preservation. A second one was established by Provincial or District Government and managed by Ministry of Marine and Fisheries i.e District Marine Conservation Area. We synthesized the area of MPA in each FMA from the report of Marine Protected Areas Governance [95]. The largest MPA was in FMA 715 with a total surface area of 2 533 986.96 ha and the smallest was reported in FMA 571 with a total area of 12 001.29 hectares.

Each MPA may involve specific and important species. Indonesia comprise 11 marine ecoregions of the world (MEOW) as defined by Spalding [12] i.e. Malacca Strait, Western Sumatra,

Southern Java, Lesser Sunda, Sunda Shelf/Java Sea, Sulawesi Sea/Makassar Strait, Banda Sea, North East Sulawesi/Tomini Bay, Halmahera, Papua and Arafuru Sea. Each ecoregion involves a specific habitat type. We used the Report of the Directorate of Conservation for Area and Fish Species, Ministry of Marine Affairs and Fisheries on 2012 [106]. Based on this report, we focused on important species, namely coral reef fish, cetaceans, sea turtles, mangrove, sea grass, dugongs, and seabirds. The associated MPA-related data in each FMA were synthesized in Table 4.4

TABLE 4.4 – Considered MPA-based ecological data for each FMA : number of species for coral reef fish, sea turtles, mangrove and seabirds, total seagrass area, number of dugong populations, total MPA area.

FMA	coral reef fish species	cetaceans spots	seaturtles species	mangrove species	seagrass area (hectares)	dugongs populations	seabirds species	area of MPA (hectares)
571	952	0	3	35	162,4	0	63	12 001.29
572	915	1	6	0	2 132,4	1	19	865 807.45
573	3238	1	5	47	2 059,8	100	321	4 200 451.99
711	1509	0	6	31	38 949,87	100	374	2 055 649.77
712	1509	0	6	31	1 661,61	100	374	409 758.38
713	1785	3	0	0	33 466,05	0	0	1 169 268.68
714	1760	1	5	0	19 484,48	50	173	2 127 657.52
715	1561	2	4	20	5 664,26	50	301	2 533 986.96
716	1711	1	2	23	1 633,82	100	318	1 387 006.39
717	1728	1	4	35	621 909,56	100	96	1 832 768.64
718	1368	1	5	53	856 300	200	202	550 344.93

coral reef fish coral reef can be regarded as tropical forests of marine ecosystems [107]. coral reef are very fragile ecosystems. It is very sensitive to the alteration of environment. coral reef is a habitat for coral reef fish so that the destruction of coral reef will impacted the coral reef fish. In Indonesia there are five ecoregions whose estimated species richness of coral reef fish exceeds 1700 species i.e Sulawesi Sea/Makassar Strait, Banda Sea, Lesser Sundas, Papua, and Halmahera. It is estimated that 1785 species to live in the Sulawesi Sea and Makassar Strait ecoregion. All of these five sites are considered as habitats with an extremely high reef fish diversity. FMA 573 comprises two ecoregions (Southern Java and Lesser Sundas) with the greatest number of species (3238 species).

Cetaceans 9 FMA, contained within 6 ecoregions, stand out for their special importance for cetacean populations. Coastal cetaceans living on the nearshore waters are found on the southern coast of Papua and eastern coast of Kalimantan. In eastern Kalimantan (FMA 713) there are two spots for coastal cetaceans, one spot in the FMA 715 (Kaimana) and one spot in the FMA

718 (Arafuru Sea). Great whales and oceanic dolphins are found in the North of Bali (FMA 713), Lesser Sundas (FMA 573), Banda Sea (FMA 714), Halmahera Sea (FMA 715) and several existing MPAs, such as Bunaken National Park in North Sulawesi (FMA 716) and the Raja Ampat MPA in Papua (FMA 715) are particularly rich in marine mammal diversity because of its deep-sea near-shore environment. We faced a lack of data in Western Sumatra (FMA 712). In this area no cetacean observation data were reported even tough the presence of cetaceans in this area was acknowledged.

Sea turtles Being a habitat for six of the world's sea turtle species (Leatherback, Hawksbill, Green, Olive Ridley, Flatback, Loggerhead), Indonesian seas play a significant role in sustaining these species. Turtles may be found in different areas, several regions comprising sea turtle reproduction sites. All six sea turtle species can be found in both Western Sumatra (FMA 572) and Sunda Shelf/Java Sea (FMA 711 and FMA 712) ecoregions. Five sea turtles were found in Lesser Sunda (FMA 573) and Arafuru Sea (FMA 718).

Mangrove The mangrove forest grows in tidal areas such as coastal areas, lagoons and estuaries. This forest is always or regularly inundated by seawater and affected by tides. For mangrove ecosystems, the Arafura Sea (FMA 718) ranks first in terms of mangrove species richness with 53 species. The second region is Bali and Lombok in Lesser Sunda (FMA 573) with 47 species, followed by Papua and the Malacca Strait, each with 35 species.

Seagrass Seagrass is unique flora in the sea. It is the grass that has the roots and leaves and live submerge in the sea. Seagrass needs sunlight to live so that in general seagrass develops extensive seagrass beds on the seafloor in regions that can be reached by sufficient sunlight. Seagrass have been receiving great attention because of their importance : for stabilizing coastal sediments, providing food and shelter for diverse organisms, as well as nursery grounds for fish and invertebrates. As such, seagrass is of key importance both for small-scale fisheries. In Indonesia, the large seagrass beds are found in the Arafura Sea, Papua, the Sunda Shelf and Java Sea. The surface area in Arafura Sea (FMA 718) is 856 300 hectares [108]. Papua (FMA 717) follows with 621 909,56 hectares and Sunda Shelf (FMA 711) involves 38 949,87 hectares.

Dugongs The distribution and estimated population size of Dugongs in Indonesia closely relate to seagrass extent. The Arafura Sea involves the greatest number of dugong populations.

In Arafura Sea (FMA 718) it was estimated that there are more than 200 populations of Dugongs, and in FMA 717,FMA 716, FMA 711, FMA 712 and FMA 573 there are more than 100 populations in each of area.

Seabirds Sunda Shelf and Java Sea ecoregion is acknowledged as a important ecoregion for the conservation of mangrove ecosystem. Mangrove is a habitat for seabirds especially migratory and colonial seabirds and waterbirds. This ecoregion is the richest in seabird species (374 species). It is a habitat for a large number of endemic and threatened species. FMA 573 is the second one with 321 species, with 206 species in Lesser Sundas and 115 species in Southern Java. Sulawesi Sea and Makassar Strait ecoregion ranks third in terms of seabird richness (318 species), followed by Arafura Sea (202 species). The Arafura Sea (FMA 718) contains a regionally-important area (Wasur National Park and Rawa Biru). This is an area where seabirds rest during their migratory routes.

4.2.4 Marine fisheries data

Fishing and aquaculture are important industries which may be affected by oil spills in various ways. In this work, we considered two aspects of marine and capture fisheries production : the total production biomass for the different fish stocks and the associated economic value. Regarding the first aspect, commercially exploited fish and plants may be killed as a result of oil smothering and toxicity. Regarding the economic value, catches and cultivated stocks may become physically contaminated or may acquire an oil-derived taste referred to as 'tainting'[1] Public confidence in seafood products can quickly degrade if suspected of contamination or actually contaminated, resulting in a economical losses.

Some animals, especially bivalve molluscs, are highly vulnerable to taint. Such animals may ingest suspended oiled particles in the water column. Other animals, such as high-fat fish, typically show higher accumulation level of oil-induced molecules in their tissues [109]. The impact of oil however differs among species. As pointed out by the ITOPF, salmon, trout, and molluscs are immediately affected by an exposure to oil, whereas crabs may not be. By constrast, 60 days after an oil contamination, the remaining contamination has almost disappeared for salmon and

[1]Taint is commonly defined as an odor or flavor that is foreign to a food product. The degree of taint which may result and consumer tolerance levels for taint are different for different seafood products, communities and markets.

trout, but remains important for mussels. These elements suggest considering different species categories to assess the impact of oil spill on fisheries activities.

To analyze the impact of oil spill in each FMA, we synthesized fisheries production data from the report of MMAF 2014 [94]. Fisheries production data are categorized w.r.t. large pelagic species, small pelagic species, demersal species, crustaceans, moluscs, and other fish (seaweed,etc). We report our synthesis in Table 4.5.

For the calculation of oil spill risk levels for marine capture fisheries, we define a weighing factor for each category of fisheries production data. For the molluscs and seaweed, we considered a weighting factor of 1 since they are the most fragile species. Crustaceans are associated with a weighing factor of 0.3 and the other categories a weighing factor of 0.5, as they have greater capabilities to reduce the taint 60 days after the exposure to oil.

TABLE 4.5 – Fish production and associated economic value in each FMA

FMA	Marine Capture Fisheries Production (tonnes)							Economic Value (US $)
	Big Pelagic	Small Pelagic	Demersal	Crustacean	Molluscs	other fish (other aquatic animals, seaweeds)	Total production	
571	48 054.87	165 298.70	170 542.49	56 794.78	68 307.09	10 289.39	519 287.33	618 970 680.62
572	167 979.70	195 436.04	192 374.80	49 063.18	12 731.18	10 580.41	628 165.30	798 158 542.33
573	171 716.73	139 910.28	69 612.83	7189.67	7387.63	7527.40	403 344.56	502 048 320.11
711	129 097.55	163 837.50	255 187.41	74 172.84	45 396.04	15 777.47	683 468.81	887 424 463.25
712	211 635.05	355 803.17	361 306.71	92 165.08	59 747.78	21 823.72	1 102 481.52	1 369 786 495.97
713	172 481.12	254 066.85	189 332.59	45 197.38	14 093.06	14 759.71	689 930.71	869 398 013.25
714	179 955.19	221 737.71	164 994.94	3323.87	11 686.31	10 626.09	592 324.11	697 969 715.30
715	229 470.90	146 485.70	82 855.38	3721.29	4552.28	5565.13	472 650.68	580 848 485.04
716	209 596.67	73 790.80	30 958.92	6611.61	8171.29	1888.47	331 017.76	420 002 357.71
717	61 644.08	44 018.77	48 854.25	3179.35	6089.16	2777.89	166 563.50	203 308 612.21
718	117 020.14	66 302.13	223 512.67	19 870.95	10 517.17	11 379.30	448 602.36	580 153 106.53

4.2.5 Socio-economic data for fishing activities, tourism services and salt ponds

With a view to evaluating the socio-economic impact of oil spill, we consider data on fishing activities, tourism services as well as other coastal activities, namely salt ponds. Oil spill may have strong impacts on fishing gears. Fishing and cultivation gear may get oiled, leading to the risk of catches or stock becoming contaminated or fishing being halted until gear is cleaned or replaced. An other negative impact of oil spill is the interruption of subsistence, recreational and commercial fishing activity and the disruption of salt production cycles, which can have important economic consequences. Based on the report of MMAF on 2014, there are more than 8000 fishing vessels that operated in Indonesia marine water [94] in 2014. In 2015, 548 water tourism services were reported over Indonesia [110].

Traditional salt ponds is an important economic activity of Indonesia with a total production of 2 077 370.83 tonnes in 2015. The direct employment involves more than 21 000 persons [110]. MMAF reported a total surface area of traditional salt ponds of 25 766.13 hectares. This sector is vulnerable to oil spills since the intake of salt ponds uses fresh sea water directly from the ocean. Traditional salt ponds spread over 43 districts and cities in Indonesia. We categorized the location of these ponds into 11 FMA and we calculated the total surface area, production level and workers number of traditional salt ponds in each area.

TABLE 4.6 – Considered socio-economic characteristics of fisheries activities, maritime tourism activities and traditional salt ponds in each FMA.

FMA	Number of fishing boat	Number of water tourism service	Traditional Salt Production		
			Area (hectares)	Production (tonnes)	Labor
571	197	18	123,45	9135.84	1080
572	748	5	0	0	0
573	977	22	706,89	26 033.10	2040
711	1917	0	0	0	0
712	236	13	21 867.66	2 485 939.53	11020
713	693	168	2980.93	264 712.07	6840
714	213	73	0	0	0
715	528	124	87,2	709,83	70
716	478	98	0	0	0
717	575	27	0	0	0
718	1500	0	0	0	0

4.3 Proposed methodology

We detail in this section the proposed methodology for the evaluation of oil spill-related risk indices in Indonesia. We follow the general framework introduced in [101]. For each type of data, the risk indices are computed as percentages and typically account for weighing factors, which weigh the relative contribution or impact of associated categories (e.g., oil spill categories for ship accident data, species categories for ecological data,...). We detail below the proposed indices for each type of data.

We first introduce oil spill risk indices with respect to different oil spill sources and the associated collected data (Section 4.3.1). We then define vulnerability indices with respect to ecological and socio-economical impacts (Section 4.3.2). These indices are used to define global FMA-level risk indices (Section 4.3.3). In a second, we explore a vulnerability analysis at finer space-time scales on MPA (Section 4.3.4).

The identification of oil spill risk indices are using the average percentage risk. The average percentage risk is the percentage risk of critical variable divided by number of critical variables considered at the national scale. In the calculation of percentage risk of critical variable, for some variables we considered using the weighting factor. For example on the calculation of ship accident related percentage risk that will be discussed later in the subsection 4.3.1, we used the three weighting factor for three class different. For some other variables that we have not had enough detail information, we considered not using the weighting factor.

4.3.1 Oil spill risk indices

4.3.1.1 Ship-accident-related risk indices

From Table 4.2 and using the criteria from ITOPF, we assigned weights to each tier of the oil spill ship accidents as follows : (w_i), $w_1 = (7 \div 700) = 0.01$, $w_2 = ((7 + 700) \div (2 \times 700) = 0.51$, and $w_3 = 1$. We calculated risk indices associated with oil spills due to ship accidents in each of FMA as follows :

$$PR_{shipaccident} = \left[\sum_{i=1}^{n} w_i \times \frac{f_i}{FI_i}\right] \times \frac{100}{\sum_{i=1}^{n} w_i} \tag{4.1}$$

where f_i is cumulative frequencies of oil spill from ship accident observed during the period at tier i for the FMA interest and FI_i is highest frequencies of oil spill from ship accident at tier i observed at one of the 11 FMA.

For instance, the cumulative frequencies of oil spill from ship accident in FMA 573 are 2,0,2 for category 1,2,3 whereas the FI_i at each tier is 7 accidents (in FMA 711), 2 accidents (in FMA 712) and 4 accidents (in FMA 571). The PR_shipaccident for FMA 573 was estimated as follows :

$$\begin{aligned} PR_{shipaccident-FMA573} &= \left[(w_1 \times \frac{f_1}{FI_1}) + (w_2 \times \frac{f_2}{FI_2}) + (w_3 \times \frac{f_3}{FI_3})\right] \\ &\quad \times \frac{100}{(w_1 + w_2 + w_3)} \\ &= \left[(0.01 \times \frac{2}{7}) + (0.51 \times \frac{0}{2}) + (1 \times \frac{2}{4})\right] \\ &\quad \times \frac{100}{0.1 + 0.51 + 1} = 66.07 \end{aligned}$$

We estimated the $PR_{shipaccident}$ for all FMA using this method and the results are shown in Table 4.7 in column PR_s1.

4.3.1.2 Oil-activity-related risk indices

We calculated risk indices for oil spills from oil platforms through the number of oil platforms observed in a FMA zone of interest normalized by the maximum number of oil platforms encountered in one of the 11 FMA. We did not assign any weighing factor because we did not know the capacity of production and related activities that might cause oil spills with varying amounts. For instance, 30 oil platforms were observed in the zone FMA 712, whereas the highest number of oil platforms was found in the zone FMA 713 with 35 oil platforms. The resulting risk index ($PR_{oilplatform}$) in zone FMA 712 is thus equal to :

$$PR_{oilplatform-FMA712} = \frac{30}{35} \times 100 = 85.71 \tag{4.2}$$

We calculated risk indices from oil refinery and oil distribution port data with the same method for each zone of FMA. The result of $PR_{oilplatform}$, $PR_{oilrefineries}$, $PR_{oildistributionport}$ for all FMA are shown in Table 4.7 in column PR_s2, PR_s3, PR_s4 respectively.

4.3.1.3 Maritime-traffic-related risk indices

From maritime traffic density data reported in Table 4.2, we defined oil spill risk indices from the ship density observed on each FMA normalized by the highest ship density among the 11 FMA. In this calculation, we did not assign any weighing factor because we had no complementary information on the vessel types and nor on their oil capacity. For instance, a ship density of 348 points was observed in FMA 571, whereas the highest ship density was found in FMA 712 with a density of 357. The resulting risk index ($PR_{shipdensity}$) in FMA 571 is thus equal to :

$$PR_{shipdensity-FMA571} = \frac{348}{357} \times 100 = 97.48 \tag{4.3}$$

Proceeding similarly for all FMA, we report in Table 4.7 in column PR_s5 the oil risk indices issued from maritime traffic data.

4.3.1.4 SAR-derived risk indices

From the collected SAR-derived oil spill data reported in Table 4.2, we define SAR-derived oil spill risk indices. We used as weighing factors, the total surface area of the SAR-derived oil spill detection in each FMA divided by the total surface area of the FMA (Table 4.3). Hence, associated risk indices are defined as follows for each FMA :

$$\begin{aligned} PR_{detectionSAR} &= \left[\frac{d_i}{DI}\right] \times 100 \\ d_i &= \left[\frac{AreaPolygonOil_i}{AreaSAR_i}\right] \times AreaFMA_i \end{aligned} \tag{4.4}$$

where d_i is the total area of the SAR-derived oil spill detection and DI is highest value among the 11 FMA.

For instance, the total oil spill area detected in SAR observations on FMA 573 is 112.37 km^2 for a global SAR coverage of 631 994.95 km^2 and a total surface area of 987 492.11 km^2 of FMA 573. The value of d_i in FMA 573 is :

$$d_{573} = \left[\frac{112.37}{631\,994.95}\right] \times 987\,492.11 = 175.58$$

We calculated the value of d_i for each zone of FMA and the maximum of d_i (DI) was found in FMA 711 with value 1448.13, so that the PR_detectionSAR for FMA 573 was estimated as follows :

$$PR_{detectionSAR-FMA573} = \left[\frac{175.58}{1448.13}\right] \times 100 \quad = 12.12$$

We estimated the $PR_{detectionSAR}$ the other FMA similarly. Results are shown in column PR_s6 in Table 4.7 .

TABLE 4.7 – Oil spill risk indices derived from different data sources for the 11 FMA. We let the reader refer to the main text for the definition of the different indices PR_s k

FMA	PR_s1	PR_s2	PR_s3	PR_s4	PR_s5	PR_s6
571	66.07	25.71	37.50	0	97.48	25.55
572	0	5.71	0	0	15.97	6.96
573	33.08	2.86	25	42.86	60.78	12.12
711	50.33	45.71	50	28.57	29.97	100
712	33.55	85.71	100	100	100	25.87
713	16.78	100	25	42.86	77.03	55.82
714	0	14.29	0	28.57	30.25	0.29
715	0	62.86	12.50	0	31.03	0
716	0	28.57	0	0	8.05	5.69
717	0	14.29	0	0	3.74	0
718	0	22.86	0	0	10.34	0

4.3.2 Environmental and socio-economical vulnerability indices

4.3.2.1 MPA-derived vulnerability indices

From the MPA data collected above, we derive environmental vulnerability indices with respect to oil spill pollution at the FMA level. For each MPA-related ecological feature described in Table 4.4, we derive a vulnerability index from the ecological feature observed for a given FMA divided by the greatest value among the 11 FMAs. In this calculation, we did not assign any feature-specific weighing factors. We give the same relative significance to all the considered ecological features. For instance, regarding the vulnerability index for coral reef fish, 952 species of coral reef fish were observed in FMA 571, whereas the highest number of species of coral reef

fish was found in FMA 573 with 3238 species. The resulting vulnerability index for coral reef fish ($PR_{coralfish}$) in FMA 571 is thus equal to :

$$PR_{coralfish-FMA571} = \frac{952}{3238} \times 100 = 29.40$$

We proceeded similarly for all the ecological features to derive vulnerability indices $PR_{coralfish}$, $PR_{cetaceans}$, $PR_{seaturtles}$, $PR_{mangorove}$, $PR_{seagrass}$, $PR_{dugongs}$, $PR_{seabirds}$, and PR_{MPA} as shown in Table 4.8 from column PR_env1 to column PR_env8 respectively.

TABLE 4.8 – Vulnerability indices computed for each FMA from MPA-level ecological features. We let the reader refer to the main text for the definition of the different indices PR_end k.

FMA	PR_env1	PR_env2	PR_env3	PR_env4
571	29.40	0.00	50.00	66.04
572	28.26	33.33	100.00	0.00
573	100.00	33.33	83.33	88.68
711	46.60	0.00	100.00	58.49
712	46.60	0.00	100.00	58.49
713	55.13	100.00	0.00	0.00
714	54.35	33.33	83.33	0.00
715	48.21	66.67	66.67	37.74
716	52.84	33.33	33.33	43.40
717	53.37	33.33	66.67	66.04
718	42.25	33.33	83.33	100.00
FMA	PR_env5	PR_env6	PR_env7	PR_env8
571	0.02	0.00	16.84	0.29
572	0.25	0.50	5.08	20.61
573	0.24	50.00	85.83	100.00
711	4.55	50.00	100.00	48.94
712	0.19	50.00	100.00	9.76
713	3.91	0.00	0.00	27.84
714	2.28	25.00	46.26	50.65
715	0.66	25.00	80.48	60.33
716	0.19	50.00	85.03	33.02
717	72.63	50.00	25.67	43.63
718	100.00	100.00	54.01	13.10

4.3.2.2 Fisheries-related vulnerability indices

Proceeding similarly to the MPA-derived indices, we define fisheries-related vulnerability indices from the fisheries production data reported in Table 4.5 as follows :

$$PR_{fishproduction} = \left[\sum_{i=1}^{n} w_i \times \frac{f_i}{FI_i}\right] \times \frac{100}{\sum_{i=1}^{n} w_i} \tag{4.5}$$

where f_i refer to fish production for different fish species observed during the period at tier i for the FMA interest and FI_i is the highest production level at tier i among the 11 FMA.

For instance, fish production in FMA 573 is respectively of 171 716.73 tonnes, 139 910.28 tonnes, 69 612.83 tonnes, 7189.67 tonnes, 7387.64 tonnes, 7527.41 tonnes, for large pelagic species, small pelagic species, demersal species, crustaceans, moluscs, and other fish (seaweed,etc) whereas the greatest production FI_i is respectively of 229 470.90 tonnes for large pelagic species (in FMA 715), 355 803.17 tonnes, 361 306.71 tonnes, 92 165.08 tonnes, 21 823.72 tonnes for small pelagic, demersal, crustaceans, and others fish species (in FMA 712) and 68 307.09 tonnes for molluscs (in FMA 571). Thus vulnerability index PR_fishproduction for FMA 573 was estimated as follows :

$$\begin{aligned}
PR_{fishproduction-FMA573} = &[(w_1 \times \frac{f_1}{FI_1}) + (w_2 \times \frac{f_2}{FI_2}) + (w_3 \times \frac{f_3}{FI_3}) \\
&+(w_4 \times \frac{f_4}{FI_4}) + (w_5 \times \frac{f_5}{FI_5}) + (w_6 \times \frac{f_6}{FI_6})] \\
&\times \frac{100}{(w_1 + w_2 + w_3 + w_4 + w_5 + w_6)} \\
=&[(0.5 \times \frac{171\,716.73}{229\,470.90}) + (0.5 \times \frac{139\,910.28}{355\,803.17}) \\
&+(0.5 \times \frac{69\,612.83}{361\,306.71}) + (0.3 \times \frac{7189.67}{92\,165.08}) \\
&+(1.0 \times \frac{7387.64}{68\,307.09}) + (1.0 \times \frac{7527.41}{21\,823.72})] \\
&\times \frac{100}{(0.5 + 0.5 + 0.5 + 0.3 + 1.0 + 1.0)} \\
&= 30.09
\end{aligned}$$

We proceeded similarly for the 11 FMA and synthesized our results in column PR_soc1 of Table 4.6.

We derived similarly vulnerability indices based on the economic value of each fisheries. For instance, in FMA 571 the economic value of marine capture fisheries is US $618 970 680.62, whereas the highest economic value was found in FMA 712 with US $1 369 786 495.97. The resulting vulnerability index ($PR_{economic-value}$) in FMA 571 is thus equal to :

$$PR_{economic-value-FMA571} = \frac{618\,970\,680.62}{1\,369\,786\,495.97} \times 100 = 45.19$$

We proceeded similarly for the 11 FMA and synthesized our results in column PR_soc2 of Table 4.6.

4.3.2.3 Human-activity-related indices

Based on the data collected on coastal and marine human activities (Table 4.6), we derived associated vulnerability indices. For instance, for salt pond production, we computed indices based on the total production covered by traditional salt ponds in one FMA normalized by the maximum production among the 11 FMA. Considering FMA 571 as example, traditional salt ponds production was 9135.84 tonnes, whereas the largest production was found in FMA 712 with 2 485 939.53 tonnes. The resulting salt-pond-related vulnerability index ($PR_{salt-ponds}$) in FMA 571 is thus equal to :

$$PR_{salt-ponds-FMA571} = \frac{9135.84}{2\,485\,939.53} \times 100 = 0.37$$

We computed similar vulnerability indices for the other socio-economic features synthetsized in Table 4.6, referring respectively to fishing vessels, maritime tourism activities and salt pond production. The resulting indices $PR_{fishing-boat}$, $PR_{tourism}$, $PR_{salt-ponds}$ are shown in Table 4.6 in column PR_soc3, PR_soc4 and PR_soc5.

4.3.3 Global FMA-level risk index

Based on the different oil spill-related risk and vulnerability indices introduced in the previous sections, we define a global index (GRI) summarizing the overall vulnerability of a given FMA w.r.t. oil spill pollution. In summary, we defined six oil spill risk indices(PR_s1 to PR_s6) and eight environmental vulnerability indices (PR_env1 to PR_env8) and five socio-economical vulnerability indices (PR_soc1 to PR_soc5). The proposed GRI is the following :

$$GRI = \frac{\sum_{i=1}^{N} PR_{source}}{N_{source}} \times \left(\frac{\frac{\sum_{i=1}^{N} PR_{env}}{N_{env}} + \frac{\sum_{i=1}^{N} PR_{soc}}{N_{soc}}}{2} \right) \tag{4.6}$$

To make easier the analysis of this global index, we introduce a four-level categorization of the GRI as detailed in Table 4.3.2. The same categorization may be applied to the other risk and vulnerability indices.

TABLE 4.9 – Categorization of the Global Risk Index (GRI) (Eq.4.6).

Risk level	GRI range
High	RI $\geq$ 45%
Medium	RI = 35-45 %
Low	RI = 25 -35 %
Minimal	RI $\leq$ 25 %

We report in Table 4.11 the synthesis of the GRI computed for the 11 FMAs along with the associated risk level according to the category defined in Table 4.3.2.

4.3.4 MPA-level vulnerability analysis

In addition to the above FMA-level risk assessment analysis, we performed a MPA-level analysis. Such finer spatial scales also advocate for considering finer time scales as meteological-oceanographic (metocean) conditions may greatly affect the dynamics of an oil spill and its regional impact onto the offshore and coastal environment and associated human activities. For the different oil spill sources identified above, we aim at evaluating their potential impact on MPA and how this impact may evolve in relation with the variabilities of the metocean conditions.

The proposed scheme exploited Mobidrift developed by CLS France [75] to simulate the drift of an oil spill conditionally to given metocean conditions. We considered the following parameter setting : a wind drift factor C_w in eq. (3.1) = 0.03, a sea surface current drift factor C_c =1.0 and 500 particles. We ran drift simulations for a duration between 3 and 6 days from January to December with a 6-hours time step. As oil spill source, we might consider the different sources identified in Section 4.3.1. Here, we used the ship density map as oil spill source input. We used the metocean conditions for year 2015 as reference conditions. For a given simulation, we evaluated the number of particles entering in a MPA.

For this MPA-level analysis, we focus on high-risk FMA 711 and 712. There are 14 MPA in FMA 711 and 7 MPA in FMA 712 as shown in Figure 4.6 and 4.5. From Mobidrift simulations using the ship density map as oil spill sources, we determined the number of particles entering each MPA on a monthly basis. Results are reported in Table 4.12. We then computed MPA-level risk index as :

$$PR_{MPA} = \left[\frac{p_i}{PI}\right] \times 100 \tag{4.7}$$

where p_i is the number of particles that entered MPA ^{i} from the considered Mobidrift simulations and PI is the greatest number of particles that entered one of the MPA in the considered FMA. For a given FMA, for instance FMA 712, we refer to MPA 712.k as the kth MPA in FMA 712.

For instance, for Karimun Jawa MPA (MPA 712.6) located in FMA 712, 48 (resp. 248) particles entered the FMA for Mobidrift simulations run for January metocean conditions with a 3-day (resp. 6-day) duration, where MPA 712.1 (Seribu Islands) evolved the greatest numbers of particles (resp. 3761 and 5139 particles for 3-day and 6-day simulation duration). Hence, the risk indices for MPA 712.6 are given by

$$PR_{oil-particles-MPA7126} = \frac{48}{3761} \times 100 = 1.28 \text{ (for duration = 3 days)}$$
$$PR_{oil-particles-MPA7126} = \frac{248}{5139} \times 100 = 0.90 \text{ (for duration = 6 days)}$$

We proceeded similarly for all MPA in FMA 711 and 712. The results are reported in Table 4.13, 4.14, 4.15 and 4.16 .

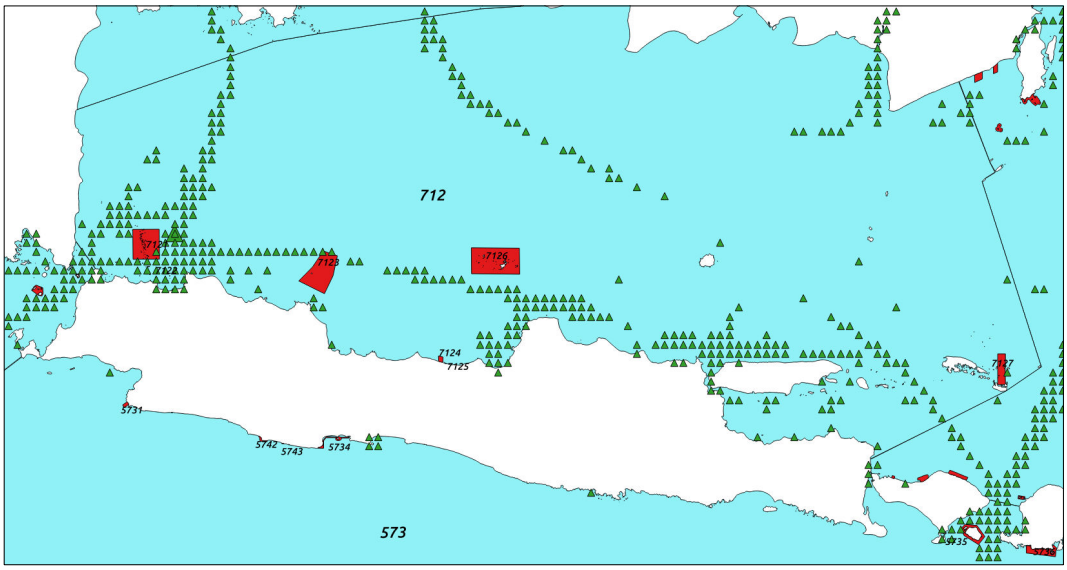

FIGURE 4.5 – Mapping of 7 zones of MPA in FMA 712 (red) along with potential oil spill sources (green triangles) associated with high-traffic points in the area determined from AIS-derived traffic density maps.

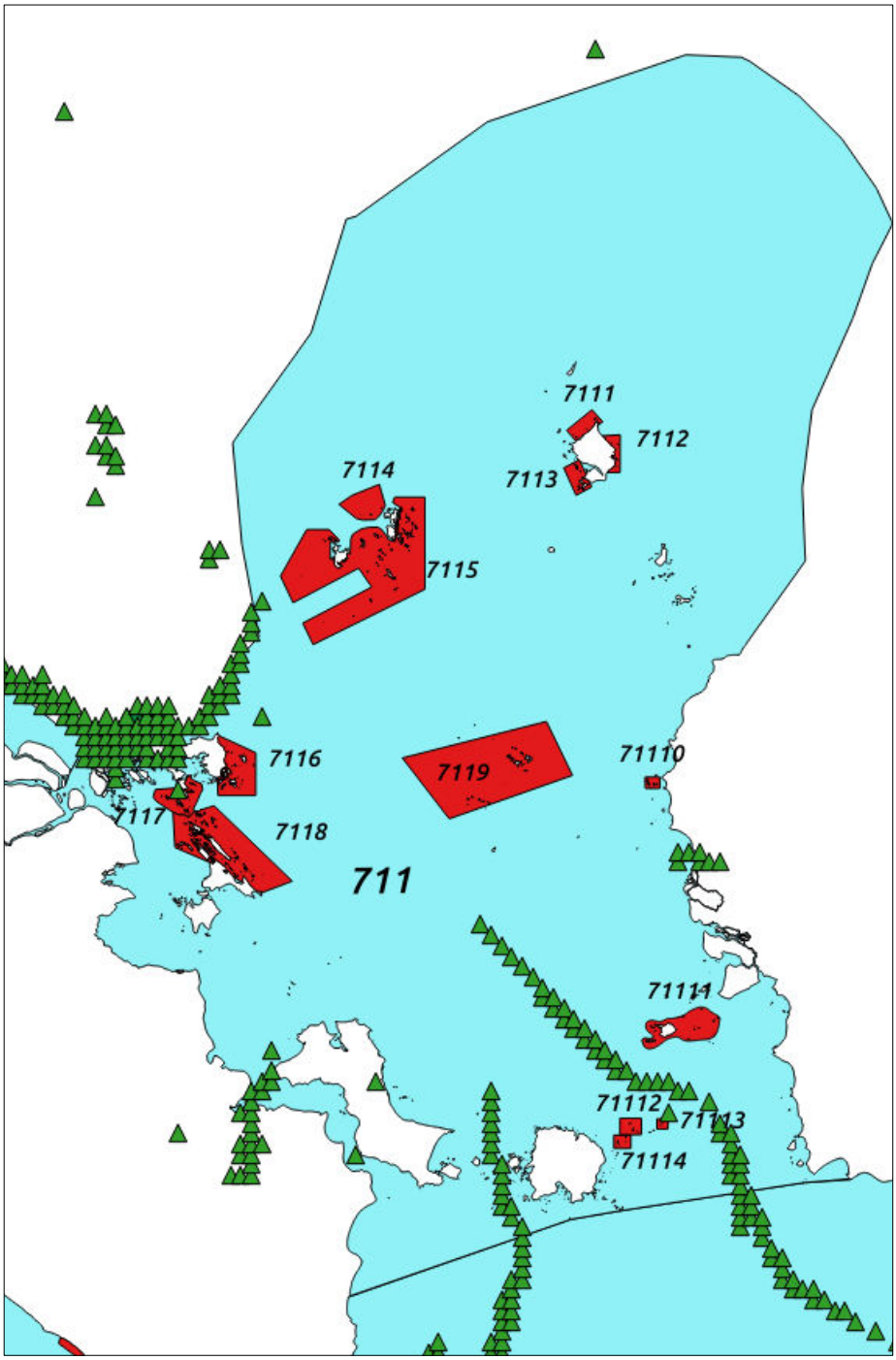

FIGURE 4.6 – Mapping of 14 zones of MPA in FMA 711 (red) along with potential oil spill sources (green triangles) associated with high-traffic points in the area determined from AIS-derived traffic density maps.

4.4 Results and Discussion

Table 4.10 showed that FMA 712, 713 and 711 involve the highest oil-spill-risk level. In Natuna Sea, Java Sea and Makassar Strait, the density of the maritime traffic, of oil platform as well as of oil transportation activities is very high. FMA 571 has medium risk level that related mostly to the maritime traffic number in the Malacca Strait. By contrast, FMA 573 depicts a low risk level in the Indian Ocean on the South of Indonesia. Other FMA were categorized as minimum risk level.

Regarding environment-related vulnerability indices, 4 zones, namely FMA 573,711,717 and 718, were categorized as high-vulnerability areas. FMA 712, 715 and 716 involved a medium level, FMA 713 and 714 only a low level, and FMA 571 and 572 a minimal level.

Regarding socio-economic impacts, FMA 711,712 and 713 (Natuna Sea, Java Sea and Makassar Strait) depict a high-risk level. FMA 717 depicted a minimal-risk level and the remaining 7 FMA a low-risk level.

TABLE 4.10 – Synthesis of FMA-level risk and vulnerability indices

FMA	Risk Index	Cost Environment	Cost Socioeconomic
571	42.05	18.07	25.04
572	4.77	20.89	29.20
573	29.45	60.16	26.37
711	50.76	45.40	46.08
712	74.19	40.56	63.15
713	52.91	20.76	52.71
714	12.23	32.80	29.53
715	17.60	42.86	34.83
716	7.02	36.79	27.16
717	2.99	45.70	14.76
718	5.49	58.45	31.48

For a synoptic analysis, we report GRI values for all FMA in Table 4.11. It clearly points out FMA 711 and 712 as high-risk areas. FMA 711 is the most vulnerable one because it has high-risk for different oil spill sources and also depict a high vulnerability both in terms of environmental and socioeconomic impacts. By contrast, FMA 712 depicts a high vulnerability level in terms of socioeconomic factors but only a medium vulnerability level in terms of environmental impact. Two zones, FMA 573 and 713, are categorized as medium-risk areas. FMA 573 involves a high-risk impact w.r.t. environment factors but a low-risk level in terms of oil spill exposure and socioeconomic impacts. FMA 713 depicts a high risk/vulnerability level in

terms of socioeconomic impacts and oil spill exposure, but a medium-level risk level regarding environmental factors. Overall, the other FMA seem to relatively safe w.r.t. oil spill pollution with a low-risk level for FMA 571 and 715 and a minimal-risk level for FMA 572, 714, 716, 717 and 718.

TABLE 4.11 – Global Risk Index (GRI) for each FMA

FMA	Global Risk Index	Category
571	906.40	Low
572	119.57	Minimal
573	1274.17	Medium
711	2321.95	High
712	3846.93	High
713	1943.89	Medium
714	381.25	Minimal
715	683.76	Low
716	224.37	Minimal
717	90.33	Minimal
718	246.85	Minimal

4.5 MPA-level risk assessment

Based on the above FMA-level analysis, we performed a vulnerability analysis at finer space and time scales within the two high-risk FMA, namely FMA 711 and 712. We applied the scheme detailed in Section 4.3.7. For FMA 711, we ran Mobidrift simulations with 107 source points from the vessel density map. One simulation example is illustrated in Figure 4.7 for condition on North West monsoon, 4.9 for condition on SouthEast monsoon, 4.8 and 4.10 for condition on Transition 1 and Transition 2 monsoon. In these simulations the position of the oil spill source is point 0° 36' 0" S and 107° 5' 60" E. We depict simulations with two durations (3 and 6 days) for different metocean conditions from January to December. The seasonal variability of these metocean conditions clearly affect the drift of the oil spill and its impacts on nearby MPA. During the SouthEast monsoon period (June - August), oil spill mostly drifts to the SouthEast and threats MPA 711.9. During the North West monsoon period, the oil spill drifts towards MPA 711.11 and 711.12.

We also report simulation examples for FMA 712, which involve 357 oil spill source points, in Figure 4.11. In these simulations, the oil spill source is located 5° 30' 0" S and 106° 54' 0" E. We ran the simulation with 3-day and 6-day durations for metocean conditions from January to December. From these simulations, the SouthEast monsoon period (June-August) and September-November period (Transition 1), a 3-day drift impacted MPA 712.1. During the North West monsoon, on December, the drift impacted MPA 711.1 for 6-day simulations. By contrast, on January and February the drift was directed towards MPA 711.3. From March to May (Transition 2) the simulations showed that MPA 711.3 is still under threat on March but no more on April and May, where the drift is directed towards MPA 711.1.

We synthesized the outputs of these simulations through the number of particles entering each MPA in Table 4.12. MPA-level vulnerability indices (4.7) are given in Table 4.13, 4.14, 4.15 and 4.16 respectively for FMA 711 and 712, 3-day and 6-day simulations. We computed the mean vulnerability indices for each MPA in Table 4.17 for FMA 711 and in Table 4.18.

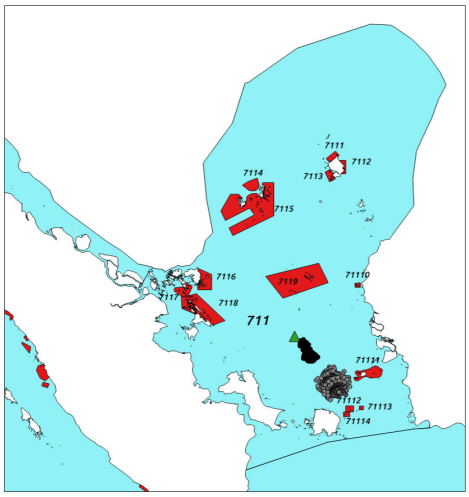

December

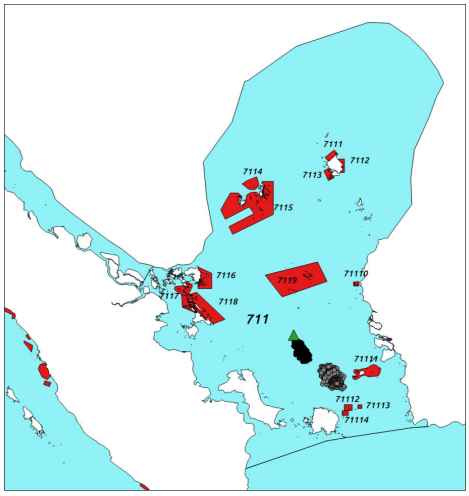

January

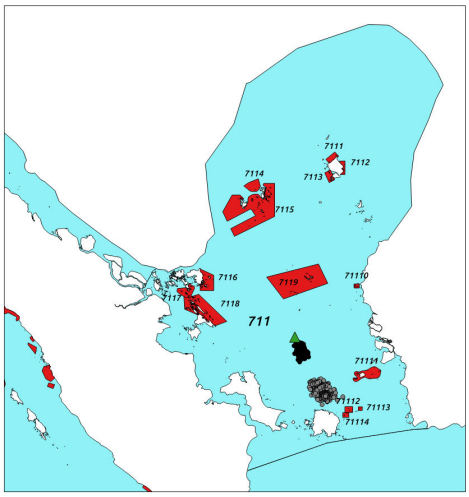

February

FIGURE 4.7 – Oil spill drift simulations from one source point located at 0° 36' 0" S and 107° 5' 60" E (green triangle) in FMA 711 with 3-day and 6-day durations (resp. black and gray dots) for metocean conditions in the Northwest monsoon from December to February.

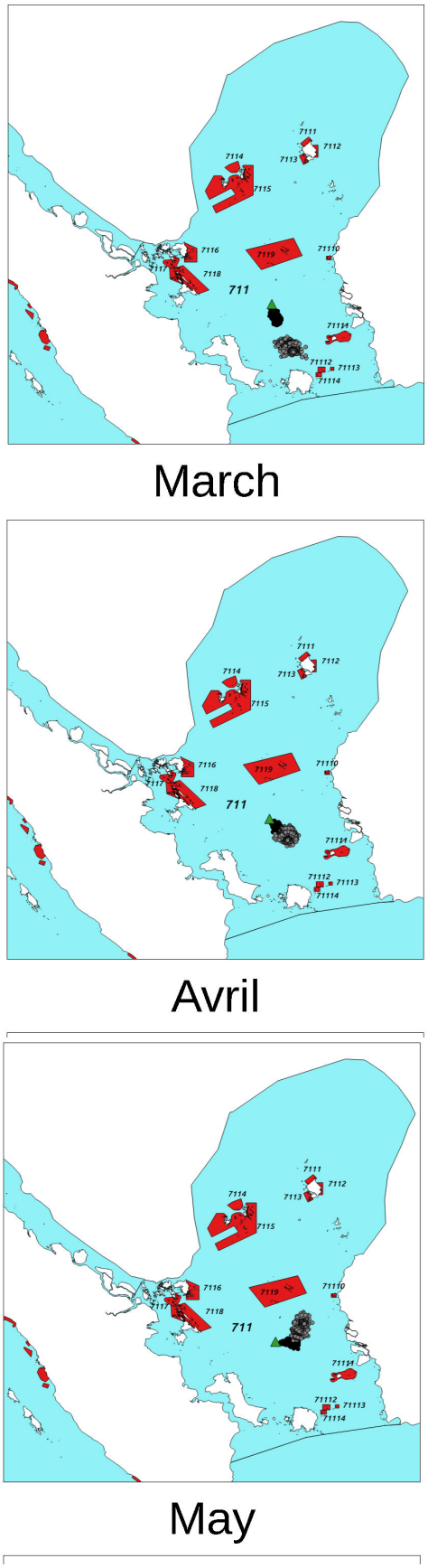

FIGURE 4.8 – Oil spill drift simulations from one source point located at 0° 36' 0" S and 107° 5' 60" E (green triangle) in FMA 711 with 3-day and 6-day durations (resp. black and gray dots) for metocean conditions in the Transition 1 monsoon from March to May.

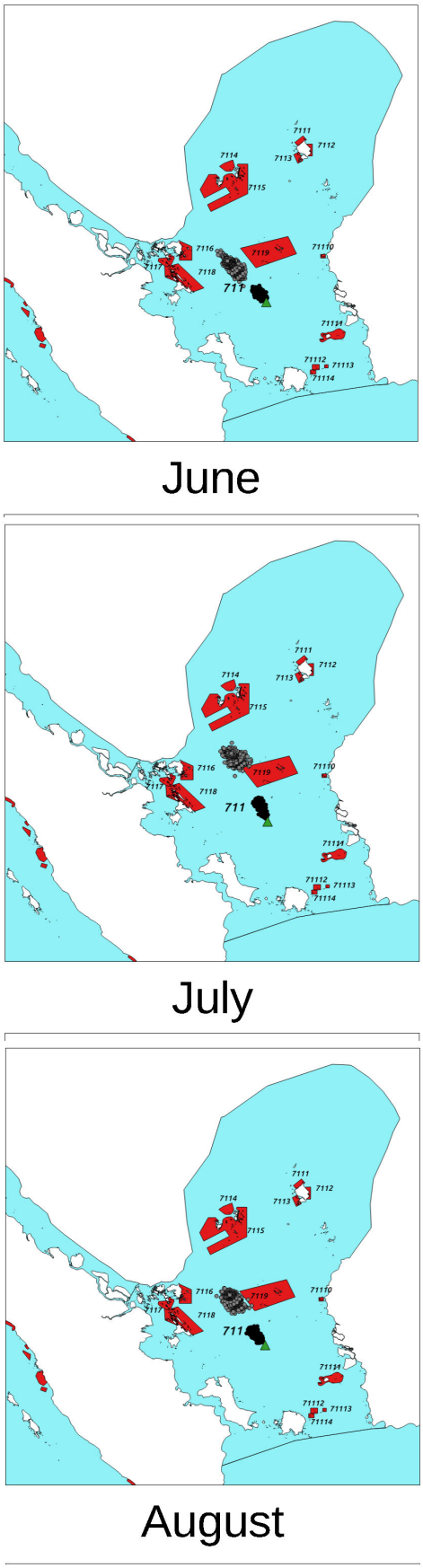

FIGURE 4.9 – Oil spill drift simulations from one source point located at 0° 36' 0" S and 107° 5' 60" E (green triangle) in FMA 711 with 3-day and 6-day durations (resp. black and gray dots) for metocean conditions in the SouthEast monsoon from June to August.

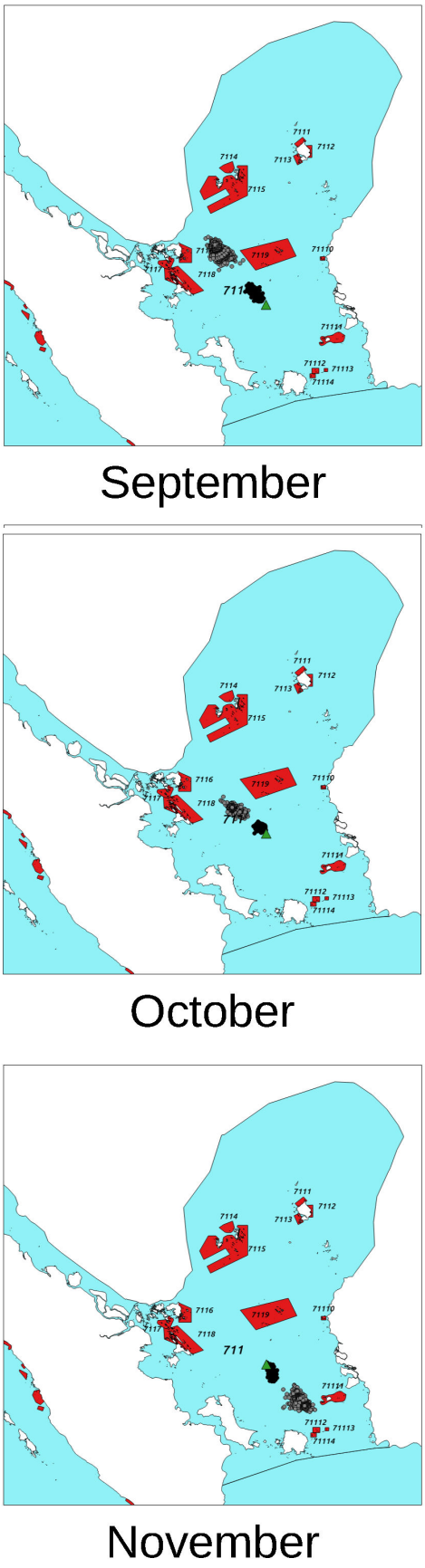

FIGURE 4.10 – Oil spill drift simulations from one source point located at 0° 36' 0" S and 107° 5' 60" E (green triangle) in FMA 711 with 3-day and 6-day durations (resp. black and gray dots) for metocean conditions in the Transition 2 monsoon from September to November.

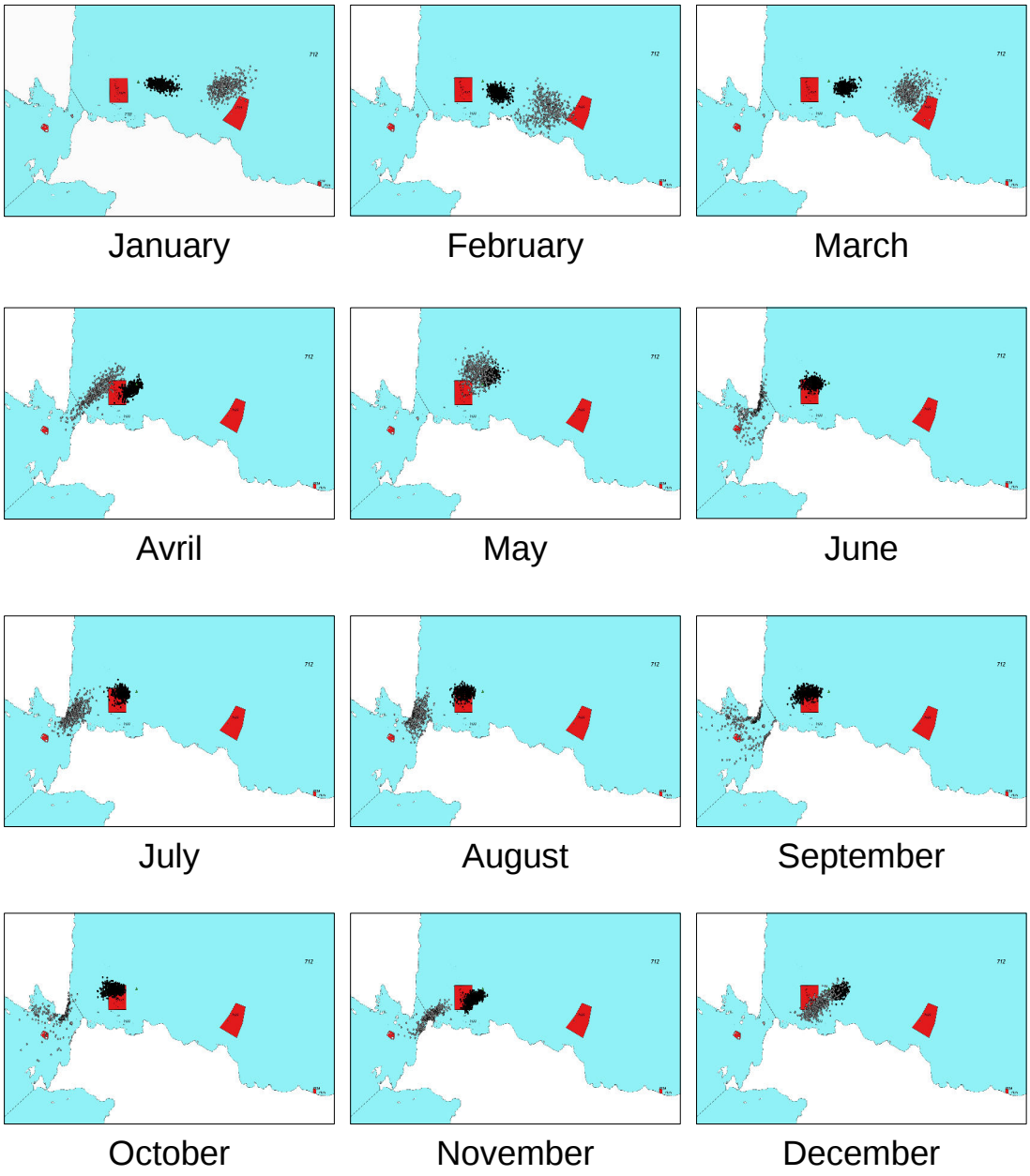

FIGURE 4.11 – Oil spill drift simulations from one source point located at 5° 30' 0" S and 106° 54' 0" E (green triangle) in FMA 712 with 3-day and 6-day durations (resp. black and gray dots) for metocean conditions from January to December.

TABLE 4.12 – Number of particles entering each MPA in FMA 711 and 712 for oil spill drift simulations with January-to-December metocean conditions. AIS-derived Vessel density maps were used to generate oil spill source points.

	Number of simulated oil spill particles entering a MPA																							
MPA	January		February		March		April		May		June		July		August		September		October		November		December	
	d=3	d=6	d=3	d=6	d=3	d=6	d=3	d=6	d=3	d=6	d=3	d=6	d=3	d=6	d=3	d=6	d=3	d=6	d=3	d=6	d=3	d=6	d=3	d=6
711.1	0	0	0	0	0	0	0	0	0	0	0	0	0	0	0	0	0	0	0	0	0	0	0	0
711.2	0	0	0	0	0	0	0	0	0	0	0	0	0	0	0	0	0	0	0	0	0	0	0	0
711.3	0	0	0	0	0	0	0	0	0	0	0	0	0	0	0	0	0	0	0	0	0	0	0	0
711.4	0	0	0	0	0	0	0	0	0	0	0	0	0	0	0	0	0	0	0	0	0	0	0	0
711.5	0	0	0	0	0	0	0	5	0	277	0	0	0	0	0	0	0	0	0	0	0	0	0	0
711.6	268	170	69	634	27	595	84	407	3	0	0	0	0	0	0	0	0	0	0	0	7	385	294	460
711.7	541	640	486	475	489	535	481	464	458	449	362	336	330	300	235	313	366	215	496	360	385	505	460	460
711.8	21	252	13	514	3	11	1	0	0	0	0	0	0	0	0	0	0	0	0	0	0	10	0	0
711.9	0	0	0	0	0	0	0	0	0	28	0	0	0	2200	0	8	0	0	0	0	0	0	0	0
711.10	0	0	0	0	0	0	0	0	0	28	0	0	0	69	0	51	0	28	0	0	0	0	0	0
711.11	0	2	0	10	0	59	0	1	29	1545	0	0	3	845	0	340	2	428	3	502	0	3	0	0
711.12	3	0	0	149	1	217	43	6	43	6	0	2	0	2	1	230	0	0	0	35	0	0	0	362
711.13	0	0	0	69	0	157	2	0	0	0	0	20	0	0	0	2	0	5	0	53	0	20	0	23
711.14	0	0	0	0	0	4	0	0	0	0	0	0	0	0	0	0	0	0	0	2	0	16	0	0
712.1	1110	10	1946	64	3692	317	2530	1661	1995	5139	3645	1587	2813	1014	3283	808	3423	938	3761	1407	2212	2177	1257	2379
712.2	0	0	7	0	2	1	3	0	2	2	3	1	8	7	5	2	3	2	2	0	11	5	2	5
712.3	989	1998	374	1414	707	2272	805	251	89	18	274	1224	152	40	147	241	138	21	190	926	721	431	597	558
712.4	0	0	0	0	0	0	0	18	0	46	0	9	0	1	0	0	0	0	0	2	0	0	0	0
712.5	0	0	0	0	0	0	0	0	0	0	0	0	0	0	0	0	0	0	0	0	0	0	0	0
712.6	48	248	34	1289	13	1283	0	569	190	2578	14	1602	38	1665	41	1506	34	2481	47	866	1	251	92	800
712.7	0	137	37	23	0	96	232	3	317	0	71	0	69	0	162	0	81	0	9	0	147	0	58	48

Table 4.13 – MPA-level vulnerability indices in FMA 711 issued from oil spill drift simulations for a 3-day drift duration and January-to-December metocean conditions.

MPA ID	January	February	March	April	May	June	July	August	September	October	November	December
711.1	0	0	0	0	0	0	0	0	0	0	0	0
711.2	0	0	0	0	0	0	0	0	0	0	0	0
711.3	0	0	0	0	0	0	0	0	0	0	0	0
711.4	0	0	0	0	0	0	0	0	0	0	0	0
711.5	0	0	0	0	0	0	0	0	0	0	0	0
711.6	49.54	12.75	4.99	15.53	0.55	0	0	0	0	0	1.29	54.34
711.7	100	89.83	90.39	88.91	84.66	66.91	61.00	43.44	67.65	91.68	71.16	85.03
711.8	3.88	2.40	0.55	0.18	0	0	0	0	0	0	0	0
711.9	0	0	0	0	0	0	0	0	0	0	0	0
711.10	0	0	0	0	0	0	0	0	0	0	0	0
711.11	0	0	0	0	5.36	0	0.55	0	0.37	0.55	0	0
711.12	0.55	0	0.18	7.95	7.95	0	0	0.18	0	0	0	0
711.13	0	0	0	0.37	0	0	0	0	0	0	0	0
711.14	0	0	0	0	0	0	0	0	0	0	0	0

Table 4.14 – MPA-level vulnerability indices in FMA 711 issued from oil spill drift simulations for a 6-day drift duration and January-to-December metocean conditions.

MPA ID	January	February	March	April	May	June	July	August	September	October	November	December
711.1	0	0	0	0	0	0	0	0	0	0	0	0
711.2	0	0	0	0	0	0	0	0	0	0	0	0
711.3	0	0	0	0	0	0	0	0	0	0	0	0
711.4	0	0	0	0	0	0	0	0	0	0	0	0
711.5	0	0	0	0.23	12.59	0	0	0	0	0	0	0
711.6	7.73	28.82	27.05	18.50	0	0	0	0	0	0	17.50	20.91
711.7	29.09	21.59	24.32	21.09	20.41	15.27	13.64	14.23	9.77	16.36	22.95	20.91
711.8	11.45	23.36	0.50	0	0	0	0	0	0	0	0.45	0
711.9	0	0	0	0	1.27	0	100	0.36	0	0	0	0
711.10	0	0	0	0	1.27	0	3.14	2.32	1.27	0	0	0
711.11	0.09	0.45	2.68	0.05	70.23	0	38.41	15.45	19.45	22.82	0.14	0
711.12	0	6.77	9.86	0.27	0.27	0.09	0.09	10.45	0	1.59	0	16.45
711.13	0	3.14	7.14	0	0	0.91	0	0.09	0.23	2.41	0.91	1.05
711.14	0	0	0.18	0	0	0	0	0	0	0.09	0.73	0

Table 4.15 – MPA-level vulnerability indices in FMA 712 issued from oil spill drift simulations for a 3-day drift duration and January-to-December metocean conditions.

MPA ID	January	February	March	April	May	June	July	August	September	October	November	December
712.1	29.51	51.74	98.17	67.27	53.04	96.92	74.79	87.29	91.01	100	58.81	33.42
712.2	0	0.19	0.05	0.08	0.05	0.08	0.21	0.13	0.08	0.05	0.29	0.05
712.3	26.30	9.94	18.80	21.40	2.37	7.29	4.04	3.91	3.67	5.05	19.17	15.87
712.4	0	0	0	0	0	0	0	0	0	0	0	0
712.5	0	0	0	0	0	0	0	0	0	0	0	0
712.6	1.28	0.90	0.35	0	5.05	0.37	1.01	1.09	0.90	1.25	0.03	2.45
712.7	0	0.98	0	6.17	8.43	1.89	1.83	4.31	2.15	0.24	3.91	1.54

Table 4.16 – MPA-level vulnerability indices in FMA 712 issued from oil spill drift simulations for a 6-day drift duration and January-to-December metocean conditions.

MPA ID	January	February	March	April	May	June	July	August	September	October	November	December
712.1	0.19	1.25	6.17	32.32	100	30.88	19.73	15.72	18.25	27.38	42.36	46.29
712.2	0	0	0.02	0	0.04	0.02	0.14	0.04	0.04	0	0.10	0.10
712.3	38.88	27.52	44.21	4.88	0.35	23.82	0.78	4.69	0.41	18.02	8.39	10.86
712.4	0	0	0	0.35	0.90	0.18	0.02	0	0	0.04	0	0
712.5	0	0	0	0	0	0	0	0	0	0	0	0
712.6	4.83	25.08	24.97	11.07	50.17	31.17	32.40	29.31	48.28	16.85	4.88	15.57
712.7	2.67	0.45	1.87	0.06	0	0	0	0	0	0	0	0.93

TABLE 4.17 – Mean MPA-level vulnerability indices in FMA 711 for January-to-December metocean conditions

MPA ID	SouthEast		Transition 1		NorthWest		Transition 2	
	3days	6days	3days	6days	3days	6days	3days	6days
711.1	0	0	0	0	0	0	0	0
711.2	0	0	0	0	0	0	0	0
711.3	0	0	0	0	0	0	0	0
711.4	0	0	0	0	0	0	0	0
711.5	0	0	0	0	0	0	0	4.27
711.6	0	0	0.43	5.83	38.88	19.15	7.02	15.18
711.7	57.12	14.38	76.83	16.36	91.62	23.86	87.99	21.94
711.8	0	0	0	0.15	2.09	11.61	0.25	0.17
711.9	0	33.45	0	0	0	0	0	0.42
711.10	0	1.82	0	0.42	0	0	0	0.42
711.11	0.18	17.95	0.31	14.14	0	0.18	1.79	24.32
711.12	0.06	3.55	0	0.53	0.18	7.74	5.36	3.47
711.13	0	0.33	0	1.18	0	1.39	0.12	2.38
711.14	0	0	0	0.27	0	0	0	0.06

TABLE 4.18 – MPA-level vulnerability indices in FMA 712 under different monsoon conditions.

MPA ID	SouthEast		Transition 1		NorthWest		Transition 2	
	3days	6days	3days	6days	3days	6days	3days	6days
712.1	86.33	22.11	83.28	29.33	38.23	15.91	72.83	46.16
712.2	0.14	0.06	0.14	0.05	0.08	0.03	0.06	0.02
712.3	5.08	9.76	9.30	8.94	17.37	25.75	14.19	16.48
712.4	0	0.06	0	0.01	0	0	0	0.42
712.5	0	0	0	0	0	0	0	0
712.6	0.82	30.96	0.73	23.34	1.54	15.16	1.80	28.73
712.7	2.68	0	2.10	0	0.84	1.35	4.87	0.64

Table 4.17 showed that MPA 711.7 is the most vulnerable all year long. This MPA is more vulnerable during the NorthWest and Transition 2 monsoon. Hence, the surveillance should be enhanced in this region during that period. Other vulnerable MPA in FMA 711 are MPA 711.6 and MPA 711.9. MPA 711.6 was threatened on the NorthWest monsoon and MPA 711.9 on the SouthEast monsoon.

Regarding, FMA 712, as showed on Table 4.18, MPA 712.1 was the most threatened MPA by the oil spill. This MPA is more vulnerable on the SouthEast, Transation 1 and Transation 2 monsoon. MPA 712.1 needs more surveillance on the Transation 2 monsoon because on this period both oil spill coming from 3 and 6 days simulation were threatened this area. The others MPA that needs attention are FMA 712.3 and 712.6. FMA 712.3 was threatened on the NorthWest monsoon and FMA 712.6 on the Transition 2 and SouthEast monsoon.

4.6 Conclusion and Discussion

In this work, we developed a novel method for the assessment of the vulnerability of marine and coastal Indonesian ecosystems to oil spill pollution. The proposed approach combined a variety of potential oil spill sources documented from maritime traffic density data, oil-related activities and satellite-derived oil spill detection. The calculation of oil spill risk on each FMA based on the value of average percentage rate of each critical variable considered. Regarding the limitation of data and information, the calculation of average percentage rate is sometimes different between each variable. For example on the variable risk coming from ship accident we used the weighting factor as described from ITOPF because we had the information related to the volume of oil spilled for each accident. In other example, we analyzed the risk from the variable maritime density not using the weighting factor because no information related to the type of vessel and volume of oil that being transported. It would be better for the further analysis if we can be provided by more information but at least this analysis can be identified which area that more vulnerable from the oil spill.

We evaluated the impact of oil spill pollution both in terms of ecological and socioeconomic impacts. Our analysis was spatially structured with respect to 11 Fisheries Management Areas implemented by Indonesia. Same with the methodology used in the calculation of risk, the calculation of oil spill impact on each FMA based on the value of average percentage rate of each critical variable considered in the ecological and socioeconomic. As a final result, we proposed a global risk index (GRI) combining all information sources at the MFA level.

The result of our analysis clearly pointed out FMA 711 and 712 as the areas the most vulnerable to oil spill. Medium-risk levels were reported from FMA 573 and FMA 713 and the remaining ones involved a low-risk or minimal-risk level. Its worth to note that the data used for the calculation of oil spill impact on the environment the data used in the analysis is coming from ecoregion data which is quite different with Fishing Management Area. In ecoregion FMA 573 divided into 2 ecoregions different namely South Java and Lesser Sunda. This explained why the FMA 573 is categorized as medium-risk. In FMA 573, even the oil spill risk is low but the oil spill impact is high considering the marine biodiversities in FMA 573 that combining from two ecoregions.

In FMA 712, the risk level is the highest. Java Sea has an important role in terms of maritime activities and fisheries production, meanwhile it has dense ship traffic and a lot of activities linked to oil and gas production and distribution. Seribu Islands (MPA 712.1) in the North of Jakarta is the most threatened MPA. This MPA is threatened almost all year long from January to December with the highest risk level during the SouthEast monsoon from June to August. Situated in the North of Semarang (Capital of Central Java Province) with a dense ship traffic, Karimunjawa (MPA 712.6) is the second most threatened MPA in FMA 712 but involved a low-risk level.

In FMA 711, the most vulnerable MPA are Batam Islands (MPA 711.7 and 711.6) and Tambelan and Karimata Islands (MPA 711.9 and 711.11). Batam Islands are vulnerable due to its location near Singapore ports that have very high ship traffic density. The enhancement of the surveillance should be conducted on these islands. The surveillance and mitigation should be focused on North West monsoon period from December to February and on the transition period from March to May. Other MPA in FMA 711 that require particular attention is the MPA in Tambelan and Karimata Islands located in the Karimata Strait. The Tambelan and Karimata Islands are close to major sea lanes. For this MPA, the focus should be given to the June-August period (Monsoon SouthEast), with a main threat related to relatively longer drifts (6-day duration).

The result of our study should be analyzed with respect to reported oil spill occurences. Regarding for instance the Seribu Island and Batam Islands. In Seribu Islands, several oil spills were reported on December 2003, April, May and October 2004, June 2007 and February, March and August 2011. In FMA 711 particularly in Batam Islands, the last oil spills were found on January and February 2017. These reported oil spill events and impacts support the significance of our study, which also identified these zones as being among the most vulnerable ones to oil spill pollution.

We believe this study to be relevant to decision makers, government officials and local communities in avoiding or limiting the oil spill risk in vulnerable zones. The related regulations on marine shipping and vessel navigation on the vulnerable zone could be improved based on the risk levels established through the proposed approach. The determination of vulnerability indices conditionally to metocean conditions also open the possibility for surveillance and mitigation plans adapted to the seasonal and inter-annual variabilities of the metocean conditions.

Using SAR-based surveillance in conjunction with surveillance vessel operating in predefined areas of interest, especially high-risk ones, could improve law enforcement. Our study of the MPA-level vulnerability further stresses the importance of using high-quality metocean data, including bathymetry and tidal information, with a view to predicting realistic oil spill drifts as well as for risk assessment issues as explored in our study as in mitigation for oil spill disasters. Overall, the proposed methodology could be implemented within INDESO system, including routine updates from newly documented oil spill events as well as updated knowledge on the presence of oil-related acitvies (e.g., refinery, platform,....).

Chapitre 5

Conclusions and Perspectives

5.1 Conclusion 106
5.2 Perspectives 108

5.1 Conclusion

Oil spill monitoring in the Indonesian seas is one of the main objective of the INDESO project. In this framework, this thesis aimed to propose new methodologies and analyses. This thesis involved two main contributions. The first contribution addressed the retrieval of oil spill drift parameters from a joint analysis of SAR observations of an oil spill and of outputs of a Lagrangian oil spill transport model. We applied the proposed methodology on the most famous oil spill accident in Indonesia, the Montara case. The second contribution was the global assessment of oil spill risk in Indonesia.We focused on the 11 Indonesia Fisheries Management Area to support the sustainability development of marine and fisheries. In this analysis we proposed methodology that considered the oil spill from different source and their impacts not only to the environment, but also from social and economic perspectives. For the assessment of vulnerability of Marine Protected Areas to oil spill pollution, we also exploited the oil spill trajectory model.

In the first part of this thesis, we aimed to estimate oil spill drift parameters. The proposed framework exploited a Lagrangian oil spill transport model such that the simulated oil spill drift could match a SAR-based observation of an oil spill. In the considered 2D Lagrangian model there were two dominant factors, i.e. wind and surface current. To confirm the origin of the oil spill detected on a given date through a SAR observation, we performed simulations with various leakage starting dates, leakage durations, and different values of wind and current weighing coefficients. We developed a novel framework for the assimilation of these oil leakage parametersfrom a SAR-derived detection of an oil spill. This framework states this assimilation as the minimization of a level-set representations of the SAR-derived oil spill detection and of 2D transport model simulations. We illustrated its relevance on the Montara oil spill case study. We showed that the observed oil spill on 02 September 2009 was mainly due to the oil leakage from August 21 until September 02 with majority of slick is coming from five first days of leakage (August 21-25, 2009). The estimated wind and current drift factors were in agreement with values previously reported in the literature. They were however significantly different from nominal parameters and shown to affect the match between the observed oil spill and transport model simulations.

The second part of this thesis addressed the assessment of the vulnerability of Indonesian sea areas to oil spill pollution. The focus was given to Fisheries Management Areas as a means to

provide synoptic analysis over the entire Indonesian maritime territory. Using different information from many institutional reports, we collected and analyzed the potential source of oil spill in each FMA. Each FMA has specific characteristics in terms environmental and socioeconomic features. We assessed the oil spill risk in each FMA based on all these factors. In total, we have computed a Global Risk Index (GRI) at the FMA level that combined all information sources. The resulting distribution of the GRI over the 11 FMA showed that FMA in the North of Java and Natuna Sea are the most vulnerable ones to oil spill. Furthermore, we exploited oil spill drift simulations into these two FMA to further assess the vulnerability at a finer spatial scale, focusing on Marine Protected Areas, and a finer time scale, namely up to a monthly scale, with a view to assessing the impact of the variabilities of the meteorological and oceanographic conditions. Among 14 MPA in the zone of FMA Natuna Sea the most vulnerable MPA are in Batam Islands, Bintan Islands and Tambelan & Karimata Islands. The surveillance and mitigation should be focused on North West monsoon on December until February and on the transition period from March until May. Meanwhile, in the FMA on the North of Java the most vulnerable MPA is in Seribu Islands. This MPA is threatened almost all the year long from January until December with a peak during the South East monsoon from June until August.These results are consistent with recurrent oil spill events reported in the Seribu Island and Batam Islands. The result of this study can be used in the mitigation planning to reduce the negative impacts of oil spill. It might be useful for decision makers, government officials and local communities in avoiding or limiting the oil spill risk in vulnerable zones. The related regulations on marine shipping and vessel navigation in the highly-vulnerable zone should be improved. At the operational level, we might suggest the joint use of the SAR-based surveillance in conjunction with vessels operating at set.This coordination could reinforce the law enforcement.

In summary, we have proposed several methods for the monitoring of oil spills and their impacts into Indonesian marine ecosystems and activities, which benefit from both satellite observation technologies and operational oceanography tools, both aspects being at the core of INDESO project.

5.2 Perspectives

The study on the assimilation of SAR images in oil spill trajectory models opens new research avenues for the satellite-based operational monitoring of oil spills. Future work will further investigate the assimilation of oil leakage parameters from multi-date observations as well as other oil leakage configurations, such as illegal oil discharges from natural oil seeps or vessels. The two novel applications would be of key interest in the framework of INDESO project.

The analysis of oil spill risk showed that several areas are categorized as highly vulnerable areas. In such high-risk zones, the oceanographic data such as bathymetry and current, wind and tidal information should be acquired and prepared better in advance with a view to being fully-operational in case of most often unexpected oil spill disasters. One may consider the development and parameterization of zone-specific oil spill drift models for high-risk zones. Regarding the implementation of the proposed oil spill monitoring tools, a critical issue if the availability of supporting data. In our study, we calculated oil spill risk indices from oil spill drift simulations using only ship positions as sources. Information on the positions of oil platforms would further improve the analysis of the oil spill risk and the mapping of this risk at the national and regional scale. The simulation of oil spill will be better considering the evaporation and emulsification process. In the future simulation using 3D setting will be more clearly identified the impact of oil spill to the marine environment.

The expertise in object trajectory model and satellite image analysis for marine applications remains fairly limited in Indonesia. This thesis can be used in supporting the operational of Indeso especially for the oil spill monitoring in Indonesia sea territory. Our work can be used in law enforcement, response and mitigation planning. In the future, sea pollution can be expected to catch more and more the attention of stakeholders as maritime and fisheries activities tend to be one of the most important source of growth of the economy. Marine pollution does not restrict to oil spill pollution. The world's oceans are now facing mountains of debris. Indonesia sea territory is among the most affected ones. Indonesia is also stirringly suspected to be one of the biggest marine polluter in the world. In this respect, INDESO is a critical tool to support the the government of Indonesia in combating this issue. With the comprehensive observation data acquired within INDESO along with the modeling and analysis tools implemented are clearly of great interest to address this issue. For instance, one might combine the detection to marine

debris to drift trajectory models to forecast the impact of marine debris pollution onto the coastal Indonesian ecosystems. The detection of the marine debris is a real challenge as debris are is relatively small and mainly found in the subsurface. New solutions and operational plan have then to be developed in response to the operational needs.

Bibliography

[1] J. A. Sethian, *Level set methods and fast marching methods.* Cambridge University Press, 1999. [Online]. Available : http://hrcak.srce.hr/file/69388?origin=publicationDetail

[2] A. Jordi, M. Ferrer, G. Vizoso, A. Orfila, G. Basterretxea, B. Casas, A. Álvarez, D. Roig, B. Garau, M. Martínez *et al.*, "Scientific management of mediterranean coastal zone : A hybrid ocean forecasting system for oil spill and search and rescue operations," *Marine Pollution Bulletin*, vol. 53, no. 5, pp. 361–368, 2006.

[3] P. J. Webster, A. M. Moore, J. P. Loschnigg, and R. R. Leben, "Coupled ocean-atmosphere dynamics in the indian ocean during 1997-98," *Nature*, vol. 401, no. 6751, pp. 356–360, 1999.

[4] A. Gordon, "Oceanography of the Indonesian Seas," *Oceanography*, vol. 18, no. 4, pp. 13–13, 2005.

[5] Y. Masumoto and T. Yamagata, "Seasonal variations of the indonesian throughflow in a general ocean circulation model," *Journal of Geophysical Research : Oceans*, vol. 101, no. C5, pp. 12 287–12 293, 1996.

[6] R. D. Susanto, A. L. Gordon, and Q. Zheng, "Upwelling along the coasts of java and sumatra and its relation to enso," *Geophysical Research Letters*, vol. 28, no. 8, pp. 1599–1602, 2001.

[7] J. T. Potemra and N. Schneider, "Interannual variations of the indonesian throughflow," *Journal of Geophysical Research : Oceans*, vol. 112, no. C5, 2007.

[8] R. D. Susanto, A. L. Gordon, and J. Sprintall, "Observations and proxies of the surface layer throughflow in lombok strait," *Journal of Geophysical Research : Oceans*, vol. 112, no. C3, 2007.

[9] J. Sprintall, S. E. Wijffels, R. Molcard, and I. Jaya, "Direct estimates of the indonesian throughflow entering the indian ocean : 2004–2006," *Journal of Geophysical Research : Oceans*, vol. 114, no. C7, 2009.

[10] C. Caviedes, *El Niño in history : storming through the ages.* University Press of Florida, 2001.

[11] J. S. Gray, "Marine biodiversity : patterns, threats and conservation needs," *Biodiversity & Conservation*, vol. 6, no. 1, pp. 153–175, 1997.

[12] M. D. Spalding, H. E. Fox, G. R. Allen, N. Davidson, Z. A. Ferdaña, M. Finlayson, B. S. Halpern, M. A. Jorge, A. Lombana, S. A. Lourie, K. D. Martin, E. McManus, J. Molnar, C. A. Recchia, and J. Robertson, "Marine ecoregions of the world : A bioregionalization of coastal and shelf areas," *BioScience*, vol. 57, no. 7, p. 573, 2007. [Online]. Available : +http://dx.doi.org/10.1641/B570707

[13] C. H. Hidrovo and D. P. Hart, "Emission reabsorption laser induced fluorescence (erlif) film thickness measurement," *Measurement Science and Technology*, vol. 12, no. 4, p. 467, 2001.

[14] E. Donnay, "Use of unmanned aerial vehicle (uav) for the detection and surveillance of marine oil spills in the belgian part of the north sea," in *Proceedings of the 32 AMOP technical seminar on environmental contamination and response*, vol. 2, 2009.

[15] F. Carnesecchi, V. Byfield, P. Cipollini, G. Corsini, and M. Diani, "An optical model for the interpretation of remotely sensed multispectral images of oil spill," in *Proc. SPIE*, vol. 7105, 2008, p. 710504.

[16] R. Belore, "A device for measuring oil slick thickness," *Spill Technology Newsletter*, vol. 7, no. 2, pp. 44–47, 1982.

[17] M. F. Fingas and C. E. Brown, "Review of oil spill remote sensing," *Spill Science & Technology Bulletin*, vol. 4, no. 4, pp. 199–208, 1997.

[18] K. Grüner, R. Reuter, and H. Smid, "A new sensor system for airborne measurements of maritime pollution and of hydrographic parameters," *GeoJournal*, vol. 24, no. 1, pp. 103–117, 1991.

[19] A. Samberg, "The state-of-the-art of airborne laser systems for oil mapping," *Canadian Journal of Remote Sensing*, vol. 33, no. 3, pp. 143–149, 2007.

[20] M. N. Jha, J. Levy, and Y. Gao, "Advances in remote sensing for oil spill disaster management : state-of-the-art sensors technology for oil spill surveillance," *Sensors*, vol. 8, no. 1, pp. 236–255, 2008.

[21] C. Brekke and A. H. S. Solberg, "Oil spill detection by satellite remote sensing," *Remote Sensing of Environment*, vol. 95, no. 1, pp. 1–13, 2005.

[22] O. Calla, N. Ahmadian, and S. Hasan, "Estimation of emissivity and scattering coefficient of low saline water contaminated by diesel in cj band (5.3 ghz) and ku band (13.4 ghz)," *84.37.+ q ; 84.40. xb ; 92.05. Hj*, 2011.

[23] O. Calla, H. K. Dadhich, and S. Singhal, "Oil spill detection using ssm/i satellite data over bombay high location in arabian sea," *IJRSP Vol.42(1) February 2013*, 2013.

[24] L. Yujiri, M. Shoucri, and P. Moffa, "Passive millimeter wave imaging," *IEEE microwave magazine*, vol. 4, no. 3, pp. 39–50, 2003.

[25] C. Giri, J. Long, and L. Tieszen, "Mapping and monitoring louisiana's mangroves in the aftermath of the 2010 gulf of mexico oil spill," *Journal of Coastal Research*, vol. 27, no. 6, pp. 1059–1064, 2011.

[26] R. Goodman, "Remote sensing resolution and oil slick inhomogeneities," in *Proceedings of the second thematic conference on remote sensing for marine and coastal environments : needs, solutions and applications. ERIM, Ann Arbor, p I-1-17*, 1994.

[27] C.-S. Yang, Y.-S. Kim, K. Ouchi, and J.-H. Na, "Comparison with l-, c-, and x-band real sar images and simulation sar images of spilled oil on sea surface," in *Geoscience and Remote Sensing Symposium, 2009 IEEE International, IGARSS 2009*, vol. 4. IEEE, 2009, pp. IV–673.

[28] D.-j. Kim, W. M. Moon, and Y.-S. Kim, "Application of terrasar-x data for emergent oil-spill monitoring," *IEEE Transactions on Geoscience and Remote Sensing*, vol. 48, no. 2, pp. 852–863, 2010.

[29] B. Minchew, C. E. Jones, and B. Holt, "Polarimetric analysis of backscatter from the deepwater horizon oil spill using l-band synthetic aperture radar," *IEEE Transactions on Geoscience and Remote Sensing*, vol. 50, no. 10, pp. 3812–3830, 2012.

[30] R. Solberg and N. Theophilopoulos, "Envisys–a solution for automatic oil spill detection in the mediterranean," Environmental Research Institute of Michigan, Ann Arbor, MI (United States), Tech. Rep., 1997.

[31] Y. Zhang, H. Lin, Q. Liu, J. Hu, X. Li, and K. Yeung, "Oil-spill monitoring in the coastal waters of hong kong and vicinity," *Marine Geodesy*, vol. 35, no. 1, pp. 93–106, 2012.

[32] Z. Yongzhi, L. Hujun, W. Xiao, and W. Dan, "Edge extraction of marine oil spill in sar images," in *Challenges in Environmental Science and Computer Engineering (CESCE), 2010 International Conference on*, vol. 1. IEEE, 2010, pp. 439–442.

[33] F. Zhang, Y. Shao, W. Tian, and S. Wang, "Oil spill identification based on textural information of sar image," in *Geoscience and Remote Sensing Symposium, 2008. IGARSS 2008. IEEE International*, vol. 4. IEEE, 2008, pp. IV–1308.

[34] M. Tello, R. Bonastre, C. Lopez-Martinez, J. J. Mallorqui, A. Danisi, G. Di Martino, A. Iodice, G. Ruello, and D. Riccio, "Characterization of local regularity in sar imagery by means of multiscale techniques : application to oil spill detection," in *Geoscience and Remote Sensing Symposium, 2007. IGARSS 2007. IEEE International.* IEEE, 2007, pp. 5228–5231.

[35] D. Chaudhuri, A. Samal, A. Agrawal, A. Mishra, V. Gohri, R. Agarwal *et al.*, "A statistical approach for automatic detection of ocean disturbance features from sar images," *IEEE Journal of Selected Topics in Applied Earth Observations and Remote Sensing*, vol. 5, no. 4, pp. 1231–1242, 2012.

[36] A. Mishra, D. Chaudhuri, C. Bhattacharya, and Y. Rao, "Ocean disturbance feature detection from sar images—an adaptive statistical approach," in *Synthetic Aperture Radar (APSAR), 2011 3rd International Asia-Pacific Conference on.* IEEE, 2011, pp. 1–4.

[37] O. Garcia-Pineda, I. MacDonald, and B. Zimmer, "Synthetic aperture radar image processing using the supervised textural-neural network classification algorithm," in *Geoscience*

and Remote Sensing Symposium, 2008. IGARSS 2008. IEEE International, vol. 4. IEEE, 2008, pp. IV–1265.

[38] D. I. Morales, M. Moctezuma, and F. Parmiggiani, "Detection of oil slicks in sar images using hierarchical mrf," in *Geoscience and Remote Sensing Symposium, 2008. IGARSS 2008. IEEE International*, vol. 3. IEEE, 2008, pp. III–1390.

[39] M. Robson, J. Secker, and P. Vachon, "Evaluation of ecognition for assisted target detection and recognition in sar imagery," in *Geoscience and Remote Sensing Symposium, 2006. IGARSS 2006. IEEE International Conference on.* IEEE, 2006, pp. 145–148.

[40] C. Ozkan, C. Ozturk, F. Sunar, and D. Karaboga, "The artificial bee colony algorithm in training artificial neural network for oil spill detection," *Neural Network World*, vol. 21, no. 6, p. 473, 2011.

[41] S. Singha, T. J. Bellerby, and O. Trieschmann, "Detection and classification of oil spill and look-alike spots from sar imagery using an artificial neural network," in *Geoscience and Remote Sensing Symposium (IGARSS), 2012 IEEE International.* IEEE, 2012, pp. 5630–5633.

[42] ——, "Satellite oil spill detection using artificial neural networks," *IEEE Journal of Selected Topics in Applied Earth Observations and Remote Sensing*, vol. 6, no. 6, pp. 2355–2363, 2013.

[43] K. Topouzelis, V. Karathanassi, P. Pavlakis, and D. Rokos, "Detection and discrimination between oil spills and look-alike phenomena through neural networks," *ISPRS Journal of Photogrammetry and Remote Sensing*, vol. 62, no. 4, pp. 264–270, 2007.

[44] K. N. Topouzelis, "Oil spill detection by SAR images : Dark formation detection, feature extraction and classification algorithms," *Sensors*, vol. 8, no. 10, pp. 6642–6659, 2008.

[45] K. Topouzelis, V. Karathanassi, P. Pavlakis, and D. Rokos, "Potentiality of feed-forward neural networks for classifying dark formations to oil spills and look-alikes," *Geocarto International*, vol. 24, no. 3, pp. 179–191, 2009.

[46] M. Fingas, *Oil spill science and technology.* Gulf professional publishing, 2016.

[47] A. Berry, T. Dabrowski, and K. Lyons, "The oil spill model oiltrans and its application to the celtic sea," *Marine Pollution Bulletin*, vol. 64, no. 11, pp. 2489 – 2501, 2012. [Online]. Available : http://www.sciencedirect.com/science/article/pii/S0025326X12003578

[48] A. Galeev and S. Ponikorov, "Numerical analysis of the process of heated oil evaporation from the emergency spill surface," *Journal of Engineering Physics and Thermophysics*, vol. 84, no. 6, pp. 1398–1407, 2011.

[49] D. Mackay and C. D. McAuliffe, "Fate of hydrocarbons discharged at sea," *Oil and Chemical Pollution*, vol. 5, no. 1, pp. 1–20, 1989.

[50] M. Nazir, F. Khan, P. Amyotte, and R. Sadiq, "Multimedia fate of oil spills in a marine environment—an integrated modelling approach," *process safety and environmental protection*, vol. 86, no. 2, pp. 141–148, 2008.

[51] W. Stiver and D. Mackay, "Evaporation rate of spills of hydrocarbons and petroleum mixtures," *Environmental science & technology*, vol. 18, no. 11, pp. 834–840, 1984.

[52] S. Wang, Y. Shen, and Y. Zheng, "Two-dimensional numerical simulation for transport and fate of oil spills in seas," *Ocean Engineering*, vol. 32, no. 13, pp. 1556–1571, 2005.

[53] Z. Zhong and F. You, "Oil spill response planning with consideration of physicochemical evolution of the oil slick : A multiobjective optimization approach," *Computers & Chemical Engineering*, vol. 35, no. 8, pp. 1614–1630, 2011.

[54] D. Rasmussen, "Oil spill modeling—a tool for cleanup operations," in *International Oil Spill Conference*, vol. 1985, no. 1. American Petroleum Institute, 1985, pp. 243–249.

[55] H. Xie, P. D. Yapa, and K. Nakata, "Modeling emulsification after an oil spill in the sea," *Journal of Marine Systems*, vol. 68, no. 3, pp. 489–506, 2007.

[56] X. Chao, N. J. Shankar, and H. F. Cheong, "Two-and three-dimensional oil spill model for coastal waters," *Ocean engineering*, vol. 28, no. 12, pp. 1557–1573, 2001.

[57] J. C. Huang, "A review of the state-of-the-art of oil spill fate/behavior models," in *International Oil Spill Conference*, vol. 1983, no. 1. American Petroleum Institute, 1983, pp. 313–322.

[58] S. A. Lonin, "Lagrangian model for oil spill diffusion at sea," *Spill Science & Technology Bulletin*, vol. 5, no. 5, pp. 331–336, 1999.

[59] M. L. Spaulding, "A state-of-the-art review of oil spill trajectory and fate modeling," *Oil and Chemical Pollution*, vol. 4, no. 1, pp. 39–55, 1988.

[60] M. Reed, E. Gundlach, and T. Kana, "A coastal zone oil spill model : development and sensitivity studies," *Oil and Chemical Pollution*, vol. 5, no. 6, pp. 411–449, 1989.

[61] E. Howlett, K. Jayko, and M. Spaulding, "Interfacing real-time information with oilmap," Tech. Rep., 1993.

[62] K. Korotenko, R. Mamedov, and C. Mooers, "Prediction of the dispersal of oil transport in the caspian sea resulting from a continuous release," *Spill Science & Technology Bulletin*, vol. 6, no. 5, pp. 323–339, 2000.

[63] CLS, "Product User Manual – Meteorological data," INDESO Project, Tech. Rep., 2015.

[64] M. Girin, "Operational pollution at sea," *Safer Seas Symposium Brest*, 2007.

[65] A. Jernelöv, "The threats from oil spills : now, then, and in the future," *AMBIO*, vol. 39, no. 6, pp. 353–366, 2010, doi :10.1007/s13280-010-0085-5.

[66] PTTEP-Australasia, "Montara Well Release Monitoring Study Oil Fate and Effects Assessment :Spill Trajectory Analysis," PTTEP-Australasia, Tech. Rep. October, 2010.

[67] MMAF-Indonesia, "Zone and Management Plan Sawu Seas, KEPMEN No.6/KEPMEN-KP/2014," 2014.

[68] M. Reed, Ø. Johansen, P. J. Brandvik, P. Daling, A. Lewis, R. Fiocco, D. MacKay, and R. Prentki, "Oil spill modeling towards the close of the 20th century : Overview of the state of the art," *Spill Science and Technology Bulletin*, vol. 5, no. 1, pp. 3–16, 1999, doi = 10.1016/S1353-2561(98)00029-2.

[69] Y. Cheng, X. Li, Q. Xu, O. Garcia-Pineda, O. B. Andersen, and W. G. Pichel, "SAR observation and model tracking of an oil spill event in coastal waters," *Marine Pollution Bulletin*, vol. 62, no. 2, pp. 350–363, 2011.

[70] Y. Liu, A. MacFadyen, Z.-G. Ji, and R. Weisberg, "Monitoring and Modeling the Deepwater Horizon Oil Spill : A Record-Breaking Enterprise," *Washington DC American Geophysical Union Geophysical Monograph Series*, vol. 195, 2011.

[71] Y. Liu, R. Weisberg, C. Hu, and L. Zheng, "Tracking the Deepwater Horizon Oil Spill : A Modeling Perspective," *Eos Trans. AGU*, vol. 92, no. 6, pp. 45–46, 2011, doi : 10.1029/2011EO060001.

[72] Y. Liu, R. H. Weisberg, C. Hu, and L. Zheng, "Trajectory Forecast as a Rapid Response to the Deepwater Horizon Oil Spill," *Geophys. Monogr. Ser.*, vol. 195, pp. 153–165, 2011, doi :10.1029/2011GM001121.

[73] Q. Xu, X. Li, Y. Wei, Z. Tang, Y. Cheng, and W. G. Pichel, "Satellite observations and modeling of oil spill trajectories in the Bohai Sea," *Marine Pollution Bulletin*, vol. 71, no. 1-2, pp. 107–116, 2013, http ://dx.doi.org/10.1016/j.marpolbul.2013.03.028.

[74] Y. Cheng, B. Liu, X. Li, F. Nunziata, Q. Xu, X. Ding, M. Migliaccio, and W. G. Pichel, "Monitoring of oil spill trajectories with COSMO-skymed X-band SAR images and model simulation," *IEEE Journal of Selected Topics in Applied Earth Observations and Remote Sensing*, vol. 7, no. 7, pp. 2895–2901, 2014, doi= 10.1109/JSTARS.2014.234157.

[75] CLS France, "Manuel d'Utilisation de MOBIDIRIFT," CLS France, Tech. Rep., 2012.

[76] J. Lellouche, O. Le Galloudec, M. Drévillon, C. Régnier, E. Greiner, G. Garric, N. Ferry, C. Desportes, C. Testut, C. Bricaud *et al.*, "Evaluation of global monitoring and forecasting systems at mercator océan," *Ocean Sci*, vol. 9, no. 1, pp. 57–81, 2013.

[77] L. Parent, N. Ferry, B. Barnier, M. Drevillon, and E. Greiner, "Global Ocean Reanalysis Simulations at Mercator Océan GLORYS1 : the Argo years 2002-2008," in *EGU General Assembly Conference Abstracts*, ser. EGU General Assembly Conference Abstracts, D. N. Arabelos and C. C. Tscherning, Eds., vol. 11, Apr. 2009, p. 10679.

[78] W. J. Lehr and D. Simecek-Beatty, "The relation of langmuir circulation processes to the standard oil spill spreading, dispersion, and transport algorithms," *Spill Science & Technology Bulletin*, vol. 6, no. 3, pp. 247–253, 2000.

[79] A. J. Abascal, S. Castanedo, F. J. Mendez, R. Medina, and I. J. Losada, "Calibration of a lagrangian transport model using drifting buoys deployed during the prestige oil spill," *Journal of Coastal Research*, pp. 80–90, 2009.

[80] P. Lange and H. Hühnerfuss, "Drift response of monomolecular slicks to wave and wind action," *Journal of Physical Oceanography*, vol. 8, no. 1, pp. 142–150, 1978.

[81] M. F. Fingas, "The evaporation of oil spills : development and implementation of new prediction methodology," in *International Oil Spill Conference*, vol. 1999, no. 1. American Petroleum Institute, 1999, pp. 281–287.

[82] N. Longepe, A. Mouche, M. Goacolou, N. Granier, L. Carrere, J. Lebras, P. Lozach, and S. Besnard, "Polluter identification with spaceborne radar imagery, {AIS} and forward drift modeling," *Marine Pollution Bulletin*, vol. 101, no. 2, pp. 826 – 833, 2015.

[83] European Maritime Safety Agency, *Pollution Preparedness and Response Activities of The European Maritime Safety Agency.* European Maritime Safety Agency, 2013, no. 107.

[84] C. E. Jones, B. Minchew, B. Holt, and S. Hensley, "Studies of the Deepwater Horizon Oil Spill With the UAVSAR Radar," *Monitoring and Modeling the Deepwater Horizon Oil Spill : A Record Breaking Enterprise*, no. June, pp. 33–50, 2013.

[85] B. Zhang, W. Perrie, X. Li, and W. G. Pichel, "Mapping sea surface oil slicks using radarsat-2 quad-polarization sar image," *Geophysical Research Letters*, vol. 38, no. 10, pp. n/a–n/a, 2011, l10602. [Online]. Available : http://dx.doi.org/10.1029/2011GL047013

[86] F. Girard-Ardhuin, G. Mercier, F. Collard, and R. Garello, "Operational oil slick characterization by SAR imagery and synergistic data," *IEEE Trans. on Oceanic Engineering*, vol. 30, no. 3, Jul. 2005.

[87] L. Chang, Z. S. Tang, S. H. Chang, and Y. L. Chang, "A region-based GLRT detection of oil spills in SAR images," *Pattern Recognition Letters*, vol. 29, no. 14, pp. 1915–1923, 2008.

[88] Powell MJD, "An efficient method for finding the minimum function of several variables without calculating derivatives," *Computer Journal*, vol. 7, no. 2, pp. 155–162, 1964.

[89] I. Leifer, W. J. Lehr, D. Simecek-Beatty, E. Bradley, R. Clark, P. Dennison, Y. Hu, S. Matheson, C. E. Jones, B. Holt *et al.*, "State of the art satellite and airborne marine oil spill remote sensing : Application to the bp deepwater horizon oil spill," *Remote Sensing of Environment*, vol. 124, pp. 185–209, 2012.

[90] P. Burrows, C. Rowley, and D. Owen, "Torrey canyon : A case study in accidental pollution*," *Scottish Journal of Political Economy*, vol. 21, no. 3, pp. 237–258, 1974. [Online]. Available : http://dx.doi.org/10.1111/j.1467-9485.1974.tb00195.x

[91] Indonesia's National Maritime Council, "Policy Evaluation for Implementation of International Ocean Laws (UNCLOS 1982) In Indonesia," Indonesia's National Maritime Council, Jakarta, Tech. Rep., 2008.

[92] Ministry of Environment Indonesia, "Country report on pollution in the BOBLME - Indonesia," Ministry of Environment Indonesia, Tech. Rep., 2011.

[93] B. G. Gautama and R. Fablet, "Assimilative 2-D Lagrangian Transport Model for the Estimation of Oil Leakage Parameters From SAR Images : Application to the Montara Oil Spill," *IEEE Journal of Selected Topics in Applied Earth Observations and Remote Sensing*, vol. 9, no. 11, pp. 4962–4969, 2016.

[94] Ministry of Marine and Fisheries Indonesia, "Statistic of Marine Capture Fisheries in Indonesia Fishing Management Area, 2005-2014," Ministry of Marine and Fisheries Indonesia, Jakarta, Tech. Rep., 2015.

[95] I. Yulianto, Y. Herdiana, M. H. Halim, P. Ningtias, A. Hermansyah, and S. Campbell, "Spatial Analysis to Achieve 20 Million Hectares of Marine Protected Areas For Indonesia by 2020," Marine Protected Areas Governance (MPAG), Jakarta, Tech. Rep., 2013. [Online]. Available : http://www.wcs.or.id

[96] Y. Loya and B. Rinkevich, "Effects of oil pollution on coral reef communities," *Marine Ecology Progress Series*, vol. 3, no. 2, pp. 167–180, 1980. [Online]. Available : http://www.jstor.org/stable/24813665

[97] J. D. Bell and R. Galzin, "Influence of live coral cover on coral-reef fish communities," *Marine Ecology Progress Series*, vol. 15, no. 3, pp. 265–274, 1984. [Online]. Available : http://www.jstor.org/stable/24815943

[98] E. R. Gundlach and M. O. Hayes, "Vulnerability of coastal environments to oil spill impacts," *Marine technology society Journal*, vol. 12, no. 4, pp. 18–27, 1978.

[99] M. G. Barron, "Ecological impacts of the deepwater horizon oil spill : implications for immunotoxicity," *Toxicologic pathology*, vol. 40, no. 2, pp. 315–320, 2012.

[100] P. Fattal, M. Maanan, I. Tillier, N. Rollo, M. Robin, and P. Pottier, "Coastal Vulnerability to Oil Spill Pollution : the Case of Noirmoutier Island (France)," *Journal of Coastal Research*, vol. 26, no. 5, pp. 879–887, 2010.

[101] N. Singkran, "Classifying risk zones by the impacts of oil spills in the coastal waters of Thailand," *Marine Pollution Bulletin*, vol. 70, no. 1-2, pp. 34–43, 2013. [Online]. Available : http://dx.doi.org/10.1016/j.marpolbul.2013.02.004

[102] X. Liu, R. Meng, Q. Xing, M. Lou, H. Chao, and L. Bing, "Assessing oil spill risk in the Chinese Bohai Sea : A case study for both ship and platform related oil spills," *Ocean and Coastal Management*, vol. 108, pp. 140–146, 2015. [Online]. Available : http://dx.doi.org/10.1016/j.ocecoaman.2014.08.016

[103] Statistics Indonesia, *Statistics of Marine and Coastal Resources*. Jakarta : BPS Indonesia, 2011.

[104] JICA, "The study for the maritime traffic safety system development plan in the Republic of Indonesia," Ministry of Transportation Indonesia, Tech. Rep., 2002.

[105] Special Task Force for Upstream Oil and Gas Business Activities Indonesia, "Annual Report 2014," SKK MIGAS, Jakarta, Tech. Rep. 9, 2014.

[106] T. Huffard, C.L., Erdman, M.V., Gunawan, "Geographic priorities for marine biodiversity conservation in Indonesia," Directorate of Concervation for Area and Fish Species, Directorate General of Marine, Coasts, and Small Islands Ministry of Marine Affairs and Fisheries, Jakarta, Tech. Rep., 2012.

[107] J. H. Connell, "Diversity in tropical rain forests and coral reefs," *Science*, vol. 199, no. 4335, pp. 1302–1310, 1978.

[108] L. McKenzie, R. Coles, and P. Erftemeijer, "Seagrass ecosystems of papua," *The Ecology of Papua, Part Two. AJ Marshall and BM Beehler. Singapore, Periplus Editions*, 2007.

[109] The International Tanker Owners Pollution Federation Limited, “Effects of Oil on Fisheries and Aquaculture,” Tech. Rep. 3, 2004. [Online]. Available : http://www.imo.org/en/OurWork/Environment/PollutionResponse/OilPollutionResources/Documents/Platformforinforamtionsharing/Seafoodsafety/TechnicalInformationPaper.pdf

[110] Ministry of Marine And Fisheries Indonesia, “Marine and Fisheries in Figures 2015,” Ministry of Marine And Fisheries Indonesia, Tech. Rep., 2015.

Résumé

L'observation de la nappe du pétrole à la mer d'Indonésie

L'Indonésie, l'une de plus grands archipels, a été menacé avec la pollution provenant de la marée noire. Le gouvernement d'Indonésie en coopération avec le gouvernement Français a développé un système d'observation de l'océan par satellite afin de supporter de développement durable. Ce système est intégré dans les systèmes d'océanographie opérationnelle dans le cadre du projet de développement des infrastructures de l'océanographie spatiale (INDESO). Le contexte de cette thèse est dans le cadre du projet INDESO notamment dans applications d'INDESO pour suivre des déversements de pétrole dans les mers d'Indonésie. Dans ce contexte, cette thèse propose de nouvelles méthodologies et analyses. Cette thèse comportait deux contributions principales. La première contribution est sur la récupération des paramètres de dérive des déversements d'hydrocarbures à partir d'une analyse conjointe des observations SAR (Synthetic Aperture Radar) et des résultats d'un modèle de transport de déversement de pétrole. Dans cette première partie, nous estimons les paramètres de dérive de pétrole. On a exploité un modèle de transport de déversement de pétrole lagrangien, de sorte que la dérive simulée de déversement d'hydrocarbures modèles puisse correspondre à l'observation de satellite. Pour confirmer l'origine du déversement de pétrole détecté à une date donnée par une observation de SAR, nous avons effectuaient des simulations avec différentes dates de début de fuite, duré de fuite et différentes valeurs de pondération deux facteurs dominants i.e. vent et courant. Nous avons développé une nouvelle méthode pour l'assimilation de ces paramètres de fuite de pétrole à comparer avec d'une détection dérivée d'un déversement d'hydrocarbures. Nous avons appliqué la méthodologie proposée sur le plus grand accident en Indonésie, l'accident de Montara. La deuxième contribution est l'évaluation globale du risque de déversement d'hydrocarbures en Indonésie. Nous sommes concentrés sur la zone de gestion des pêches de l'Indonésie. Dans cette analyse, nous avons proposé une méthodologie qui considère le déversement de pétrole, qui a des sources différentes et leurs impacts à l'environnement, mais aussi sur les perspectives sociales et économiques. Pour l'évaluation de la vulnérabilité des zones marines protégées, nous avons également exploité le modèle de 2D lagrangien. L'accent mis sur les zones de gestion des pêches (FMA) afin de fournir une analyse synoptique sur l'ensemble du territoire maritime d'Indonésie. Chaque FMA présente les caractéristiques spécifiques des paramètres environnementaux et socio-économiques. Nous avons évalué le risque de déversement d'hydrocarbures dans chaque zone de gestion sur la base de tous ces facteurs. Le résultat de cette étude peut être utilisé dans la planification d'une action pour réduire les impacts négatifs du déversement d'hydrocarbures.

Mots-clés : Déversement d'hydrocarbures, Indonésie, Synthétique Aperture Radar, Modèle de trajectoire, Océanographie opérationnelle

Abstract

Oil spill observation in Indonesia

Indonesia as the biggest archipelago has a major threat coming from oil spill. Due to the increasing concerns of environment protection for sustainable development, the government of Indonesia in cooperation with government of France developed an ocean observation system with one of its pilot applications is oil spills monitoring. This system is integrated in the operational oceanography systems within the project of Infrastructure Development of Space Oceanography (INDESO). The context of this thesis is in the frame of INDESO project particularly in the monitoring of oil spill in the Indonesian seas. Within the context above, this thesis propose new methodologies and analyses. This thesis involved two main contributions. The first contribution addressed the retrieval of oil spill drift parameters from a joint analysis of SAR observations of an oil spill and of outputs of a Lagrangian oil spill transport model. In this first part, we estimate oil spill drift parameters. The proposed framework exploited a Lagrangian oil spill transport model such that the simulated oil spill drift could match a SAR-based observation of an oil spill. In the considered 2D Lagrangian model there were two dominant factors, i.e. wind and surface current. To confirm the origin of the oil spill detected on a given date through a SAR observation, we performed simulations with various leakage starting dates, leakage durations, and different values of wind and current weighing coefficients. We developed a novel framework for the assimilation of these oil leakage parameters from a SAR-derived detection of an oil spill. We applied the proposed methodology on the most famous oil spill accident in Indonesia, the Montara case. The second contribution was the global assessment of oil spill risk in Indonesia. We focused on the 11 Indonesia Fisheries Management Area to support the sustainability development of marine and fisheries. In this analysis we proposed methodology that considered the oil spill from different source and their impacts not only to the environment, but also from social and economic perspectives. For the assessment of vulnerability of Marine Protected Areas to oil spill pollution, we also exploited the oil spill trajectory model. The focus was given to Fisheries Management Areas as a means to provide synoptic analysis over the entire Indonesian maritime territory. Using different information from many institutional reports, we collected and analyzed the potential source of oil spill in each FMA. Each FMA has specific characteristics in terms environmental and socioeconomic features. We assessed the oil spill risk in each FMA based on all these factors. The result of this study can be used in the mitigation planning to reduce the negative impacts of oil spill.

Keywords: Oil spill, Indonesia, Synthetic Aperture Radar, Trajectory model, Oceanography operational

IMT Atlantique
Bretagne-Pays de la Loire
École Mines-Télécom

N° d'ordre : 2017IMTA0036

IMT Atlantique Bretagne-Pays de la Loire - www.imt-atlantique.fr

Campus de Brest
Technopôle Brest-Iroise
CS 83818
29238 Brest Cedex 03
T +33 (0)2 29 00 11 11
F +33 (0)2 29 00 10 00

Campus de Nantes
4, rue Alfred Kastler - La Chantrerie
CS 20722
44307 Nantes Cedex 3
T +33 (0)2 51 85 81 00
F +33 (0)2 51 85 81 99

Campus de Rennes
2, rue de la Châtaigneraie
CS 17607
35576 Cesson Sévigné Cedex
T +33 (0)2 99 12 70 00
F +33 (0)2 99 12 70 08